TÉCNICO LISBOA

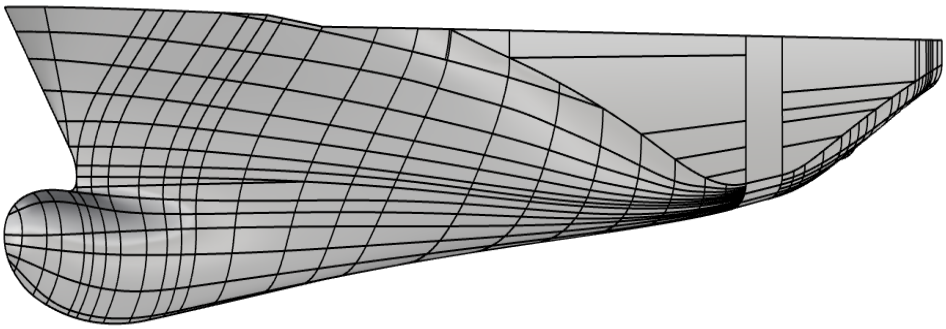

Parametric Modelling of Hull Forms for Merchant Ships

Pedro Henrique Campos Reis

Thesis to obtain the Master of Science Degree in

Naval Architecture and Ocean Engineering

Supervisor(s): Prof. Manuel Filipe Simões Franco Ventura

Examination Committee

Chairperson: Prof. Ângelo Manuel Palos Teixeira
Supervisor: Prof. Manuel Filipe Simões Franco Ventura
Member of the Committee: Prof. Tiago Alexandre Rosado Santos

November 2022

Declaration

I declare that this document is an original work of my own authorship and that it fulfils all the requirements of the Code of Conduct and Good Practices of the Universidade de Lisboa.

Signature

Acknowledgments

I would like to thank Professor Manuel Ventura for the freedom to explore interesting topics and the extremely valuable guidance given to me during the development of this work, especially in the writing phase.

I also have to thank my family, especially my parents, grandmother and sister, that gave me the support to successfully complete this work during these months. Thank you for always believing in me even when i didn't.

Also i want to thank my friends for helping getting through these though years in Técnico. For giving me memories that i will keep and cherish. A special thanks to the friends who live with me who, during these months, have not stopped giving me words of encouragement and allowing me to unwind my problems.

Finally, i want to dedicated this thesis to my grandfather that unfortunately passed away during my time at Técnico. The memories you have given me throughout my life have given me the strength to overcome any challenge that has arisen during these past few months.

Resumo

O objectivo desta tese é criar um modelo totalmente paramétrico que possa criar um modelo wireframe de navios mercantes para ser usado na fase de projecto de conceito. O primeiro passo será analisar as formas do casco de diferentes tipos de navios mercantes, com foco em graneleiros, Ro-Ro, navios-tanque e navios porta-contentores. Os objectivos desta análise são: identificar as curvas importantes para definir a forma do casco, os parâmetros necessários para defini-las e a faixa de valores de cada parâmetro. As curvas são classificadas em dois tipos: curvas geométricas e de variação de propriedades. São identificadas oito curvas geométricas e três curvas de variação de propriedade. O modelo paramétrico é implementado em uma ferramenta de programação visual chamada Grasshopper, um plug-in do Rhinoceros 3D. O modelo inicia com a entrada de oitenta parâmetros, ou menos, dependendo da complexidade da forma do casco, que criam pontos, depois as curvas geométricas e de variação de propriedades e, por fim, o modelo wireframe. As curvas são criadas com curvas Non-Uniform Rational B-Spline. Após a implementação do procedimento parámetrico, é apresentado a sua validação. O procedimento de validação consiste em uma validação numérica, onde os resultados hidrostáticos são comparados, e uma validação gráfica, onde é criado um plano geométrico onde as secções paramétricas e reais são sobrepostas. Os resultados mostram erros hidrostáticos baixos e com as secções paramétricas a apresentarem formas aceitáveis embora em alguns casos apresentem diferenças nas áreas.

Palavras-chave: Modelação Paramétrica, Grasshopper, Forma do Casco, Projeto de Navio

Abstract

The objective of this thesis is to create a fully parametric model that can create a wireframe model of merchant ships to be used in the concept design phase. The first step is analyse the hull shapes of different types of merchant ships, focusing on bulk carriers, Ro-Ro, tankers and container ships. The objectives of this analysis are: identifying the most important curves to define hull's shape, the necessary parameters to define them and the values range of each parameter. The curves are classified in two types: geometric curves and property variation curves. Eight geometric curves and three property variation curves were identified. The parametric model is implemented in a visual programming tool called Grasshopper, which is a Rhinoceros 3D plug-in. The model starts with input of eighty parameters, or less, depending on the complexity of the hull shape, which create points, then the geometric and property distribution curves, and finally the wireframe model. Curves are created with Non-Uniform Rational B-Spline curves. After the parametric procedure is implemented, a validation of the parametric model is presented. This validation is carried out with five ships, with different characteristics. The validation procedure consist on a numerical validation, where the hydrostatic results are compared, and a graphical validation, where a body plan is created where the parametric and real sections were superimposed. The results show acceptable errors for hydrostatics and with the parametric sections showing acceptable shapes although in some cases they presented some difference in its areas.

Keywords: Parametric Modelling, Grasshopper, Hull Form, Ship Design

Contents

List of Tables

List of Figures

Symbology

A_{BT}	Bulb Cross-Sectional Area at Forward Perpendicular
A_{BL}	Area of Ram Bow in Longitudinal Plane
A_{MS}	Midship Section Area
B	Ship Breadth
B_b	Bulb Breadth
BM_t	Transverse Metacentric Radius
B_{wl}	Maximum Design Waterline Breadth
C_b	Block Coefficient
C_M	Midship Coefficient
C_P	Prismatic Coefficient
C_{WP}	Design Waterline Coefficient
h_{aft}	Distance Between Aft Sections
h_{fwd}	Distance Between Forward Sections
I_{xx}	Transverse Moment of Inertia
KB	Buoyancy Centre Ordinate
KM_t	Transverse Metacentric Height
L_{pp}	Length between Perpendiculars
L_{pr}	Protruding Length of Bulb
L_{wl}	Length of Design Waterline
T	Ship Draught
T_{FP}	Draught at Forward Perpendicular
Z_b	Bulb Tip Height
∇	Displacement Volume

Acronyms

BEM	Boundary Element Method
CAD	Computer Aided Design
CAE	Computer Aided Engineering
CFD	Computer Fluid Dynamics
DWL	Design Waterline
DWT	Deadweight
FFD	Free Form Deformation
FOB	Flat of Bottom
FOS	Flat of Side
GUI	Graphical User Interface
IGA	IsoGeometric Analysis
KMt	Transverse Metacentric Height
LCB	Longitudinal Center of Buoyancy
LOA	Length Overall
MARIN	Maritime Research Institute Netherlands
NSGA-II	Fast Elitist Nondominated Sorting Genetic Algorithm II
NURBS	Non-Uniform Rational B-Spline
PCC	Pure Car Carrier
PM	Parametric Modeller
PCTC	Pure Car and Truck Carrier
RBF	Radial Basis Functions
Ro-Ro	Roll-on/roll-off
SAC	Sectional Area Curve
SAC-BPD	Sectional Area Curve-Balanced Parametric Design
TEU	Twenty-foot Equivalent Units
VLCC	Very Large Crude Carrier
VLOC	Very Large Ore Carrier
ULCC	Ultra Large Crude Carrier
ULCV	Ultra Large Container Vessel

Chapter 1

Introduction

Ship design is a very complex and iterative task where the aim is to create a new design or modify an existing one that meets a set of requirements set by the ship owner, such as required cargo capacity, service speed, autonomy, etc. Traditionally this process is divided into 4 phases, of which the first two are known as basic design: concept design, preliminary design, contract design, detailed design.

At concept design the first approach is made to the requirements made by the ship owner, where an estimate is made of the main dimensions of the ship (length, beam, draught, depth, block coefficient, etc.). One or more designs alternatives are explored that meet the initial parameters and at the same time are economically viable for the ship owner. Today this phase is very quick. The preliminary phase aims at delivering a series of documents (drawings and studies) with which the construction costs of the ship can be estimated. This set of documents consists of: a general arrangement sketch of the main and auxiliary spaces, a lines plan that allows an assessment of the stability and cargo capacities, definition of the propulsion system, cargo-handling equipment and ship's hull form. All documents submitted must comply with the rules of the classification societies and all maritime authorities, be they national or international. This phase is a lot more work than the concept phase. The third phase aims at finalising all drawings and studies, as well as creating a technical specification of the ship, so that a contract can be drawn up between the ship owner and the shipbuilder. In the last phase of the ship's design, documents are produced containing all the information about the structural elements, arrangement of piping systems, also technical information for ship's construction and pipes. This documentation is then delivered to the shipyard responsible for the construction of the ship. The thesis project is focused on providing a tool to be used in basic design.

Nowadays, ship design is a field under pressure due to the International Maritime Organisation (IMO) to make ships less polluting, aiming for new ships to meet the Energy Efficiency Design Index (EEDI) regulations in order to achieve a 40% reduction in greenhouse gases by 2030 and 50% by 2050. This objective puts pressure on ship owners and ship designers to create ships that are more environmentally friendly, so it is important that there are tools that allow you to explore various design options.

To achieve this goal, Computer Aided Design (CAD) plays a very important role as it allows changes to be made to the shape of the hull. The most used techniques to modify the geometry of the hull shape are: parametric modelling, conventional modelling.

Parametric modelling can have a fully or partial parametric modelling approach. In the first approach the ship hull is described with a finite numbers of form parameters that can have geometric information associated to them. The benefits of this method are the possibility of doing quick modifications of the form parameters in a way that the person responsible for the modifications doesn't need to have lots of experience. It is the most economic method but if there is the need of build one from the ground up it can be very challenging for a person with low know-how. In the second approach only a part of the hull geometry is parametrized, this method can be very useful to optimize for example the bulbous bow. The main advantage of this method is that it isn't necessary a big know-how to set-up and use.

Conventional modelling is the creation or modification of a hull form without any type of form parameters. This method requires a lot of previous experience, it is very time consuming, it is the less economic in comparison with the two types of parametric approaches and it very difficult to reproduce the same hull form two times.

The objective of this thesis is to develop a fully parametric model to produce wireframe models that represent the hull shapes of merchant ships to be used in the basic design. This parametric procedure must be able to reproduce the most used forms of merchant ships with the input of parameters that describe it. It must also be able to create connections between the curves that define geometric and properties characteristics of ships, with the ability to make changes in the input parameters without losing the real shape of the hull. This is an important objective as it makes the optimization procedure faster and easier, which is very important given the need to reduce greenhouse gas emissions.

The thesis has the following structure. In chapter two, an analysis of the history related to hull shape modelling is made, presenting and discussing some of the relevant studies presented over the years. In chapter three is presented a study of the most usual hull forms with the main objective of identifying the necessary curves to define the the hull shape. The fully parametric procedure implementation is presented in chapter five, with a description of all the parameters and points necessary to create the curves identified in chapter four. In addition, the wireframe model generation is also explained. In chapter six, the parametric modeller validation is carried out with the presentation of numerical and graphical results. There are five ships used with different characteristics between them. The last chapter presents the conclusions of the work based on the validation of the model and suggestions for future work.

Chapter 2

State of Art

Numerical representations of the shape of the hull date back to the 18th century, the first study being attributed to Fredrik Chapman in 1760, as stated in [1]. At that time, more practical methods, such as weights and battens, were preferred to control hull shape until computers became accessible and CAD programs begin to be developed.

In the first half of the 20th century more attempts were made to mathematically represent the shape of the hull, driven by hydrodynamic analysis. Taylor in 1915 [2] used polynomials to develop a set of ships similar to an existing ship to be able to analyse the effect of form parameters used on ship resistance. In 1940 Benson [3] improved on Taylor's work to the extent that he was able to generate sections and waterlines, which allowed to be used as a design tool. As analysed in [1] the approach of mathematical representation of the shape of the hull has as a negative point the fact that a large amount of displacement data points is required to define the polynomials, which makes its manipulation complicated.

In the second half of the 20th century, and with computers increasingly efficient and powerful, new ways of representing the hull surface began to be presented, based on the Taylor method [2]. In 1970 Kuiper [4] presented a method based on initial parameters to create shape curves (waterlines, bag, profile). This method, despite being a step forward and applied in different methods used later, still had the limitations related to polynomials which make more complicated shapes difficult to represent. This method was the first parametric hull modelling technique.

An alternative representation of the shape of the hull was presented by Von Kerczek in 1969 [5], called conformal mapping. To try to overcome the limitations of the polynomials Nowacki and Reed [6] presented a solution that combined polynomials, used above the waterline, with conformal mapping, used below the waterline. This allowed to represent more shapes of ships.

Parallel to the introduction of parametric modelling, new forms of curve representation were also developed, such as Bézier curves [7], B-splines [8] and NURBS [9]. All these new representations meant an advance in relation to polynomials and conformal mapping, as they are easier to work with and can represent more geometric shapes. Among these three, the NURBS curves are the easiest to manipulate and the ones that best adapt to parts of the ship where the shapes are more complicated,

such as the bow or stern bulb. Because of this flexibility, it has become the most used representation of curves in CAD systems.

At this time, manual geometry manipulation was the norm in Computer Aided Geometric Design (CASD), but with the evolution of CAD programs it was possible to create techniques to modify or create new hull shapes in a more efficient and simple way. These geometric modelling techniques are classified by Harries, Abt and Hochkirch in [10]. They classified them into 3 different types, see figure 2.1: conventional, partial parametric and fully parametric. Having characterized these 3 forms of geometric modelling in terms of flexibility, efficiency and effectiveness. Three years later, they presented a more in-depth characterization that can be consulted in [11] or in the figure 2.2.

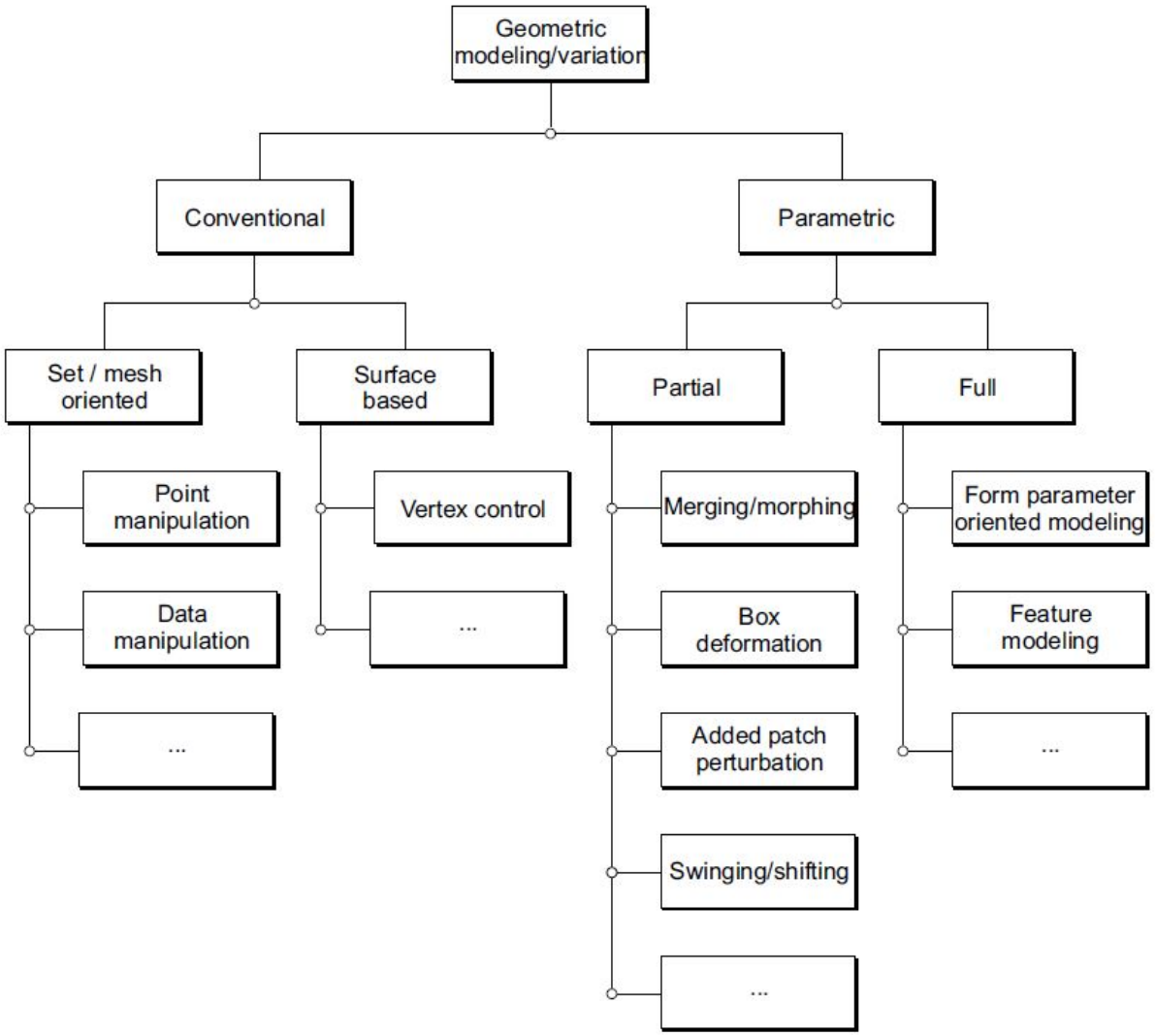

Figure 2.1: Detailed geometric modelling techniques [10]

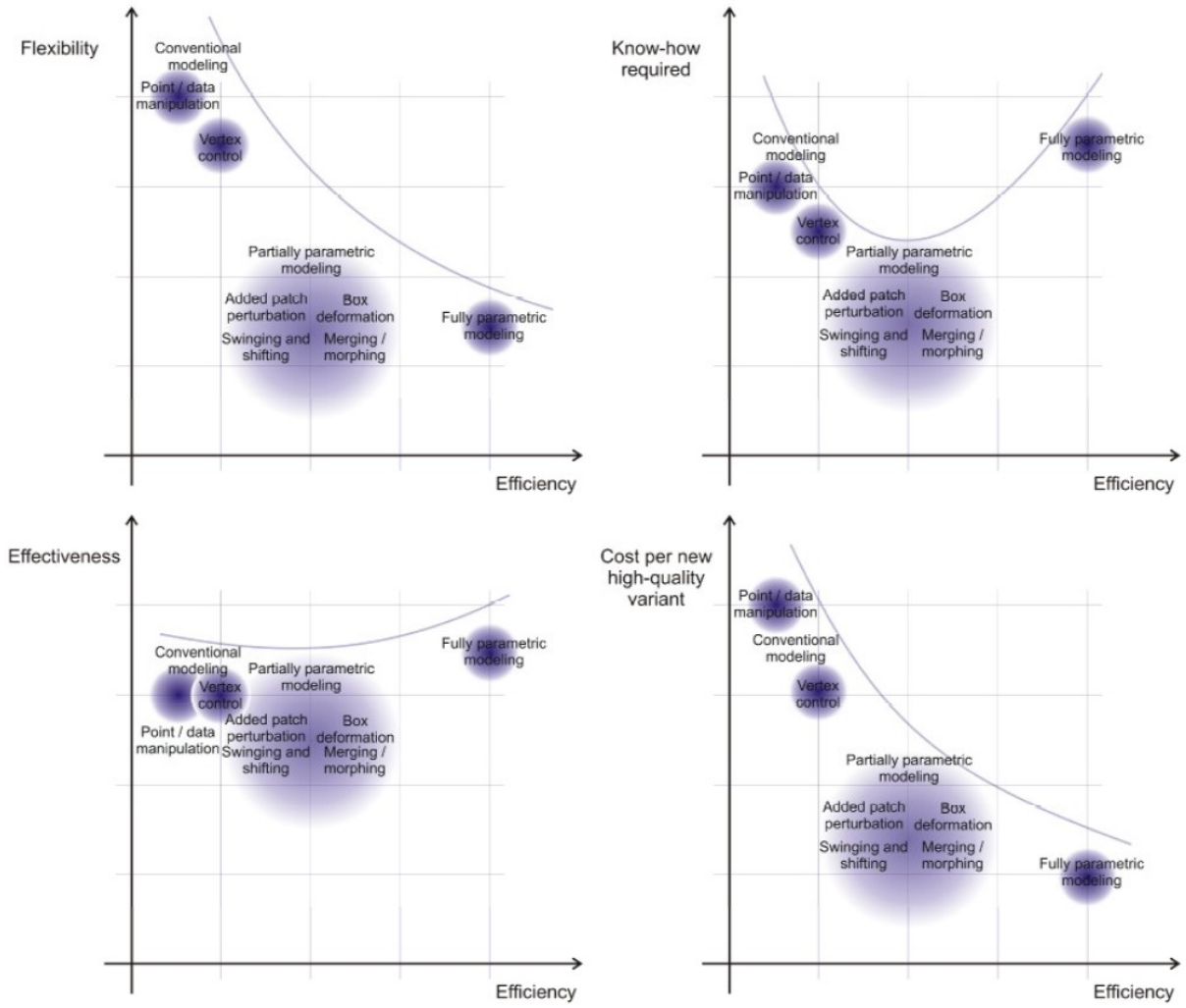

Figure 2.2: Qualitative assessment of geometric modelling techniques [11]

These three forms have already been mentioned briefly in the chapter 1, but will be discussed in more detail below, analysing the work developed in each of them over the years.

Conventional modelling techniques are based on a low-level geometry definition. Points are frequently used to define curves and surfaces. The work itself is predominantly interactive. One approach is the control of vertices, where a surface is associated with a polyhedron of vertices as in the concepts of B-spline and Bézier. To obtain the desired shape, the vertices are manipulated iteratively. The second approach begins by creating points to define curves that later define the surface.

Conventional modelling has the advantage of being very flexible, but it is needed a very large know-how and when the data necessary to represent the hull surface begins to increase any modifications are very time-consuming.

Partial parametric modelling allows you to make modifications to existing hull shapes by changing form parameters that describe the hull geometry. This type of modification can be local or global. It is widely used in optimization studies, as it allows creating a large number of different projects, quickly and easily. The main partial parametric approaches are described in figure 2.1.

Lackenby in 1950 [12] presented one of the first approaches to partial parametric modelling, more specifically a swinging and shifting technique. He came up with a way to make a systematic modification to the sectional area curve (SAC) and then move the sections longitudinally so that the new hull matches the new SAC. Nowadays, this technique continues to be used regularly in optimization studies. Shifting transformations are done by moving a point on the geometry by a specified amount in the principal directions of the chosen coordinate system. Usually the chosen coordinate system is the Cartesian plane. This type of transformation was used by Hochkirch and Bertran [13] to optimize a bulbous bow, with the objective of improving the economic aspect for a refit of a bulbous bow. The bulb was defined with 11 parameters with 3 parametric bulb modifiers, being developed in the Friendship-Framework. Another application of the shifting method to the bulbous bow was made by Zhang, Kim and Bahatmaka in 2018 [14]. This implementation was made in Grasshopper with the bulbous bow defined by 4 curves, this curves are defined by 5 points with the possibility of change the positions of three of them. For more studies where cartesian shifting is used see [15, 16].

Another shifting transformation technique is the use of radial displacements. An example is the use of radial basis functions (RBF) which is a function that is defined by the distance to the chosen centre point, a more in-depth review is made in [17]. Harries and Uharek [18] used this type os partially-parametric approach in combination with principal component analysis to reduce the time necessary to perform an hydrodynamic optimization of a catamaran. One of de negative aspects of RBF is the amount of degrees of freedom, because of this a principal component analysis is used to reduce the dimensionality of the design space and with this get a faster and easier simulation driven design. The results shows a reduction of free variables (14 to 7), which lead to a 33% reduction in computational time. Choi in 2015 [19] presented one where bell-shaped modification functions, to modify the hull shape, were used in combination with a sequential quadratic programming to perform an optimization with the objective to minimize wave resistance. A more recent resistance optimization procedure that uses shifting transformation was presented by Lu et al. [20] that uses B-splines curves to define the bulbous bow and the stern and uses the mapping method to change the hull shape. A Fast Elitist Nondominated Sorting Genetic Algorithm II (NSGA-II) is used to discover the minimum ship resistance. This year the procedure is to optimize a ice breaking bow for polar navigation [21]

The box deformation method can also be called free-form deformation (FFD), presented by Sederberg and Parry in 1986 [22]. It consists of placing a B-spline control polygon, which surrounds the geometry and has an associated control volume. Changing the shape of the geometry is done through making changes to the control polygon either by moving one or more points or applying a rotation to a set of points. For a more in-depth description check [22, 23]. This method was compared with fully parametric modelling in [23], where the optimization objective was to obtain a minimum wave resistance at design speed. The hull used for this optimization was a 48 meter deep-V hull with a wide transom stern and a flat bottom. The full parametric modeller is built in *Friendship*, and the parameters only define the part of hull that is below the spray rail at the chine. The results concluded that despite obtaining a similar reduction in wave resistance, 8.5% for the fully parametric approach and 8.4% for the FFD approach, the fully parametric approach manages to present a more realistic hull shape than the FFD method.

Morphing or merging is the interpolation of two or more baselines, which need to be topologically identical to facilitate the computation of a new geometry. This interpolation requires a morphing parameter, usually between 0 and 1, with the number of morphing parameters being equal to the number of baselines minus one. In [24, 25] the morphing technique combined with evolutionary algorithms is used to create hull shapes in a way that minimizes user input and can explore new designs efficiently and automated. They called this methodology Hybrid Evolutionary Algorithm and Morphing (HEAM).

In fully parametric modelling, the hull form is defined by form parameters. These parameters can describe three types of geometry properties: positional (length, breadth, draught, etc.), differential (tangent at a specified point, etc.), and integral (area, volume, etc.). This is a powerful modelling technique as it allows changes to be made both in the initial design phase and in the optimization phase.

Over the years, several methodologies have been presented for the fully-parametric modelling process. Harry and Abt in 1998 [26] present a modelling process for a bare hull. The process was divided in three consecutive steps, the first is to parametric design of basic curves, then define design sections derived from the basic curves, and lastly generate the surface. There are 12 basic B-splines curves. The parametrization of these curves is made by 13 form parameters, plus two comparing with the B-spline parametrization method presented by Harries and Abt [27]. Harries and Nowacki developed further with the introduction of a new skinning interpolation for the generation of B-spline surfaces [28]. Zhang et al. [29] presented a method based in Harries work to optimize the hull's hydrodynamics.

With the emergence of fully parametric approaches, hydrodynamic optimization has become a time-consuming process as they are done in different languages, which creates a bottleneck in the hull shape development, as stated in [30]. In this article [30] the hull modelling is divided in three different topology levels: appearance topology, design topology and representation topology. The different information that passes between each level makes it difficult to develop the hull shape, which makes optimization a time-consuming process. Because of these difficulties the authors of the paper presented a Computer Aided Engineering (CAE) software called FRIENDSHIP-Framework, now called CAESES. One year later, this methodology was studied in a case study of a inshore yacht [31]. The methodology proved to be capable of producing optimized yacht shapes, but the time it takes to set-up the design formulation is not acceptable for a standard sailing yacht design.

In the early 2000s, a European R&D project called FANTASTIC was carried out for a period of 3 years by 14 European partners [32]. This project resulted in three different approaches: parametric modelling of ships called FRIENDSHIP-Modeller, a model approach using NAPA and shape transformation functions via GMS/Facet. There was a great advance in the optimization procedure with the use of parametric modelling, which allows great flexibility in the variation of hull shapes. For more details of the set-up developed in the system FRIENDSHIP-Modeller used in the FANTASTIC project, see [33], but the main additions were the capability of of modelling multiple surface domains.

Over the years some papers use the CAESES platform to develop some optimization procedures. In 2011 Papanikolau et al. [34] use the platform to developed a more integrated approach for the design of ship hull forms. In 2012 Han, Lee and Choi [35] present a study where the aim was to validate the hydrodynamic optimization procedure using F-Splines (Fairness-optimized B-Spline form parameter curve) optimization. The aim of this paper is achieved with the advantages of F-Splines being: it gives always a fair curve because is generated based on optimization process for fairness, for hull form distortion F-Splines present good flexibility and simplicity in an optimization with constrains, the fully parametric ship hull design is capable of generate multiple hull forms. In 2016 Sanches [36] presented an fully parametric modeller for merchant ships. The hull geometry was defined by 9 geometric curves and seven property distributions curves. One of the objectives of this thesis was to develop a hull shape that followed the properties of the SAC, but this was not achieved. In the same year Sener [37] created a fully parametric model for a frigate. In more recent years Feng, Moctar and Schellin [38] presented an optimization procedure to reduce the total resistance of a multi-purpose wind offshore supply vessel. The CAESES software was coupled with the potential flow solver GL-Rakine to perform the optimization process. In 2020 [39] was developed a hydrodynamic optimization procedure for container ship. The container ship selected was the Duisburg Test Case (DTC). Two years later, [40] developed further and tried out the procedure for two more container ship hulls (KCS and S-175). The parametric model has design variables to describe the bulbous bow (14 parameters), the forebody (10 parameters) and the aft body (13 parameters). After an analysis the selected design variables for the KCS and DTC case were: 7 design variables for bulbous bow, the forebody is defined with 5 design variables, the aftbody is defined with 6 parameters. The S-175 is defined with: 1 parameter for the stem, 7 for the ship body and 1 for the stern. The results show the parametric modeller can be used to defined various types of hull forms.

One of the problems with parametric modelling and direct manipulation methods is the need for a lot of information to create a first reasonable iteration of a hull shape, noted in [41–43]. Bole in [41] proposed a method to combine form parameter design and conventional modelling. The advantages of dimensioning shape parameters are taken advantage of in the early stages of the project, where it is more important to have a reasonable rather than perfect hull surface, and the advantages of conventional modelling in the final stages of the design, where it is important to have a good definition of the hull surface, see figure 2.3. A hierarchy is created between form parameter design and conventional design. This concept is called IntelliHull and is implemented in PolyCad. The ship's hull is defined by 11 shape design parameters. The hull surface is divided into smaller regions that are defined by the designer with a set of geometric curves. This method was applied and discussed in Bole et al. [1] in the context of the initial design phase. For this purpose, two different hull generation techniques were created: YatchLINES and ShipLINES. The first creates a single cubic B-spline surface based on 19 geometric parameters and the second creates a B-spline surface of a single-screw cargo ship hull form with an without bulbous bow based on 25 geometric parameters. The interactive transformation of hull shape of this method is described in [44]

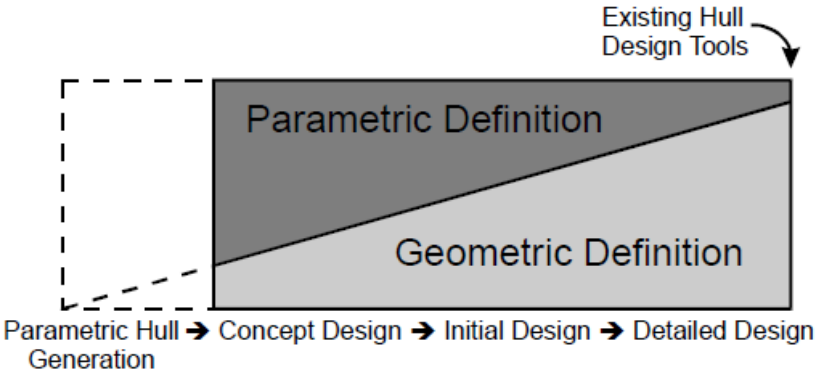

Figure 2.3: Integration of parametric and geometric definition [42]

Another design methodology was introduced by Kim and Nowacki which, unlike the one presented in [33] divides the ship hull form in a multiple domain surface topology and a associated volume [45]. This new design method is called Sectional Area Curve-Balanced Parametric Design (SAC-BPD). The method divides the hull shape into multiples free-form elementary models and blending surfaces, and then using boolean operations creates a hull form that satisfies of the SAC.

In 2008 Pérez et al. [46] presented a parametric design method for semi-displacement and displacement hulls. The structure of this method starts by defining the sectional area curve (8 parameters) and the waterline curve (7 parameters), both curves are defined by two polynomials of four degrees. Next, the designer defines the hull centre line and deck line. With these lines defined it is possible to create a wireframe of the hull stations to create a NURBS surface. Another attempt to generate planning hulls is presented by Calkins et al. [47]. This method define stations as straight lines to create the hull form. In 2014 Pérez [48] presented a parametric design method to define hard-chine ship hulls and semi-displacement hull based on a set of parameters that are related to the geometric features of hull. The objective of the method is to create B-spline surfaces, the curves are also represented with B-splines, to represent a hull based on 25 parameters (6 based on Length, 4 based on width, 6 based on height, 8 based on angles and one based on areas). The downside of these frameworks is the lack of ability to produce all types of hulls, because of this Khan et al. [49] in 2017 presented a method that allows to create planning, semi-displacement and displacement hulls. The framework consists of dividing the hull in 3 regions: entrance, middle and run region. It starts by define the deck, keel, chine and bow line, using 28 parameters. This framework in combination with a generative design algorithm and a space reduction technique is used to create the GenYatch software, more details of this software is presented by Khan et al. [50].

With the development of commercial software capable of creating parametric definitions, there has been the introduction of new parametric modellers. In 2015 year Kostas et al. [51] presented another optimization procedure that builds a T-spline ship hull parametric modeller in Rhinoceros together with a Autodesk's T-Spline plug-in. The parametric modeller uses 24 parameters to create the control cage that is used to create the T-spline surface. A Boundary Element Method (BEM) based on IsoGeometric Analysis (IGA) is used as a wave resistance solver. Ginnis et al. [52] presented a parametric modeller implemented in CATIA software. The parametric modeller uses 30 parameters. Katsoullis, Wang and Kaklis [53] developed a T-splines based parametric modeller called TshipPM to generate complex ship forms. This parametric modeller is an extension of the work presented in [51], which improves flexibility in complex areas like bulbous bow and stern and can give greater proximity in instances like moments and sectional area curve (SAC). In 2021 Ingrassia et al. [54] presented a design tool that is able to guide the designer in creating an hull form mostly based on shape coefficients and non-dimensional ratios. This tool is developed in Visual Basic for Application (VBA) for Excel. The main curves of the hull form are described with Cubic Rational Bézier curves. The hull form is divided in seven curves: three sections (fore, mid and aft), three longitudinal curves (sheer, chine and keel) and the bow. The definition of the geometric curves can be exported in ASCII and IGES format to a CAD software to create the hull surface. The software NX developed by Siemens is used by Guan et al. [55] to developed a parametric model to optimize a Unmanned Surface Vehicle (USV) in order to minimize wave resistance and seakeeping properties. The type of hull of the USV chosen was a Deep-Vee planning craft. The visual programming tool Grasshooper, a Rhinoceros plug-in used in this thesis, has already been used as a parametric modeller. In 2020 Pérez-Arribas and Calderon-Sanchez [56] developed a parametric methodology for Small Waterplane Area Twin Hull (SWATH). In the next year Romanelli [57] developed a parametric modeller for small crafts. This parametric modeller is capable of developing planning hulls and displacement hulls. Earlier this year Zhou et al. [58] created a software that uses parametric modelling process, that uses NURBS to define the hull geometry.

Chapter 3

Analysis of Hull Shapes

In this chapter, a study of the curves that define the shape of the ship is made in order to identify the important curves to define the shape of the hull. In this study curves are divided into two types: geometric curves that represent in a simplified way the shape of the hull, and property variation curves that control properties such as the area and angles of a section.

This analysis started by creating a database with various forms of hulls of merchant ships, being composed mostly of oil tankers, container ships, bulk carriers and ferries. The survey of the ships was made starting from lines plans and samples models from MaxSurf and Delftship.

The ship database is small because it is not possible to find lines plans as these are the intellectual property of those who create them. To try to counter this problem, photographs of real ships were also analysed to try to make the study cover as many hull shapes as possible.

3.1 Main Hull Particulars

The main hull particulars of the ship selected were the main dimensions and form coefficients. The main dimensions are length between perpendiculars (Lpp), width (B), draught (T) and depth (D). They depend on the type of ship, the work it will do and an important factor is its route, as there are canals, such as Panama or Suez, and ports that have limitations in terms of length, draft and breadth. The shape coefficients are the block coefficient (Cb), water plane coefficient (Cwp), prismatic coefficient (Cp) and midship coefficient (Cm). These dimensions and factors are usually selected following a set of basic factors, e.g. ship's hydrodynamic performance, stability, volume of cargo holds, etc.

Merchant ships can be classified based on their dimensions. Bulk carriers can be divided into six categories based on the Deadweight (DWT), such as: Coaster (1,000 - 10,000 DWT), Handysize (10,000 - 435,000 DWT), Handymax (35,000 - 50,000 DWT), Supramax (50,000 - 60,000 DWT), Panamax (60,000 - 80,000 DWT), Post-Panamax (80,000 - 125,000 DWT), Capesize (125,000 - 220,000 DWT) and Very Large Ore Carrier (VLOC) ($>$ 220,000 DWT). The dimensions of these bulk carriers ships can vary from 100.00 to 360.00 meters of length overall (LOA), 3.00 to 23.00 meters of draught and 20.00 to 65.00 meters of breadth.

Tankers can be divided into six categories such as: Handysize (20,000 - 30,000 DWT), Handymax ($\sim$45,000 DWT), Aframax (80,000 - 119,000 DWT), Suezmax (120,000 - 180,000 DWT), Very Large Crude Carrier (VLCC) (260,000 - 330,000 DWT) and Ultra Large Crude Carrier (ULCC) ($>$ 330,000 DWT). This results in a range of dimensions from 200.00 to 415.00 meters in LOA, 15.00 to 35.00 meters in draught and 29.00 to 63.00 meters in breadth.

The classification of container ships varies from that given for tankers and bulk carriers as the division is based on 20-foot equivalent units (TEU) rather than DWT. This type of ships can be divided in five sub-categories, such as: Feeder (300 - 3,000 TEU), Panamax (3,000 - 5,100 TEU), Post-Panamax (5,100 - 10,000 TEU), Very Large Container Carrier (VLCC) (10,000 - 20,000 TEU) and Ultra Large Container Carrier (ULCC) ($>$ 20,000 TEU). The main dimensions can vary from 100.00 to 400.00 meters in LOA, 7.00 to 17.00 meters in draught and 19.00 to 61.50 meters in breadth.

Ro-Ro ships can be divided by the type of cargo carried, such as people, cars and trucks. The subtypes of Ro-Ro ships can be: Ferries, Ro-Pax, Pure Car Carriers (PCC) and Pure Car and Truck Carriers (PCTC). Dimensions can vary between 50.00 to 220.00 meters of LOA, 1.50 to 6.80 meters of draught and 10.00 to 35.00 meters of breadth.

Table 3.1 shows a range of block coefficient values for the different types of ships studied. Container and Ro-RO ships have lower values, which is expected, as these types of ships tend to have a V-shaped section and tankers and bulk carriers often have U-shaped sections.

Table 3.1: Study of the block coefficient

	Bulk Carrier		Tanker		Container		Ro-Ro	
	Minimum	Maximum	Minimum	Maximum	Minimum	Maximum	Minimum	Maximum
Block Coefficient	0.740	0.848	0.757	0.843	0.507	0.709	0.494	0.613

3.2 Geometric Curves

By analysing the shape of the ship, it was possible to identify eight geometric curves that defined it. These curves are: bow and stern contour, midship section, flat of bottom (FOB), flat of side (FOS), transom, design waterline (DWL) and deck waterline.

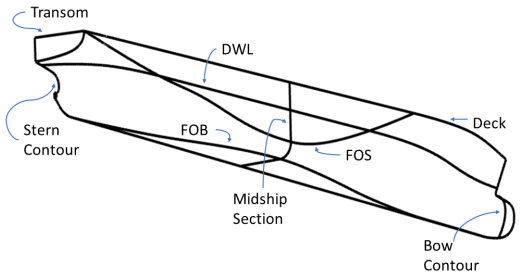

Figure 3.1: Geometric curves identified

All these geometric curves are the result of intersections between planes with the shape of the hull, for example the FOS is the curve that results from the intersection of an XZ plane located at the maximum beam point of the ship with the geometry of the hull. In lines plans the FOB and FOS curves represent the first waterline and the last buttock, respectively. Due to some models not showing a good definition of the mesh or the surfaces, the curve of the FOS and FOB was sometimes not possible to remove in its location. The solution used was to create the plane at a distance of one to three centimetres from its location.

3.2.1 Bow Contour

The bow is the first point of contact between the ship's hull and the water as the ship moves forward. Its main functions are to improve the manoeuvrability and hydrostatics of the ship, its main function being to reduce the resistance of the waves. The latter occurs mainly on merchant ships.

The bow geometry depends on the type of ship and its function. Within the scope of this thesis, 4 configurations were divided that encompass different designs, namely: bow without bulb, bulbous bow, X-bow and axe bow. The last two are bow designs that have started to be implemented in recent years. The 4 configurations will be analysed individually next.

The axe-bow was developed by the Damen together with Delft University, at the beginning of the 21st century. This type of bow is based on lowering the keel as we approach the front of the ship with a vertical stem. They have the advantage of reducing pitch motion due to their ease in passing through the waves due to the small angles of entry of the water lines. This approach to bow design was not taken into account in the model as it is not often used on merchant ships.

Another recent design is X-bow, was developed by the Ulstein group, having presented it in 2005. This type of bow has as main advantage the comfort during the voyage. This is achieved due to the increase fore ship volume comparing to the conventional bow designs, this leads to a reduction of pitch movements and slamming in rough seas, and in calm waters can split the waves causing a more evenly forces distribution over the hull surface which creates a wave piercing effect. In figure below it is possible to see this type of bow applied to a ship.

The traditional way of designing the bow is by dividing it in two, the part below and above the water. This creates the first two types of bow referred to (bow without bulb, bulbous bow). A bow without bulb configuration is often used for smaller ships where the advantages of the bulb are not taken advantage of, such as fisher vessels, etc. There are several types of bulb less bow configurations such as: parabolic, plumb, raked, spoon and clipper. To define a bow without bulb five parameters are needed, the distance between the forward perpendicular and the first and last point (X_fp and X_Deck), the vertical coordinate of the point located at the forward perpendicular (Z_fp) and two angles (α_{deck_ent}, α_{deck_run}). The parameter Z_fp has been normalized by dividing it by the draught, this creates a coefficient called $C_{Z/T}$.

Table 3.2: Parameters Study of bow without bulb

Parameter	Bulk Carrier		Tanker		Container		Ro-Ro	
	Minimum	Maximum	Minimum	Maximum	Minimum	Maximum	Minimum	Maximum
X_fp [m]	4.73	7.42	1.46	1.95	[-]	[-]	7.32	7.54
X_Deck [m]	1.80	7.80	0.12	1.94	[-]	[-]	2.77	3.10
$C_{Z/T}$	1.00	1.00	0.53	1.00	[-]	[-]	1.00	1.00
α_{deck_ent} [°]	66.00	74.60	70.00	90.00	[-]	[-]	57.00	67.00
α_{deck_run} [°]	50.60	59.07	59.42	70.00	[-]	[-]	57.00	67.06

In the table 3.2 are the results of the analysis. From the coefficient C_zp, it was possible to see that when there is no bulb, the contour point on the forward perpendicular is most often the end point of the DWL. The coefficient was not equal to one on two tankers, as the bow outline had a straight stem. From the angles studied were identified three different types of bows: two spoon type, three rake type and two parabolic type. In the column referring to container ship there are no values as all ships of this type collected had a bow with a bulb.

Nowadays, most merchant ships have a bulbous bow due to several benefits such as reducing the ship's and wave resistance, consequently they also have an impact in the ship's economy because less power is needed to make the ship move at a certain speed. Bulbs can be divided into two types, depending on their shape: integrated or added bulbs. The main difference between one type and the other is that the design of the first is made in conjunction with the hull geometry which eliminates the presence of knuckles in the hull shape.

There have already been several studies analysing the shape of the bow bulb, the best known of which is the study presented by Kratch, [59]. The result of this study allowed him to define the bulb with 6 non-dimensional parameters (3 linear and 3 non-linear) and distinguish the bulb section in 3 different types. Figure 3.2 shows the three types of bulb sections, the figure 3.3 and table 3.3 shows the non-dimensional parameters.

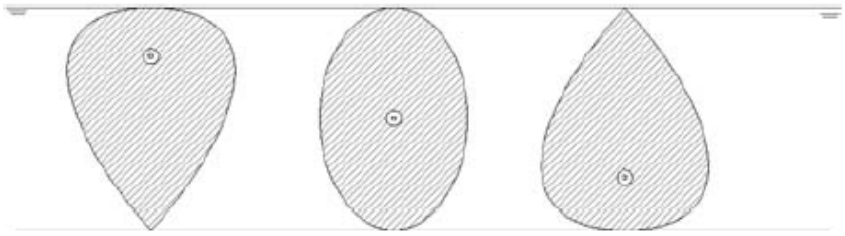

Figure 3.2: Section types: ∇ type, O type and Δ type (circles represent the centre of gravity of the traverse section) [15]

Table 3.3: Kracht parameters to define bulb

Breadth Parameter	$C_{BB} = B_b/B_{wl}$	Cross-section Parameter	$C_{ABT} = A_{BT}/A_{MS}$
Length Parameter	$C_{LPR} = L_{pr}/L_{pp}$	Lateral Parameter	$C_{ABL} = A_{BL}/A_{MS}$
Height Parameter	$C_{ZB} = Z_b/T_{FP}$	Volume Parameter	$C_{VPR} = \nabla_{PR}/\nabla$

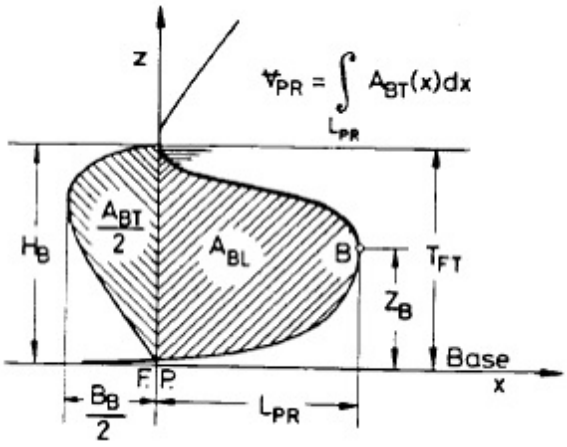

Figure 3.3: Linear and non-linear bulb parameters [59]

To define a bulbous bow you need the parameters used to define a bow without bulb plus the parameters to define the bulb. In order to properly create the shape of a bulb it was necessary to study the cross section in the forward perpendicular and a longitudinal curve starting from the forward perpendicular. The cross section of the bulb is defined by the maximum breadth point defined by two parameters (B_Bulb, Z_CG), the entrance and run angles (α_Bulb_t_l, α_Bulb_t_u) and the cross section area. The cross-section parameter of Kracht (C_ABT) was used to define the cross section area. In order to create the longitudinal contour it was necessary seven parameters. Two parameters was used to define the tip of the bulb (X_TipBulb and Z_TipBulb). The lateral parameter of Kracht (C_ABL) was used to define the longitudinal area. Also to define the first and last point it is important to have a parameter responsible for the bulb height (H_Bulb), and the height of the first point (Z_fp). The tangent angles at initial and end point of the contour are also important (α_{fp}, α_BulbUpper). It is important to note that the start and end points of the longitudinal curve are the same in the cross-section curve.

Table 3.4: Parameters Study of bow with bulb - Transversal Section

Parameter	Bulk Carrier		Tanker		Container		Ro-Ro	
	Minimum	Maximum	Minimum	Maximum	Minimum	Maximum	Minimum	Maximum
B_bulb [m]	1.33	4.30	4.18	6.99	1.07	3.67	1.53	2.31
C_{BB} [-]	0.106	0.267	0.151	0.234	0.121	0.166	0.111	0.186
Z_CG [m]	2.15	6.22	3.43	11.05	2.81	8.86	1.50	3.90
H_Bulb [m]	5.71	16.14	11.02	19.71	3.53	12.69	5.80	8.90
α_Bulb_t_l [°]	0.00	3.74	0.00	17.50	0.00	63.34	0.00	1.30
α_Bulb_t_u [°]	9.39	90.00	6.00	70.00	0.00	90.00	18.26	90.00
C_ABT [-]	0.094	0.174	0.051	0.144	0.038	0.099	0.071	0.086

After analysing the information presented in table 3.4 and 3.5, it was possible to verify that with the presence of the bulb, the first point of intersection between the forward perpendicular and the bow contour is not the last point of the DWL. This is proven by the $C_{Z/T}$ parameter being less than one. Container ships had a thinner bulb, as they have higher values for the X_TipBulb parameter and lower values for the B_Bulb parameter. In contrast, bulk carriers presented a fatter bulb.

Table 3.5: Parameters Study of bow with bulb - Longitudinal Contour

Parameter	Bulk Carrier		Tanker		Container		Ro-Ro	
	Minimum	Maximum	Minimum	Maximum	Minimum	Maximum	Minimum	Maximum
X_fp [m]	0.38	5.98	0.00	7.07	2.41	20.94	0.07	4.60
$C_{Z/T}$ [-]	0.03	0.09	0.00	0.05	0.04	0.18	0.00	0.04
X_TipBulb [m]	1.13	5.97	3.99	8.33	1.84	10.86	1.19	5.31
C_{LPR} [-]	0.007	0.021	0.019	0.026	0.007	0.041	0.011	0.027
Z_TipBulb [m]	2.14	7.55	2.64	10.50	2.97	10.90	1.50	4.00
C_{ZB} [-]	0.372	0.548	0.205	0.505	0.546	0.752	0.300	0.517
α_fp [°]	13.98	31.37	0.00	18.09	9.54	22.64	15.71	21.18
α_BulbUpper [°]	83.32	90.00	77.22	90.00	10.00	74.87	62.78	90.00
C_ABL [-]	0.076	0.169	0.105	0.165	0.094	0.296	0.080	0.191

3.2.2 Stern Contour

The stern of the ship is the most aft part of the ship. The stern design as well as the bow design can be divided into 2, the above water part, in which its shape is related to the back of the deck, and the underwater part which aims to present a system efficient propulsion. There are three basic types of sterns, namely: elliptical stern, cruiser stern and transom stern. The first two types are older designs, and as most merchant ships use stern stern, only this one has been carefully studied.

For the underwater part, there are aspects that have a strong influence on the shape of the stern, such as the configuration of the propulsion system, whether a ship with a single-propeller or twin-propeller configuration, and the presence or not of a stern bulb. Depending on the choices made, the stern may have a more complex shape, which leads to the need for more parameters to define it. Due to the lack of 3D models or line plans of ships with a double propeller configuration, it was not possible to study the shape of the stern in this situation, because of this it was not implemented in the model described in chapter 4. The two types of stern stern studied are represented in the figure 3.4.

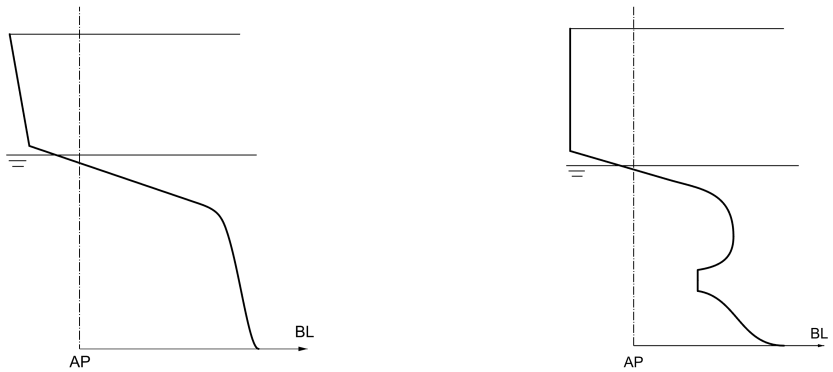

(a) Stern without bulb (b) Stern with bulb

Figure 3.4: Types of transom sterns

The stern contour starts at the same longitudinal position as the transom with a straight segment, which can present an angle of zero degree with the z axis (figure 3.4(b)) or a slight variation of angle (figure 3.4(a)), which can be positive or negative. This segment is equal in length to the transom height, described by the H_Transom parameter. The angle it makes with the z axis is related by the α_Transom_up parameter. Another important angle is the angle of the longitudinal contour with the lower

point of the straight segment, it is defined by the parameter α_Transom_bottom. The end point of the stern contour is given by the parameter X_SternEnd. For a better understanding of the parameter in the study, a coefficient ($C_{SternEnd}$) was created that divides the parameter X_SternEnd by the length between perpendiculars. With these parameters it is possible to create a stern contour without a bulb.

Table 3.6: Parameters Study of stern without bulb

Parameter	Bulk Carrier		Tanker		Container		Ro-Ro	
	Minimum	Maximum	Minimum	Maximum	Minimum	Maximum	Minimum	Maximum
$C_{SternEnd}$ [-]	[-]	[-]	0.02	0.05	0.00	0.26	0.04	0.25
α_Transom_d [°]	[-]	[-]	0.00	20.80	0.00	11.40	-4.68	19.00
α_Transom_b [°]	[-]	[-]	18.00	18.78	10.00	14.50	8.20	17.15

The $C_{SternEnd}$ coefficient have higher values for containers and Ro-Ro ships which results in a stern contour closer to a straight line with its last point furthest from the aft perpendicular than the stern contour presented in tankers. Some of the ships did not have a straight transom panel, this can be seen by the parameter α_Transom_d being different from zero. Most of them inclined towards the aft of the ship ($\alpha\_Transom\_d > 0$). This is not the case on a Ro-Ro ship, since it has a value inferior to zero in α_Transom_d parameter. In the column referring to bulk carriers there are no values as all ships of this type collected had a stern bulb.

When there is an stern bulb, the parameters used to define a bulb less stern are not sufficient. It was necessary to have information about the x and z coordinates of the propeller boss (X_Boss, Z_Boss) and for the propeller clearance (X_Clearance and Z_Clearance) and the radius of the boss (R_Boss), sometimes It was not possible to find this value because the propeller boss was represented only by a point.

Table 3.7: Parameters Study of stern bulb

Parameter	Bulk Carrier		Tanker		Container		Ro-Ro	
	Minimum	Maximum	Minimum	Maximum	Minimum	Maximum	Minimum	Maximum
X_Boss [m]	1.50	5.06	2.30	7.27	2.11	8.75	6.34	6.67
Z_Boss [m]	1.75	5.20	1.75	5.80	1.25	4.55	3.00	8.75
X_Clearance [m]	2.94	7.88	3.15	10.42	2.60	15.28	7.17	9.42
Z_Clearance [m]	2.94	8.61	2.94	10.75	2.50	8.85	3.04	6.41
R_Boss [m]	0.25	0.55	0.25	0.80	0.74	1.10	[-]	[-]
$C_{FOB\ Beg.}$ [-]	0.04	0.23	0.04	0.06	0.05	0.11	0.06	0.13
α_Transom_d [°]	0.00	18.48	0.00	14.50	0.00	10.00	0.00	0.00
α_Transom_b [°]	7.13	25.00	7.00	27.20	5.40	13.65	5.80	6.78

The longitudinal position of the shaft boss is always ahead of the perpendicular as the X_Boss parameter values are always positive and as it should be, with the clearance position being forward of the axis position of the boss. The end point of the stern contour is generally closer to the aft perpendicular than the stern contour without a bulb because it presents inferior values for the $C_{FOB\ Beg.}$ coefficient. This is not only verified on a bulk carrier. The Ro-Ro ships only had vertical transoms, and the other types of ships had a slightly lower maximum inclination (α_Transom_d) value compared to the values shown in the table 3.6.

3.2.3 Flat of Side

The FOS curve is the buttock at the maximum breadth. Depending on the type of ship it can begin at the transom, this is more visible in ships that need to have a bigger deck area for cargo like containers or Ro-Ro ships, or can begin closer to the end of the aft body, this was notice to happen more on bulk carriers and tankers.

To create the FOS it is necessary to create parameters to define the waypoints of the curve. The starting point can be located on the transom curve or on the deck, for this two parameters were created to define this point, one for its longitudinal position (X_FOS) and another for its vertical position (H_Aft_FoS). The last point is related to the deck waterline curve and is defined with a parameter that defines the length of the straight part of the deck waterline curve (L_FOS). To facilitate the understanding of these parameters, three coefficients were created: C_{AftFOS}, C_{FwdFOS} which relates the longitudinal position of the first and last FOS point with the Lpp and C_{HFOS} which relates the height of the first FOS point with the depth of the ship. To create the aft and forward curve it was necessary to find the two points that result from the intersection of the DWL and FOS. Two coefficients were created that relate the distance between the intersection points and the initial point of each segment (f_Aft, f_Fwd). The middle part of the FOS is a line with the length of the cylindrical mid body, if there isn't one this line disappears. As usual, just waypoints do not provide enough information to create a curve with the desired characteristics, so parameters were created that control the angle at the start and end point of the FOS and at the intersection points (α_Aft_FoS, α_Fwd_FoS, α_Aft_wtl_FoS, α_Fwd_wtl_FoS).

Table 3.8: Parameters Study of FOS

Parameter	Bulk Carrier		Tanker		Container		Ro-Ro	
	Minimum	Maximum	Minimum	Maximum	Minimum	Maximum	Minimum	Maximum
C_AftFOS [-]	0.166	0.295	0.098	0.241	-0.041	0.050	-0.048	0.231
C_{FwdFOS} [-]	0.653	0.818	0.770	0.839	0.740	0.867	0.832	0.862
C_{HFOS} [-]	1.00	1.00	1.00	1.00	0.73	1.00	0.67	1.00
f_Aft [-]	0.084	0.450	0.000	0.397	0.384	0.495	0.422	0.678
f_Fwd [-]	0.297	0.864	0.823	0.970	0.182	0.650	0.366	0.459
α_Aft_FoS [°]	20.00	90.00	25.24	90.00	0.00	20.34	5.91	80.73
α_Fwd_FoS [°]	16.30	74.50	24.21	90.00	2.33	17.30	9.78	48.74
α_Aft_wtl_FoS [°]	17.48	83.10	30.00	90.00	6.62	14.75	7.90	17.00
α_Fwd_wtl_FoS [°]	40.16	90.00	62.40	90.00	15.63	55.00	14.64	35.82

Some containers and Ro-Ro ships showed negative values for C_AftFOS which indicates that the FOS must start on the transom, this can be confirmed by the CHFOS parameter as the minimum value in both cases is less than one. On tankers and bulk carriers this is no longer the case, with the starting point closer to the end of the stern body.

The factor f_aft indicates that the first point of intersection between the FOS and the DWL usually occurs before the centre part of the aft segment of the FOS. This hasn't been verified just once on a Ro-Ro. Tankers and bulk carriers had the lowest minimum values, which means that they have higher entrance angles reaching 90 °. The longitudinal position of the second intersection point in Ro-Ro and containers continues to usually be behind the mid point of the forward segment. This didn't verify in the tankers and bulk carriers as the facto f_fwd is usually larger than 0.5, only in one bulk carrier it was lower.

3.2.4 Midship Section

The midship section is the section with the maximum breadth, it was considered to be at the end of the aft body and if there is the presence of a cylindrical mid body it also represents its beginning, with most merchant ships having a similar midship section. An important parameter to study was its location longitudinally, for this the parameter X_MidshipSection was created. For a better understanding of this parameter a coefficient was created that divides it by the Lpp. The coefficient was called $C_{MS/LPP}$.

After studying the shapes presented in the 3D models and drawings gathered, it was possible to verify that most of them have similar shapes. Its shape is represented by a line whose end coincides with the maximum width of the FOB, followed by a curve known as bilge, and finally by another line that coincides with the FOS. The parameters identified as necessary to create the shape described above are: bilge height and width, midship coefficient, breadth and depth. Other parameters that are important to define different shapes of the midship section are deadrise and tumblehome. Any of these parameters are not common in merchant ships, as they aim to maximize the volume of cargo. In the studied hull shapes, only one presented deadrise and none presented tumblehome.

The midship coefficient is the ratio between the submerged area of the midship section and a rectangle with the dimensions of draught per breadth. In figure 3.5 it is possible to see this relationship. In the equation 3.1 shows how the midship coefficient is calculated. Where A_{MS} is the area of the midship section below water, B and T are the breadth and draught of the ship, respectively.

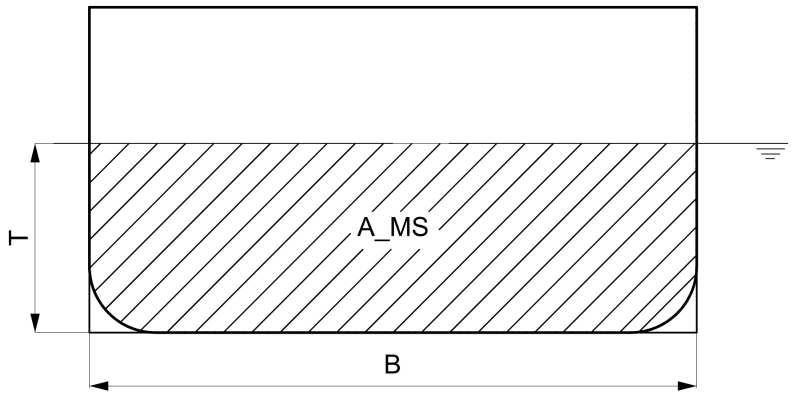

Figure 3.5: Relation between midship section with rectangle ($B * T$)

$$C_m = \frac{A_{MS}}{B * T} \tag{3.1}$$

Two different bilge shapes were identified as possible, namely: circular or elliptical. When it is a circular shape the bilge has the same height and width, and when the shape is elliptical this is not the case. By studying the results of table 3.9, it was possible to verify that the ships with the highest value for the midship coefficient had a circular bilge with the bulk carrier and the tankers were the ships where

this occurred more frequently. This was to be expected, as they feature U-shaped sections and aim to maximize cargo space. Ro-Ro ships and container ships usually have an elliptical hold with a width greater than the height.

Table 3.9: Parameters Study of Midship Section

Parameter	Bulk Carrier		Tanker		Container		Ro-Ro	
	Minimum	Maximum	Minimum	Maximum	Minimum	Maximum	Minimum	Maximum
$C_{MS/LPP}$ [-]	0.315	0.585	0.411	0.436	0.437	0.476	0.44	0.479
Bilge Height [m]	1.80	3.26	2.40	4.38	2.26	7.12	4.38	6.20
Bilge Width [m]	1.80	5.35	2.40	6.10	2.68	12.35	3.62	8.46
Midship Coefficient [-]	0.979	0.998	0.979	0.996	0.964	0.997	0.824	0.963

3.2.5 Transom

Transom is the aft most cross section of the ship's hull. It can take different forms but were generalized in three: U, normal or V shape. Since the V shape creates a knuckle and the implemented model only allows creating a knuckle in addition bulbs, this shape has not been studied. In the figure 3.6 the two forms studied are represented. The main difference is the number of curves required for its construction. This is further developed in chapter 4.

The transom is related to the stern curve as they share the start at the same longitudinal position and the length of the first line of the stern contour is equal to the height of the transom. The deck waterline curve is also related with the transom as its top contour is the first line of the deck waterline. To have a better understanding of the transom it was created a coefficient that relates the breadth of the transom with the breadth of the ship, $C_{Breadth}$. A study was also made about the entrance and run angle of the transom panel (α_Transom_bot, α_Transom_up) and the height of the transom (H_Transom).

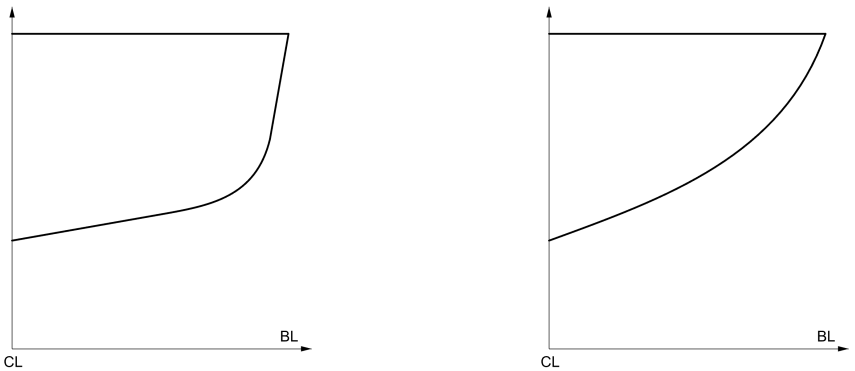

(a) U Shape (b) Normal Shape

Figure 3.6: Types of Transom shapes

Table 3.10: Parameters Study of transom panel

Parameter	Bulk Carrier		Tanker		Container		Ro-Ro	
	Minimum	Maximum	Minimum	Maximum	Minimum	Maximum	Minimum	Maximum
X_Transom [m]	-5.41	-1.07	-7.00	0.00	-7.40	-3.67	-7.80	0.00
H_Transom [m]	2.80	9.65	9.20	23.00	5.90	14.85	5.00	13.75
$C_{Breadth}$ [-]	0.37	0.85	0.20	0.63	0.99	1.00	0.80	1.00
α_Transom_bot [$^\circ$]	0.00	24.28	6.50	52.24	0.00	6.68	8.90	15.40
α_Transom_up [$^\circ$]	58.70	90.00	70.75	90.00	84.33	90.00	90.00	90.00

The X_Transom parameter shows that the transom starts at or behind the aft perpendicular, as it presents negative values or it is equal to zero. As expected, the $C_{Breadth}$ coefficient in containers and Ro-Ro ships has the highest values, because these types of ships use the aft body as cargo space. On the other hand, tankers and bulk carriers have most of the cargo holds in the parallel mid body.

3.2.6 Flat of Bottom

The FOB coincides with the lowest waterline (z=0). This curve is composed of two curves, one at the aft body and one at the fore body, and one or two linear segments, one is the line that connects the start point to the end of the FOB and if there is a cylindrical body there is another line. Usually, the start and end point coincide with the end point of the stern contour and the start point of the bow contour, respectively. As identified in the subchapter 3.2.4 the maximum breadth point of the FOB coincides with the initial point of the bilge. To build the FOB curve, it is needed more information than just the curve crossing points. With this in mind, two more parameters were created: the entry angle (α_aft_FoB) and the exit angle (α_fwd_FoB).

Table 3.11: Parameters Study of FOB

Parameter	Bulk Carrier		Tanker		Container		Ro-Ro	
	Minimum	Maximum	Minimum	Maximum	Minimum	Maximum	Minimum	Maximum
α_aft_FoB	0.00	90.00	3.66	43.15	0.00	14.56	11.36	77.90
α_fwd_FoB	9.80	90.00	2.50	86.56	0.00	12.87	5.00	90.00

These angles were difficult to measure, as some models did not have a good quality mesh closer to the longitudinal contour. With that in mind, the main conclusions were that the entrance angle in smaller FOBs presented an angle of 90 $^\circ$ and with larger FOBs presented smaller angles. The run angle showed lower values as only one tanker had the angle of 90 $^\circ$.

3.2.7 Design Waterline

The design waterline is an important curve since it has influence in ship's hydrostatics, and the area of design waterline is directly proportional to waterline coefficient, C_{WP}. It relates the area of a plane at draught with a area of a circumscribing rectangle with one of the sides equal to length and the other with breadth (figure 3.7). The equation to compute the waterline coefficient is present below. Where A_{WP} is the area, L_{wl} is the length of DWL and B is the breadth of the ship.

$$C_{WP} = \frac{A_{WP}}{L_{wl} * B} \tag{3.2}$$

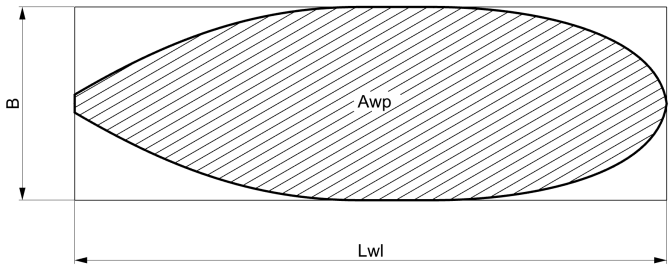

Figure 3.7: Relation between design waterline with rectangle ($L * B$)

This geometric curve is composed by three different parts: aft part, mid part and forward part. The aft part can be defined by one NURBS curve or one line and one NURBS curve, the second option happen when there is an intersection with the transom panel. A parameter was created to define the longitudinal position of the first point of the stern curve called X_DWL, with its end point being the first point of intersection between FOS and DWL. The mid part is related with the parallel mid body because this line is the connection between the two points related with the intersection between the DWL and FOS. The forward part is defined by a NURBS curve starting at the end point of the middle part and ending at the forward perpendicular. To complete the definition of the DWL curve, it was necessary to create two more parameters related to the entrance and run angle. These angles were called α_Aft_DWL and α_Fwd_DWL, respectively. For a better understanding of the X_DWL parameter, a coefficient was created that divides it by the Lpp. The coefficient was called C_{DWL}.

Table 3.12: Parameters Study of DWL

Parameter	Bulk Carrier		Tanker		Container		Ro-Ro	
	Minimum	Maximum	Minimum	Maximum	Minimum	Maximum	Minimum	Maximum
C_{DWL} [-]	-0.032	0.013	-0.021	0.205	-0.041	0.005	-0.048	0.231
C_{WP} [-]	0.783	0.945	0.839	0.896	0.761	0.853	0.741	0.773
α_Aft_DWL [$^\circ$]	21.85	63.42	29.67	33.16	40.37	84.32	23.28	44.80
α_Fwd_DWL [$^\circ$]	3.00	90.00	86.11	90.00	4.00	90.00	38.32	90.00

As expected, the coefficient C_{DWL} presents negative and positive values because the DWL can either start behind the aft perpendicular or when the DWL intersects the transom, or it can start forward of it. The entrance angle is usually lower than the run angle, with the run angle being equal to 90 $^\circ$ mainly in ships with a high block coefficient and without bulb.

3.2.8 Deck Waterline

The deck waterline curve in most models is a 2D curve but in reality this is not the case because transversally it presents camber and longitudinally it presents sheer. These two parameters can be seen in the figure 3.8. Camber is the elevation of the deck on the centreline compared to the sides with

the advantage of allowing water entering the deck to drain. These two parameters were not studied or implemented due to not being possible to verify if the implementation would be correct or not, therefore the deck curve was analysed without its influence.

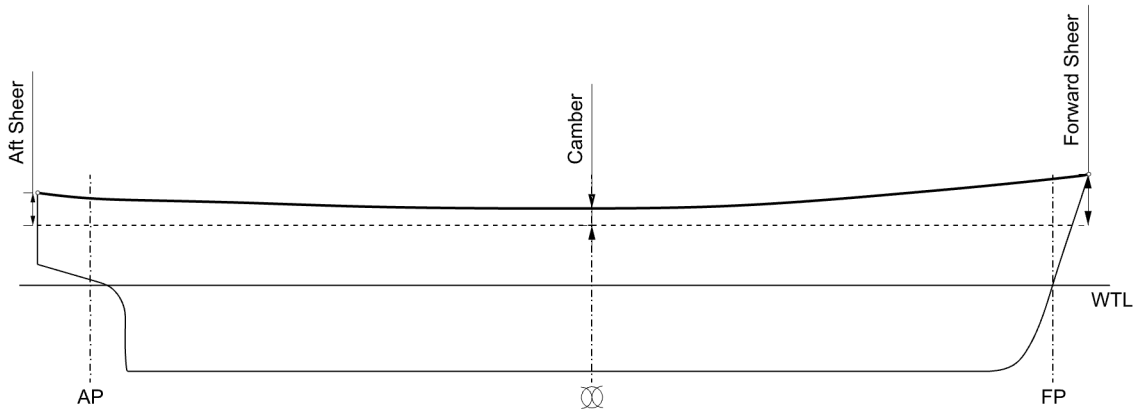

Figure 3.8: Deck with sheer and camber

The deck waterline curve can be divided into three segments, the aft, middle and forward curve. The aft curve can sometimes blend in with the middle part as it is related to the transom, and in cases where the transom width is equal to the ship's breadth, the aft curve becomes a line. If this is not the case, it is important to study the range of values for the entrance angle of the aft curve, for that a parameter called α_Deck_aft was created. The mid curve of the deck waterline is always a line in direct relation to the FOS curve. The parameter Lc is responsible for defining the length of the line. The forward curve is created between the furthest point of the FOS and the end point of the deck waterline that coincides with the highest point of the bow contour. As for certain types of ships the deck waterline area is an important parameter, a coefficient was created to analyse the relationship between the area occupied by this curve and a rectangle circumscribed with the dimensions of the length and breadth of the ship. The coefficient was called C_{Deck_Area}.

Table 3.13: Parameters Study of Deck Waterline

Parameter	Bulk Carrier		Tanker		Container		Ro-Ro	
	Minimum	Maximum	Minimum	Maximum	Minimum	Maximum	Minimum	Maximum
C_{Deck_Area}	0.908	0.966	0.911	0.956	0.919	0.968	0.920	0.964
α_Deck_aft	10.27	25.09	17.54	30.13	0.00	15.43	0.00	4.90

As expected, the entry angles for containers and Ro-Ro ships presented smaller values, since normally the transom width is equal to or very close to the width of the ship. This is confirmed by the $C_{Breadth}$ coefficient presented earlier. The range of values for the C_{Deck} coefficient is the same for all ship types. Containers and Ro-Ro ships had greater area in the aft body than in the forward body, unlike tankers and bulk carriers.

3.3 Property Variation Curves

The property variation curves described the variation of the geometric properties along the ship, either longitudinally or vertically. Three property variation curves were identified and studied, namely: sectional area curve (SAC), angles variation of sections and waterlines. The collection of numerical data on these curves sometimes proved to be complicated, once again due to the lack of precision in certain areas of the models found, the curves generated by the surface or mesh presented strange shapes along the longitudinal contour.

3.3.1 Sectional Area Curve

The SAC determines the distribution of displacement along the ship, given that the area below the SAC is equal to the displacement. Another property of the ship that it is possible to study at SAC is the longitudinal centre of buoyancy (LCB). In table 3.14 it is presented the values for the LCB.

Table 3.14: Study of the LCB

	Bulk Carrier		Tanker		Container		Ro-Ro	
	Minimum	Maximum	Minimum	Maximum	Minimum	Maximum	Minimum	Maximum
LCB [m Fwd Lpp/2]	0.33	7.03	3.52	7.47	-6.28	-0.09	-1.33	0.11
LCB [% Lpp Fwd Lpp/2]	0.44	5.02	2.25	4.52	-3.94	-0.21	-2.46	0.26

As can be seen in table 3.14 the LCB on container ships and Ro-Ro ships are located aft of midships, this is justified once again by the need that this type of ships have to have cargo space aft of the ship. This was not just the case on a Ro-Ro ship. On the other hand, bulk carriers and tankers do not have this need, which causes their LCB to be moved forward amidships.

To define a SAC it is necessary to know some important characteristics of the ship such as if it has a bulbous bow or not and if the DWL crosses the transom, as these two influence the initial and final points of the SAC. If the ship has a bulbous bow, the last point, instead of ending in the forward perpendicular, ends in the longitudinal position of the tip of the bulb and the area instead of being zero in the fore perpendicular becomes equal to the area of the transversal section of the bulb. In addition to this information, it is also necessary to know the longitudinal location and area of certain sections. In this analysis, the sections identified for which the areas were needed are the midship section, the section at the aft perpendicular, the submerged area of the transom and the cross section of the bulb. The last two can be zero. The longitudinal position of the sections that are required are from the transom, midship section, tip of the bulb and if there is the presence of the a cylindrical body the position of its final point is also needed.

3.3.2 Longitudinal Variation of Section Angles

This curve shows how the section angles evolve longitudinally, the angles are measured at 3 points: at the section exit, at the DWL and on deck. These three angles are shown in figure 3.9.

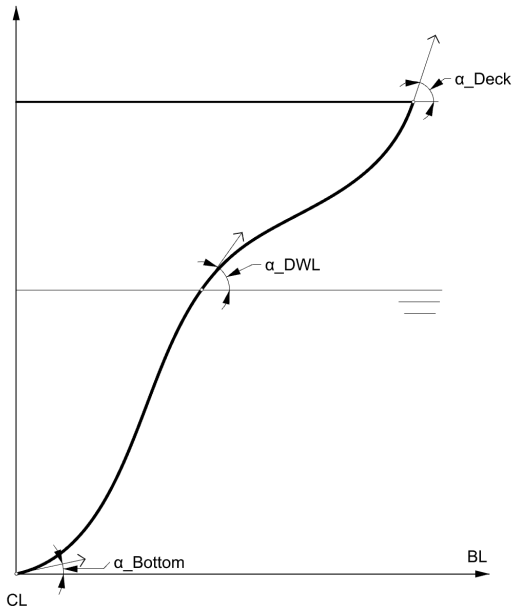

Figure 3.9: Angles of sections

To understand how the angles vary at these 3 points, an analysis was made of the available, these shapes were divided by ship type (container ships, Ro-Ro, tankers and bulk carriers). The angles were surveyed by dividing the ship into 4 parts: transom to clearance, from clearance to the forward perpendicular, stern bulb and bulbous bow, the last two may not be present in some ships. After this division are created planes with one meter spacing between them, which will be intersected with the ship's mesh and thus obtain the section curve.

The section curves are divided in two parts, with the division taking place at the height of the ship's draft (z=T). With this division, the curves are then parametrized, where in the first part of the section curve t=0 is the start of the section and t=1 is the section point on the DWL, and in the second part of the section curve t=0 is equal to t=1 of the first part of the curve and t=1 is the point on the deck waterline. With this parametrization done it is possible to calculate the derivative at the desired points and with this obtain the tangent at the 3 desired points. To measure the angle, is created a horizontal vector (0,1,0) and a vector with the tangent direction, both vectors have the same initial point. To assist this study was created two scripts in Grasshopper, where the process described above was automated, which allowed the reduction of the time required for the measurement of the angles of each ship.

In this study it was also assumed that sections intersecting the FOB exit the FOB with an exit angle of 0 degrees and those intersecting the FoS enter the FoS with an angle of 90 degrees.

It was made an attempt to create a relation between the variation of the angles and the type of ship but this prove to be not doable as the linear regression used almost always present a low value for the coefficient of determination (R^2) which indicated a high dispersion of the results.

The bottom angle in the region the transom to the clearance increases from the transom to the forward of the ship, in ships without bulb and with the an end point of the stern contour with a higher coefficient $C_{FOBBeg.}$ the variation it is slower. From the clearance to the beginning of the flat of bottom the angle decreases until it reaches 0 degrees. The opposite occurs from the ending of the FOB to the forward perpendicular. In ships with V shaped sections the angles are bigger than in the ships with U shaped sections.

The angle in draft height (α_DWL) from transom to start of FOS increases with tankers and bulk carriers usually showing higher values closer to the transom than the values showed in the cases of Ro-Ro and containers. Between the end of the FOS and the forward perpendicular decreases in tankers and bulker carriers but in Ro-Ro and container ships the decrease also verifies but closer to the forward perpendicular it begins to increase an can sometimes be higher than 90 $^\circ$.

The deck waterline angle (α_Deck) in the transom region for ships with a FOS that starts at the transom the angle is always 90 degrees. This is very common on container ships and Ro-Ro ships. In tankers and bulk carriers the angle increases towards the beginning of the FOS with the tankers presenting the lower values, around 70 $^\circ$, closer to transom. From the ending of the FOS to the tip of the deck waterline the angle decreases in all of the ships.

3.3.3 Vertical Variation of Waterline Angles

To study the variation of the angles of waterlines with vertically evolution, two angles were selected: entrance angle of the aft part, and the run angle of the forward part. To find these angles it was necessary to create an XY plane to intersect with the mesh of the 3d models of the ship, to obtain the curves of the waterlines. These intersections were made with a distance of 1 meter for each plane. With the curves found, they were divided into three or four parts depending on whether they intersect the transom or not. The two parts studied were the segments that are before (aft part) and after (forward part) the FOS. These segments were then parametrized with the entrance angle of the aft part measured at t=0, and the run angle of the forward part measured at t=1.

The entrance angle of the aft curve shows an increase from the FOB to the beginning of the stern bulb, during the stern bulb it is equal to or very similar to zero $^\circ$. When the stern bulb ends to the bottom point of the transom the angle increases. After this point is reached the angle begins to decrease as the height of the waterline gets closer to the ship depth.

The forward run angle on ships without a bulb increases from FOB to deck waterline or is constant. This happens more regularly on tankers. For ships with a bulb the angle increases from the FOB to the vertical coordinate of the tip of the bulb, then starts to decrease towards the beginning of the stem. If the bow presents a stem with a straight segment the angle is kept constant and when it ends the angle begins to increase.

3.4 Wireframe Model

A wireframe of a ship is made up of: sections, waterlines and buttocks. These curves result from the intersection of the YZ, XY and XZ planes, respectively, with the geometric curves that define the basic shape of the ship.

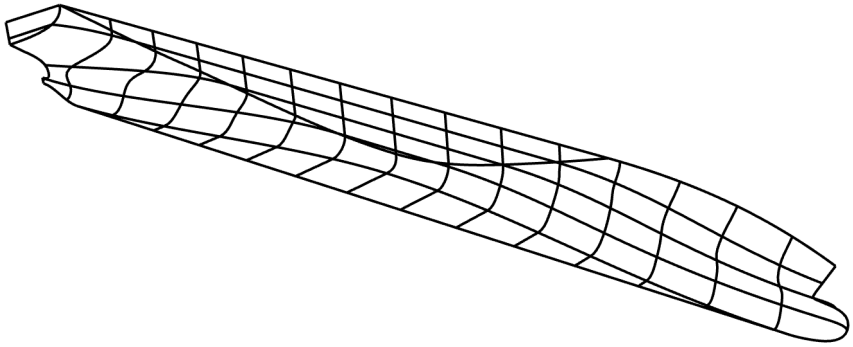

Figure 3.10: Example of a ship wireframe model

From the three curves presented in the wireframe model the buttocks are the least important, as they have no real importance in the hydrodynamics or other properties of the ship, with the buttocks being the most important FOS and longitudinal contour.

The sections of a ship can have different shapes. The most common shapes in merchant ships are the U or V-shaped sections. The U-shaped sections are more present in ships with large Cb, have a large cylindrical medium body and transport their cargo in this region. It is usually present on tankers and bulk carriers. V-shape is mostly used on Ro-Ro ships and container carriers as cargo is transported on the deck waterline and presented a lower Cb.

The form of the waterlines have influence in hydrodynamic, stability and sea keeping characteristics of the ship. Regarding the hydrodynamic aspect the entrance and run angles have an important role. Normally the ships with low Cb presented the lower values of entrance, this was verified in the studied about the waterlines. In the study this angle is refereed as the run angle of the forward part. Normally the aft and forward curves enter and exit of waterlines, respectively, with tangency at the intersection points between DWL and FOS but there is some cases where the tangency doesn't happen. The need of reduction the area under the waterlines curves can be one reason to withdrawn the tangency.

Chapter 4

Implementation

The parametric hull generation method is implemented in Grasshopper a visual programming tool available as a plug-in of Rhinoceros 3D CAD software. Visual programming has several advantages such as little abstract thinking and command automation (eg split a line into 1,000 parts). In addition, it is capable of modifying the input parameters, making it possible to check their effect almost instantly.

The first step of the implemented method is the input of parameters that define the shape of the hull. Parameters can be divided into two types: global or local. Global parameters provide information that defines the overall shape of the ship, e.g. length between perpendiculars, draught, form coefficients, etc. Local parameters define specific characteristics of a ship part like the bulb, transom, etc. It can have positional and differential properties, as one local parameter can provide a length or a height, but another can provide information about a tangent at a specific point on a curve. With the information gathered from the parameters, the curve points and boundary constrains are defined. The number of points depends on the complexity of the hull shape. The curves used are NURBS curves. The definition of these curves is done by providing the information of the start and end point and the entry and exit angles of the curve. The curves created were divided into two types: geometric curves and property variation curves. With the curves defined, it is possible to create a wireframe model that respects the initial conditions, with the possibility of making some changes to the parameters. In figure 4.1 it is described the flowchart of the parametric procedure. In Appendix A are shown parts of the Grasshopper visual code used in the parametric procedure.

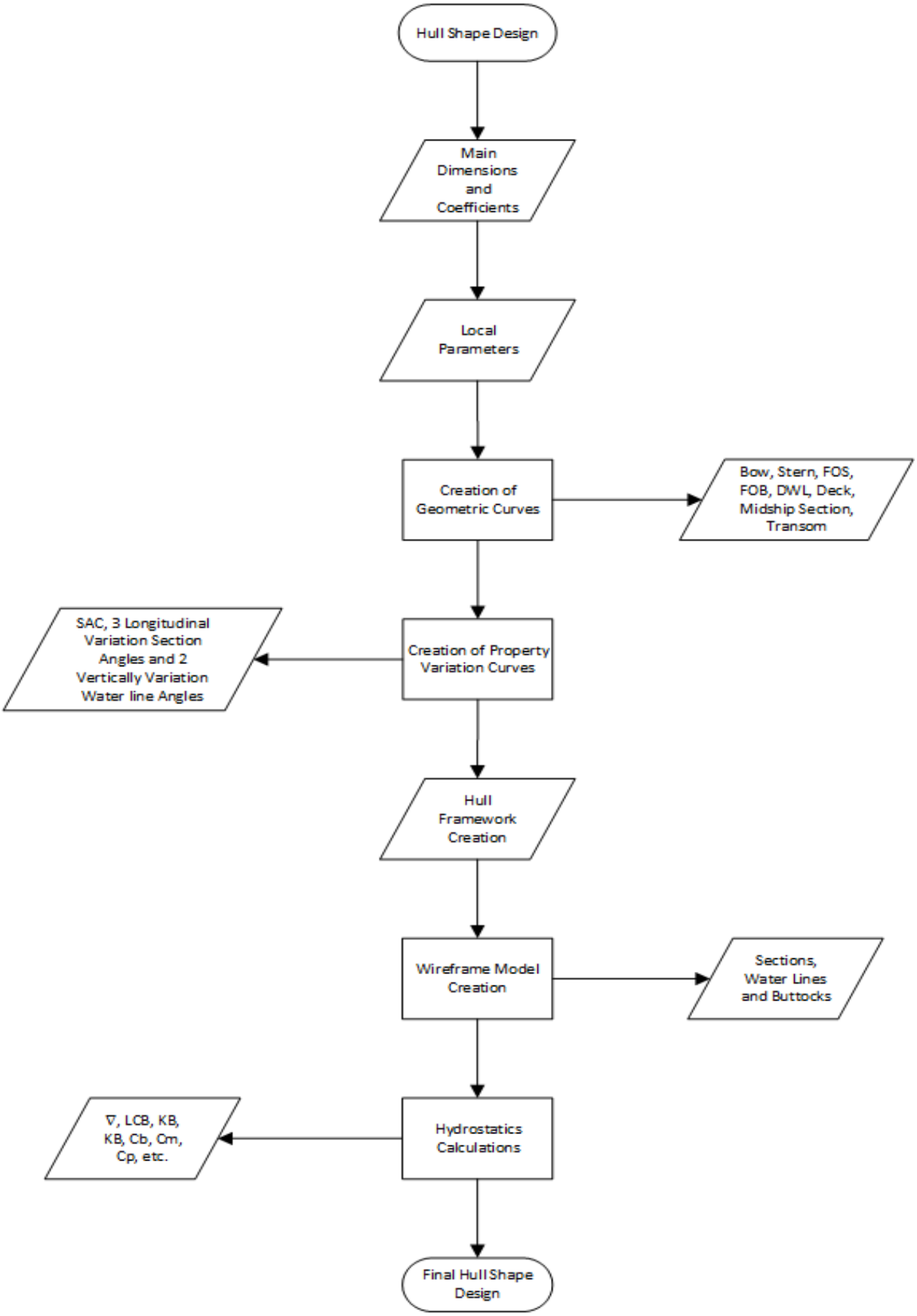

Figure 4.1: Parametric Model Flowchart

The curve creation processes present in the flowchart of parametric procedure have restrictions imposed on the curves, which makes the creation of curves an interactive process with the framework being presented in the flowchart shown in figure 4.2.

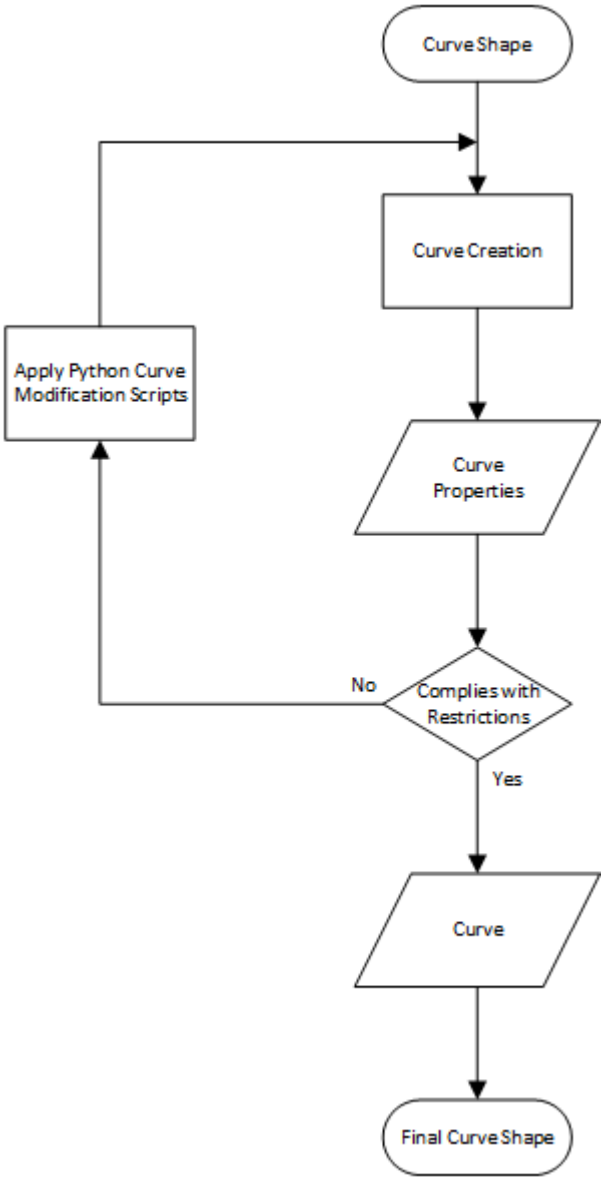

Figure 4.2: Curve Modification Framework

Some curves have an area under the curve constraint, for example DWL has an area under the curve constraint in order to comply with the waterline coefficient. To be able to adjust the curves, a Python script was created and implemented in GhPython, which is the Python interpreter available in Grasshopper. This interpreter uses the version 2.7 of IronPython.

The script starts by extracting the control points from the curve and storing them in a list. With these points, an imaginary box is created that adds a boundary constraint. Then two vectors are created: $vector_{one} = P_1^{'} - A$ and $vector_{two} = P_2^{'} - B$. To achieve the desired area under the curve, the length of the two vectors increases or decreases depending on whether the actual area (area) is larger or smaller, respectively, than the desired area (targetArea). The increase and decrease of vectors stop when the

condition presented in equation 4.1 is verified.

$$error = \frac{|area - targetArea|}{targetArea} < 1\% \tag{4.1}$$

In figure 4.3 is displayed the boundary box and the two vectors.

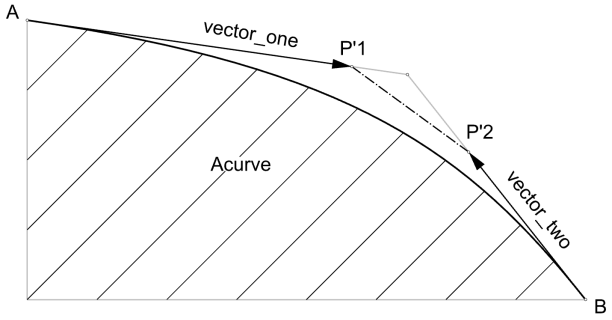

Figure 4.3: Boundary box

4.1 Main Hull Particulars

The hull main particulars are all the dimensions and coefficients that have impact in every aspect of the hull from the location of control points for each geometric curve to hull hydrostatics.

The table 4.1 shows the hull's main particulars.

Table 4.1: Hull Main Particulars

Parameter	**Description**
L_{PP}	Length between perpendiculars
B	Breadth
D	Depth
T	Draught
LCB	Longitudinal Centre of Buoyancy
C_B	Block Coefficient
C_M	Midship Section Coefficient
C_{WP}	Waterline Coefficient
L_C	Length of Cylindrical Mid Body

An important parameter that is not used as an input is the ship's displacement. The information of this parameter is taken from the block coefficient by the following formula. Where ∇ is the displacement, C_B is the block coefficient, L is the length, B is the breadth and T is the draught.

$$\nabla = C_B * L * B * T \tag{4.2}$$

4.2 Geometric Curves

Geometric curves are the curves that define the shape of the ship. Eight geometric curves were considered, as stated in sub chapter 3.2: bow and stern contours, FOB, FOS, midship section, transom, DWL and deck waterline.

In table 4.2 are represented all the parameters used to define the geometric curves as well as their units and a description of the parameter.

Table 4.2: Geometric Curves Parameters

Name	Units	Description	Interval
X_fp	m	Horizontal distance from forward perpendicular to the beginning of bow contour point	$0.0 \leq x \leq 25.0$
X_TipBulb	m	Horizontal distance from forward perpendicular to the bulb most forward point	$1.0 \leq x \leq 15.0$
X_EndKnuckle	m	Longitudinal position of knuckle last point	$1.0 \leq x \leq 10.0$
X_Stem	m	Horizontal distance from forward perpendicular to most aft point of stem	$0.0 \leq x \leq 5.0$
X_Deck	m	Horizontal distance from forward perpendicular to most foward point of deck	$0.0 \leq x \leq 10.0$
X_Transom	m	Longitudinal position of transom from the aft perpendicular	$0.0 \leq x \leq 10.0$
X_Clerance	m	Longitudinal position at the most inward point for clearance	$0.0 \leq x \leq 20.0$
X_Boss	m	Longitudinal position for the propeller boss from the aft perpendicular	$1.0 \leq x \leq 15.0$
X_MidshipSection	m	Longitudinal position of the end of aft body	$10.0 \leq x \leq 150.0$
X_FoS	m	Longitudinal position of first point from the aft perpendicular	$-15.0 \leq x \leq 100.0$
X_FoB	m	Longitudinal position of the aft point of FoB	$0.0 \leq x \leq 50.0$
X_SternEnd	m	Longitudinal position of the last stern contour point	$0.0 \leq x \leq 50.0$
L_FOS	m	Length of flat of side at deck	$0.0 \leq x \leq 125.0$
L_Keel	m	Half of the length of keel	$0.0 \leq x \leq 10.0$
L_Stem	m	Length of the straight part of stem	$0.0 \leq x \leq 25.0$
L_FOB	m	Length of the FOB	$0.0 \leq x \leq 250.0$
Z_fp	m	Height of the first point for the bow contour at forward perpendicular	$0.0 \leq x \leq 20.0$
Z_TipBulb	m	Height of most forward point of bulb	$1.0 \leq x \leq 15.0$
Z_CG	m	Height of centre of gravity of bulb	$1.0 \leq x \leq 15.0$
Z_Stem	m	Vertical distance from most inward point of stem to upper point of bulbous bow at F.P.	$0.0 \leq x \leq 2.0$
Z_Clearance	m	Height of most inward point for clearance	$1.0 \leq x \leq 15.0$
Z_Boss	m	Height of propeller boss from the aft perpendicular	$1.0 \leq x \leq 15.0$
Z_FOS	m	Height of the aft point of FOS	$4.0 \leq x \leq 30.0$
H_Bulb	m	Height of the bulb at forward perpendicular	$1.0 \leq x \leq 20.0$
H_Transom	m	Height of the transom panel	$2.0 \leq x \leq 30.0$
Transom_bh	m	Height between initial and final bilge point	$0.0 \leq x \leq 10.0$
Bilge_Height	m	Height of the final point of bilge from the baseline	$0.0 \leq x \leq 10.0$
H_Aft_FoS	m	Height of the most aft point of flat of side	$4.0 \leq x \leq 30.0$

Table 4.2 Geometric Curves Parameters (continuation)

Name	Units	Description	Interval
B_Bulb	m	Breadth of the bulb	$0.5 \leq x \leq 7.5$
Y_End_Knuckle	m	Breadth of knuckle last point	$1.0 \leq x \leq 20.0$
B_Transom	m	Width of the transom	$5.0 \leq x \leq 30.0$
Transom_bw	m	Longitudinal distance from initial point to the final point of transom bilge	$0.0 \leq x \leq 15.0$
α_fp	°	Angle at the first point at forward perpendicular	$0.0 \leq x \leq 90.0$
α_Bulb upper	°	Angle at the end of bulbous bow curve at forward perpendicular	$-90.0 \leq x \leq 90.0$
α_Bulb_t_l	°	Angle at lower point of bulb at foward perpendicular	$0.0 \leq x \leq 75.0$
α_Bulb_t_u	°	Angle at upper point of bulb at foward perpendicular	$-90.0 \leq x \leq 90.0$
α_Knuckle_ent	°	Angle at first point of knuckle	$0.0 \leq x \leq 45.0$
α_Knuckle_ext	°	Angle at last point of knuckle	$0.0 \leq x \leq 45.0$
k_rotation	°	Angle at first point of knuckle in XZ plane	$0.0 \leq x \leq 45.0$
α_Deck_ext	°	Angle at the highest point of deck	$0.0 \leq x \leq 90.0$
α_Deck_ent	°	Angle at the entrance point of top segment of bow contour	$0.0 \leq x \leq 90.0$
α_Transom_d	°	Angle between transom panel and deck	$-10.0 \leq x \leq 30.0$
α_Transom_b	°	Angle at bottom point of transom	$0.0 \leq x \leq 45.0$
α_Boss_ent	°	Angle at boss propeller at upper point of propeller boss	$0.0 \leq x \leq 90.0$
α_Boss_ext	°	Angle at boss propeller at lower point of propeller boss	$0.0 \leq x \leq 90.0$
α_Transom_bot	°	Angle at the bottom of transom panel	$0.0 \leq x \leq 45.0$
α_Transom_up	°	Angle at the side of transom panel	$25.0 \leq x \leq 90.0$
Deadrise	°	Angle between ship bottom and baseline	$0.0 \leq x \leq 45.0$
Tumblehome	°	Angle between side plate of ship and the deck	$0.0 \leq x \leq 45.0$
α_Aft_FoS	°	Angle of flat of side at first point of flat of side	$0.0 \leq x \leq 90.0$
α_Fwd_FoS	°	Angle of flat of side at last point of flat of side	$0.0 \leq x \leq 90.0$
α_Aft_wtl_FoS	°	Angle of flat of side with waterline at aft part	$0.0 \leq x \leq 90.0$
α_Fwd_wtl_FoS	°	Angle of flat of side with waterline at foward part	$0.0 \leq x \leq 90.0$
α_Aft_FoB	°	Angle of flat of bottom at first point of flat of bottom	$0.0 \leq x \leq 90.0$
α_Fwd_FoB	°	Angle of flat of bottom at last point of flat of bottom	$0.0 \leq x \leq 90.0$
α_Deck_aft	°	Angle at the transom point with maximum width of transom	$0.0 \leq x \leq 45.0$
α_Aft_DWL	°	Angle at first point of design waterline	$0.0 \leq x \leq 90.0$
α_Fwd_DWL	°	Angle at the most forward point of design waterline	$0.0 \leq x \leq 90.0$
f_WTL_Aft	[-]	Longitudinal factor of aft intersection point between FOS and DWL	$0.0 \leq x \leq 0.8$
f_WTL_Fwd	[-]	Longitudinal factor of forward intersection point between FOS and DWL	$0.1 \leq x \leq 1.0$
C_ABL	[-]	Kracth Lateral Parameter	$0.03 \leq x \leq 0.4$
C_ABT	[-]	Kracht Cross Section Parameter	$0.03 \leq x \leq 0.2$
t_fullness_aft	[-]	Area coefficient of the aft segment of DWL curve	$0.0 \leq x \leq 1.0$
t_fulness_fwd	[-]	Area coefficient of the forward segment of DWL curve	$0.0 \leq x \leq 1.0$

One of the problems encountered when modelling the curves was that simply defining the curves with parameters was not enough, as there were curves that had shapes that are not seen in real ships. An example of a curve that has an unwanted shape can be seen in the figure 4.4(a). To prevent this

from happening, a script was created to check if the control points of the curve are inside the imaginary box. The script starts by creating the boundaries of the imaginary box, then checking if any of the control points are out of bounds. If this happens, a line is created between the control point outside the boundary and the starting or ending point of the curve, then intersecting this line with the boundary of the box that is not respected. The point that results from this intersection replaces the point that is outside the imaginary box in the list of curve control points. This process can be seen in the figure 4.4.

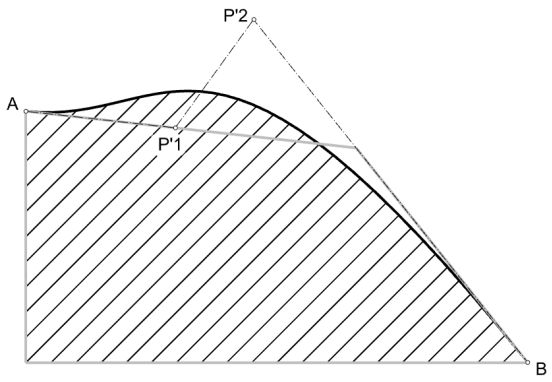

(a) Curve outside of boundary box

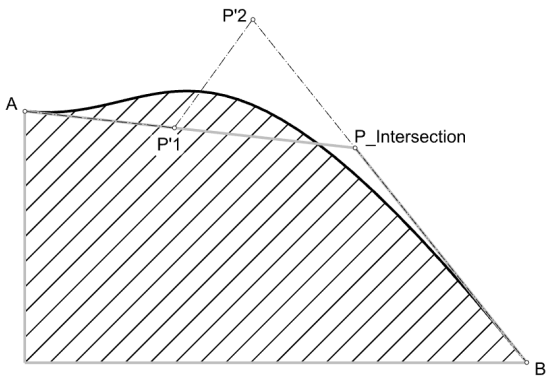

(b) Finding the intersection point between boundary box and $\overline{P'2B}$

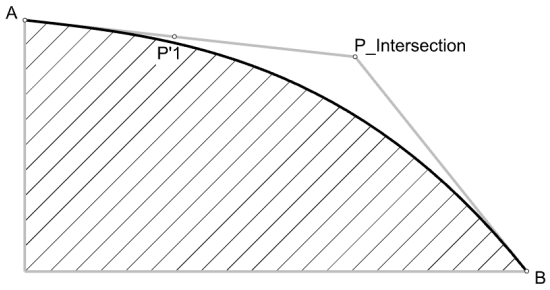

(c) Curve inside the boundary box

Figure 4.4: Process to move from a curve outside the boundary box to one inside

4.2.1 Bow Contour

As identified in the previous chapter, the bow contour was divided into two different configurations: bow without and with bulb. The bulbous bow was divided into two different types: an addition and an integrated bulb. In the model it is necessary to specify what type of bow the ship has,because the number of input parameters depends on the chosen bow configuration.

To define the bow without a bulb, three or five points are needed dividing the bow into two or three curves, respectively. In the figure 4.5 the necessary parameters for its construction are represented. By changing the parameters that control the tangents of the curve above the waterline (α_{deck_ent}, α_{deck_run}) it is possible to obtain the different types of bow without bulb identified in the previous chapter.

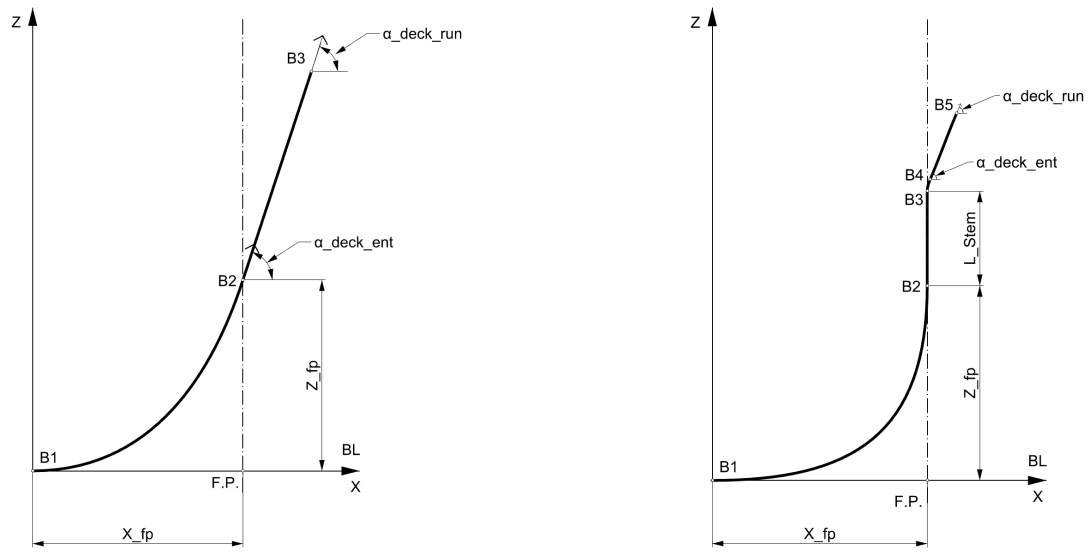

(a) Bow without Stem Straight

(b) Bow with Stem Straight

Figure 4.5: Bow Without Bulb Parameters

In table 4.3 and 4.4 describe the location of points for the two cases shown in figure 4.5. These points are created in the XZ plane.

Table 4.3: Points Position - Bow without bulb (L_Stem = 0)

Point	**X [m]**	**Z [m]**
B_1	$L_{pp} - X\_fp$	0
B_2	L_{pp}	Z_{fp}
B_3	$L_{pp} + X$	$Z_{fp} + L\_Stem$

Table 4.4: Points Position - Bow without bulb (L_Stem $\neq$ 0)

Point	**X [m]**	**Z [m]**
B_1	$L\_pp - X\_fp$	0
B_2	L_pp	Z_fp
B_3	L_pp	$Z\_fp + L\_Stem$
B_4	$L\_pp + (0.1 * X\_Deck)$	$Z\_fp + L\_Stem + (0.15 * (B_5(z) - B_3(z)))$
B_5	$L\_pp + X\_stem$	D

In the following figure are described the parameters for a addition bulb and integrated bulb. The point B_5 can become coincident with B_4 when the upper point of the bulb is located at the forward perpendicular.

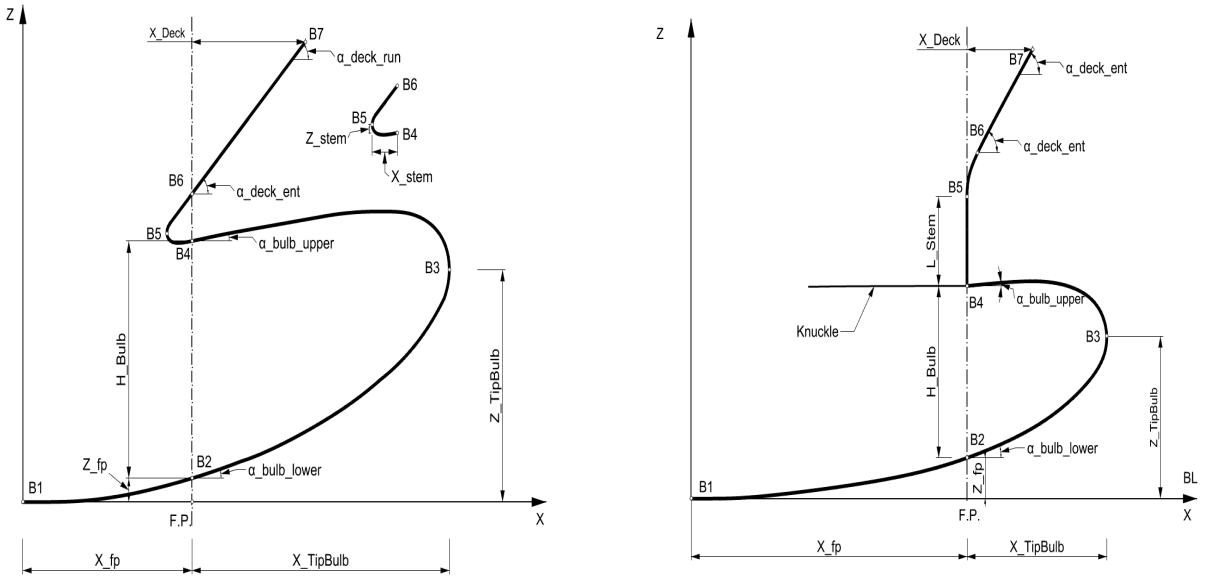

(a) Integrated Bulb

(b) Addition Bulb

Figure 4.6: Bulbous Bow Parameters

The points are created in xz plane at $y = 0$. Table 4.5 and table 4.6 describe the location of the points used to define the bow with integrated and addition bulbs, respectively.

Table 4.5: Points Position - Integrated Bulb (Longitudinal)

Point	**X [m]**	**Z [m]**
B_1	$L\_pp - X\_fp$	0
B_2	L_pp	Z_FP
B_3	$L\_pp + X\_TipBulb$	$Z\_TipBulb$
B_4	L_pp	$Z\_FP + H\_Bulb$
B_5	$L\_pp - X\_Stem$	$Z\_FP + H\_Bulb \pm Z\_Stem$
B_6	L_pp	T
B_7	$L\_pp + X\_Deck$	D

Table 4.6: Points Position - Added Bulb (Longitudinal)

Point	**X [m]**	**Z [m]**
B_1	$L\_pp - X\_fp$	0
B_2	L_pp	Z_FP
B_3	$L\_pp + X\_TipBulb$	$Z\_TipBulb$
B_4	L_pp	$Z\_FP + H\_Bulb \pm Z\_Stem$
B_5	$L\_pp - X\_Stem$	$Z\_FP + H\_Bulb \pm Z\_Stem + L\_Stem$
B_6	$L\_pp + 0.075 * X\_Deck$	$B_5(z) + 0.15(D - B_5(z))$
B_7	$L\_pp + X\_Deck$	D

As can be seen in the figure 4.6(b), when the bow present an addition bulb, there is a discontinuity on the surface of the hull with it being called a knuckle. It is defined with six parameters. The curve is first created on xy plane (see table 4.7 for points position) and then suffers a rotation on xz plane (k_rotation).

In the figure below it is represented the knuckle.

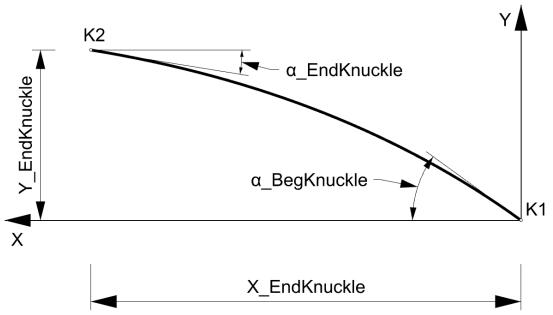

Figure 4.7: Knuckle Parameters

Table 4.7: Points Position - Knuckle

Point	X [m]	Y [m]
K_1	$L_{pp} - X_{stem}$	0
K_2	$L_{pp} - X_{endKnuckle}$	$B_{endKnuckle}$

After defining the longitudinal contour of bulbous bow, it was created a set of parameters to define a transversal section with the maximum breadth located in the forward perpendicular. It is created in the yz plane (see table 4.8 for points position), and is divided in upper and lower curve. In figure 4.8 is possible to see the parameters used to create the curves and in table 4.2 are the parameters description.

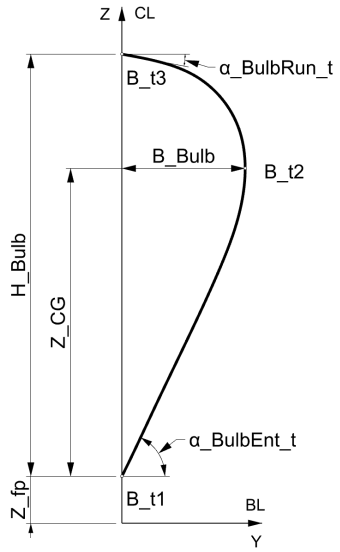

Figure 4.8: Bulb Transversal Section Parameters

Table 4.8: Points Position - Bulbous Bow (Transversal)

Point	Y [m]	Z [m]
B_{t1}	0	Z_fp
B_{t2}	B_Bulb	Z_CG
B_{t3}	0	$Z\_fp + H\_Bulb$

With the longitudinal contour and the transverse section of the bulb defined, it was necessary to create one more curve to control the maximum breadth of the transverse sections of the bulb. This curve connects the point with the maximum breadth of the bulb (B_{t2}) to the tip of the bulb (B_3) and because the points are not located in the same plane, the curve is a space curve instead of a plane curve. Despite this, in figure 4.9 it is presented the curve reflected in the xy plane. For this curve it was assumed that its running angle is always equal to 90° .

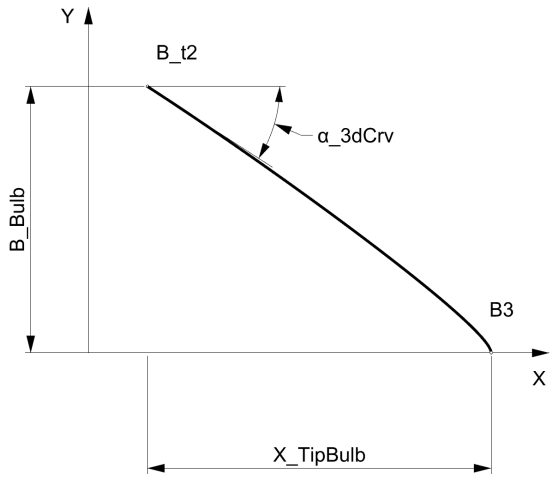

Figure 4.9: Bulb space curve parameters

4.2.2 Stern Contour

The longitudinal contour of the stern is defined by six or eight points depending on the presence of bulb or not, that are display in figure 4.10 with the parameters used to defined them. The stern contour is created in the XZ plane.

If there is no bulb, the stern contour is created with two lines and two NURBS curves, otherwise it is created with two lines and four NURBS curves. The first line in both cases is also part of the transom, with points S1 and S2 also being used to build the transom. The location of the points can be seen in the table 4.9.

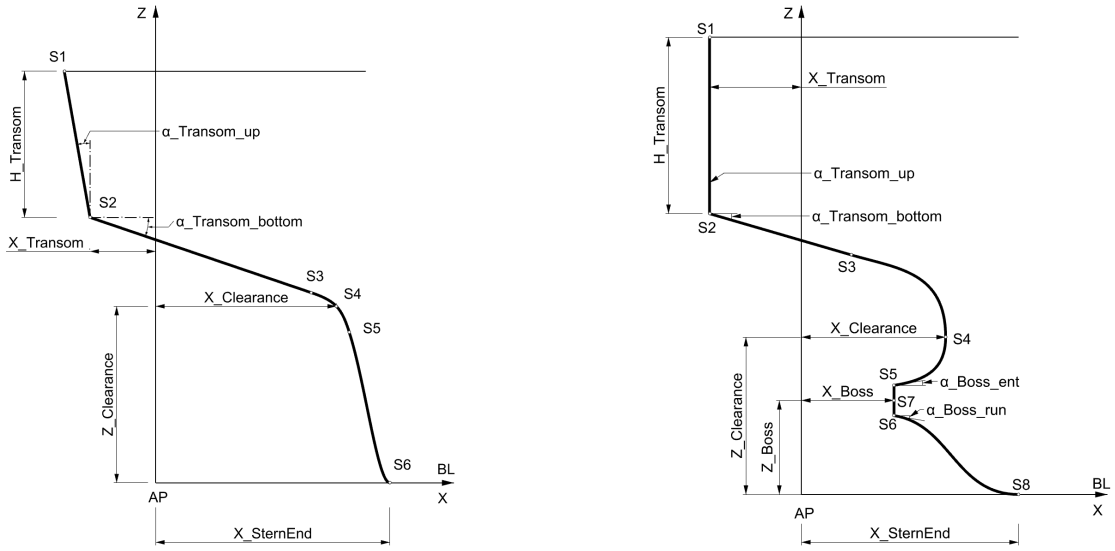

(a) Stern without bulb

(b) Stern with bulb

Figure 4.10: Stern Parameters

If there is no bulb, the stern contour is created with two lines and two NURBS curves, otherwise it is created with two lines and four NURBS curves. The first line in both cases is also part of the transom, with points S1 and S2 also being used to build the transom. The location of the points can be seen in the table 4.9.

Table 4.9: Points Position - Stern with no Bulb

Point	**X [m]**	**Z [m]**
S_1	$X\_Transom + \tan(\alpha\_Transom\_up) * H\_Transom$	D
S_2	$X\_Transom$	$D - H\_Transom$
S_3	$X\_Transom + 0.9 * (X\_Clearance - X\_Transom)$	$S_2(z) - 0.9 * (X\_Clearance - X\_Transom) * \tan(\alpha\_Transom\_bottom)$
S_4	$X\_Clearance$	$Z\_Clearance$
S_5	$X\_Clearance + 0.25 * (X\_FOB - X\_Clearance)$	$Z\_Clearance - 0.15 * Z\_Clearance$
S_6	X_FOB	0

Table 4.10: Points Position - Stern with Bulb

Point	**X [m]**	**Z [m]**
S_1	$X\_Transom + \tan(\alpha\_Transom\_up) * H\_Transom$	D
S_2	$X\_Transom$	$D - H\_Transom$
S_3	$X\_Transom + 0.6 * (X\_Clearance - X\_Transom)$	$S_2(z) - 0.9 * (X\_Clearance - X\_Transom) * \tan(\alpha\_Transom\_bottom)$
S_4	$X\_Clearance$	$Z\_Clearance$
S_5	X_Boss	$Z\_Boss + R\_Boss$
S_6	X_Boss	Z_Boss
S_7	X_Boss	$Z\_Boss - R\_Boss$
S_8	X_FOB	0

As stated in section 3.2.2, in the cases where there isn't a presence of a stern bulb the parameter X_SternEnd has influence in the shape of the stern contour curve. This was shown by the coefficient, $C_{SternEnd}$, created to study the different shapes of the stern. The conclusion was that when the coefficient was closer to or greater than 0.20 the shape of the stern contour was similar to a straight line. This created the need to modify the location of the points presented in the table 4.9 in order to define the stern contour when the previous condition was verified. In table 4.11 the number of points and their location is displayed.

Table 4.11: Points Position - Stern with no Bulb

Point	X [m]	Z [m]
S_1	$X\_Transom + \tan(\alpha\_Transom\_up) * H\_Transom$	D
S_2	$X\_Transom$	$D - H\_Transom$
S_3	$X\_Clearance$	$Z\_Clearance$
S_4	X_FOB	0

4.2.3 Flat of Side

The FOS contour is created in the XZ plane at $y = \frac{B}{2}$. To create the FOS curve, 5 to 7 points are needed depending on whether the start of the FOS is at X_FOS = X_Transom and whether there is a cylindrical body or not. The definition for six and seven points can be seen in figure 4.11. When the FOS does not start at X_FOS = X_Transom and the length of the cylindrical body is zero (L_C = 0) only five points are needed to create the FOS curve.

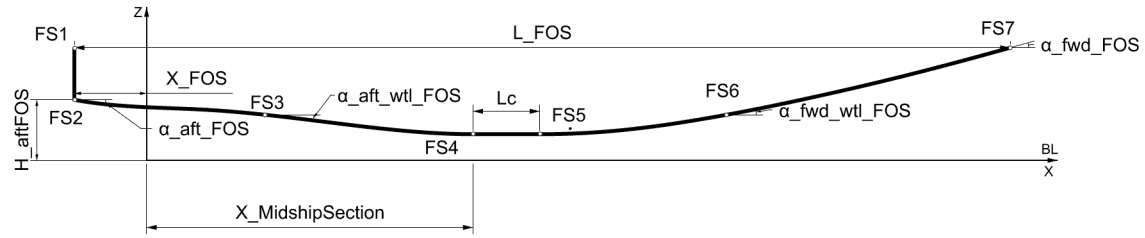

(a) FOS intersect Transom

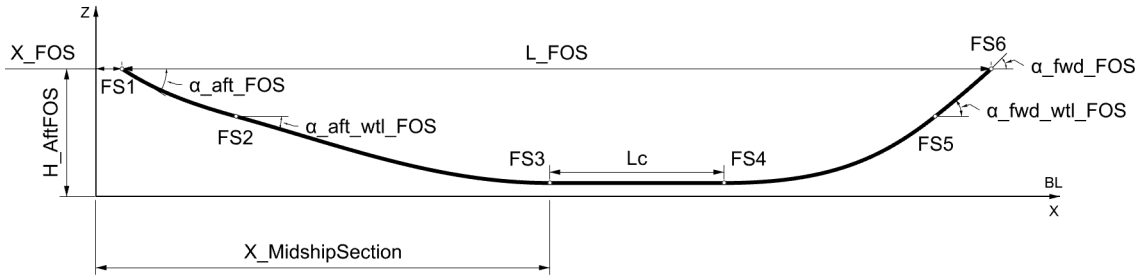

(b) FOS doesn't intersect Transom

Figure 4.11: FOS Parameters

The location of the points needed for both cases are in the table 4.12 and table 4.13. The longitudinal position of the points representing the intersection between FOS and DWL (points with z = T) is defined with the help of two factors (f_Aft and f_Fwd). The f_Aft factor is responsible for the first intersection point and can varied between 0 and 0.8. The f_Fwd factor is responsible for the second intersection point and can be varied between 0.1 and 1.

Table 4.12: Points Position - FOS at X_FOS = X_Transom

Point	**X [m]**	**Z [m]**
FS_1	X_FOS	D
FS_2	X_FOS	H_AftFOS
FS_3	$X\_FOS + f\_Aft * (X\_MidshipSection - X\_FOS)$	T
FS_4	$X\_MidshipSection$	$D - H\_Tumblehome - H\_StraightSide$
FS_5	$X\_MidshipSection + L\_c$	$D - H\_Tumblehome - H\_StraightSide$
FS_6	$FS_5 + f\_Fwd * (FS_7 - FS_5)$	T
FS_7	$X\_FOS + L\_FOS$	D

Table 4.13: Points Position - FOS at X_FOS $\neq$ X_Transom

Point	**X [m]**	**Z [m]**
FS_1	X_FOS	H_AftFOS
FS_2	$X\_FOS + f\_Aft * (X\_MidshipSection - X\_FOS)$	T
FS_3	$X\_MidshipSection$	$D - H\_Tumblehome - H\_StraightSide$
FS_4	$X\_MidshipSection + L\_c$	$D - H\_Tumblehome - H\_StraightSide$
FS_5	$FS_5 + f\_Fwd * (FS_7 - FS_5)$	T
FS_6	$X\_FOS + L\_FOS$	D

4.2.4 Midship Section

To define the midship section it is necessary a minimum of four points with a maximum of seven points, this number depends on the complexity of midship section. The parameters can be seen in figure 4.12. It was made the assumption that main frame is located at the beginning of parallel mid body. The bilge is developed with a NURBS curve, and the rest of curves are lines.

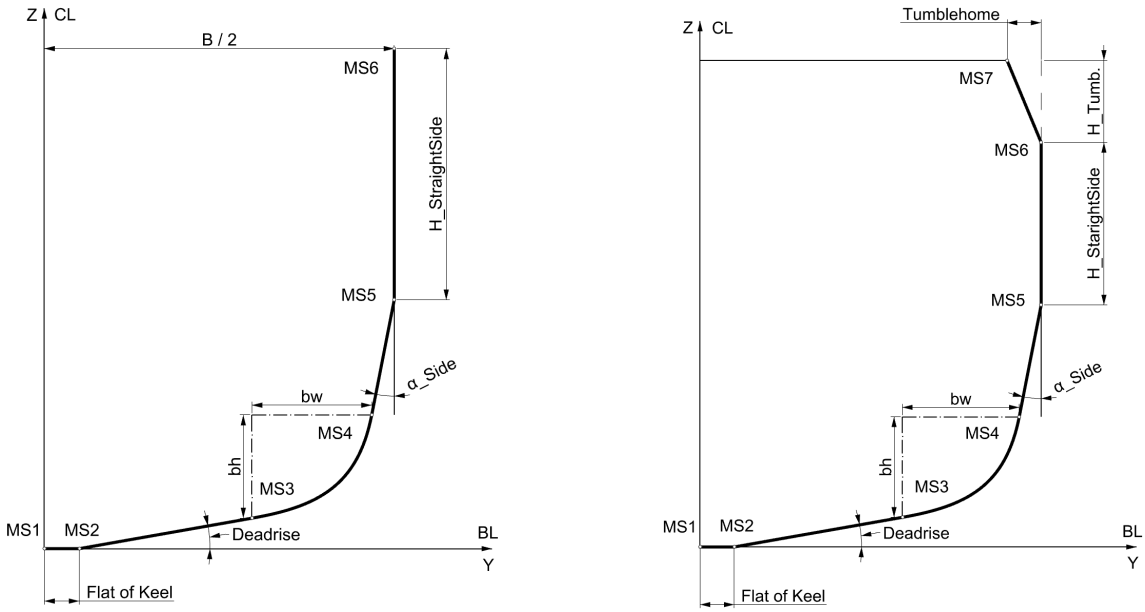

(a) Without Tumblehome

(b) With Tumblehome

Figure 4.12: Midship Section Parameters

With the parameters defined, points ($MS_1, ..., MS_i$) are created to construct the curves of midship section. This points are all located at $X = X_{MidshipSection}$ and in the plan YZ. The specific location of each point is present in the table 4.14.

Table 4.14: Points Position - Midship Section

Point	Y [m]	Z [m]
MS_1	0	0
MS_2	$FlatofKeel$	0
MS_3	$\frac{B}{2} - FlatofKeel - Bilge_W - (tan(\alpha_{Side}) * (D - Bilge_H - H_{StraightSide}))$	$tan(deadrise)(\frac{B}{2} - FlatofKeel - Bilge_W)$
MS_4	$\frac{B}{2} - (tan(\alpha_{Side}) * (D - Bilge_H - H_{StraightSide})$	$Bilge_H + tan(deadrise)(\frac{B}{2} - FlatofKeel - Bilge_W)$
MS_5	$\frac{B}{2}$	$D - H_{Tumblehome} - H_{StraightSide}$
MS_6	$\frac{B}{2}$	$D - H_{Tumblehome}$
MS_7	$\frac{B}{2} - Tumblehome$	D

In figure 4.12 all the parameters used to define a complex midship section are presented, but in most merchant ships the midship section is very simple, as it is composed of a bottom line, a curve and a lateral line. This causes many of the parameters presented above to be equal to zero, e.g. deadrise, tumblehome, etc. In figure 4.13 the parameters to define a simplified midship section are presented. In table 4.15 are described the points location.

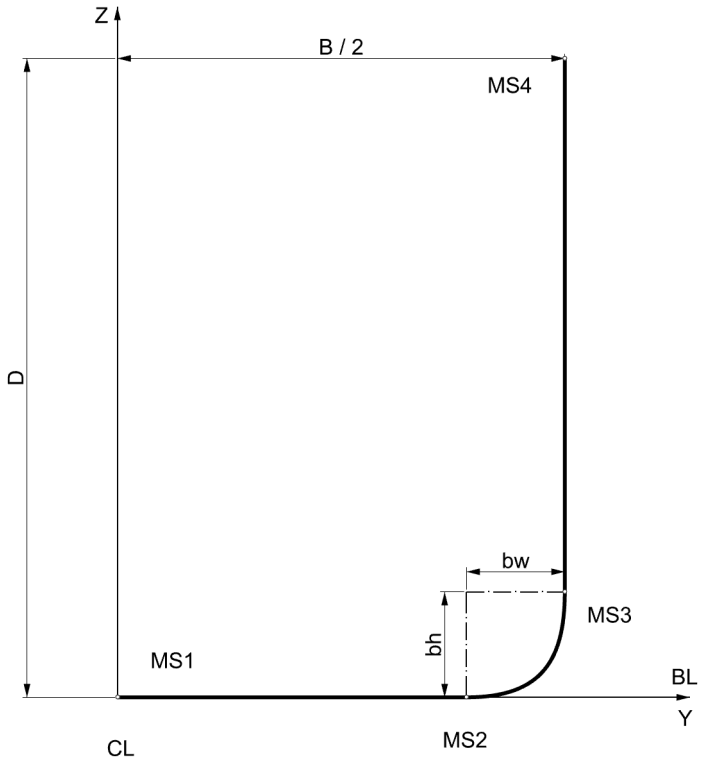

Figure 4.13: Midship Section Simplified Parameters

Table 4.15: Midship Section Simplified location points

Point	Y [m]	Z [m]
MS_1	0	0
MS_2	$\frac{B}{2} - bw$	0
MS_3	$\frac{B}{2}$	bh
MS_4	$\frac{B}{2}$	D

4.2.5 Transom

The transom panel is defined with seven parameters. The number of curves used to describe the transom changes depending on the shape of the transom (Normal or U shape). If it is a U shape it needs four curves (one is a NURBS and three are lines), if it is normal shape it only needs two curves (one NURBS and one line). These two shapes can be seen in the figure 4.14, with the parameters necessary to describe them.

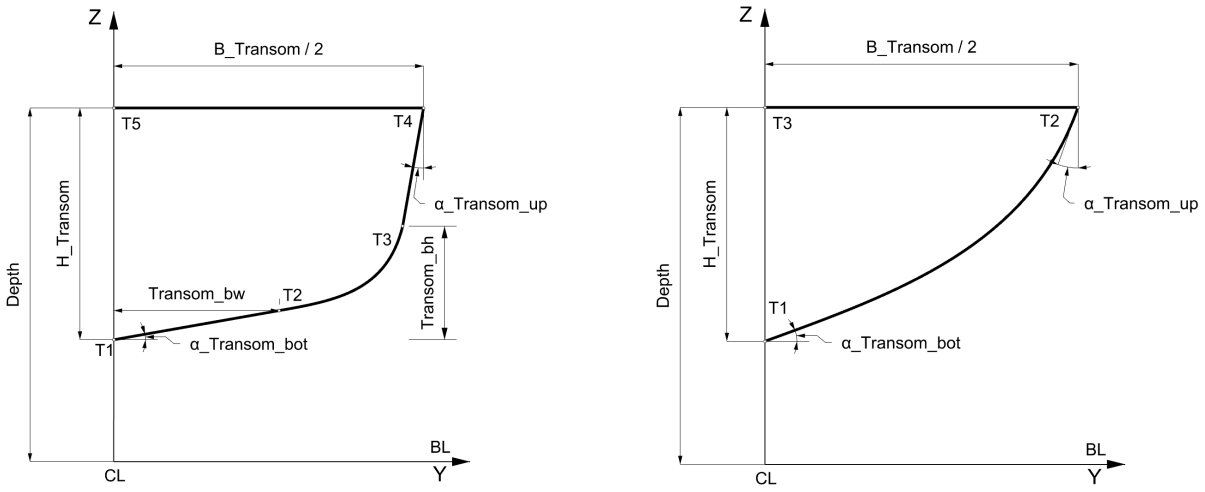

(a) U Shape

(b) Normal Shape

Figure 4.14: Transom Parameters

The points necessary are created in the plane yz at $x = x_{Transom}$. The table 4.16 shows the location of points. Once again the number of points depend on the shape of transom (U shape needs 5 points and normal shape needs 3 points).

Table 4.16: Transom location points - U Shape

Point	Y [m]	Z [m]
T_1	0	$D - H\_Transom$
T_2	$Transom\_bw$	$Transom\_bw * \tan(\alpha\_Transom\_bot)$
T_3	$\frac{B\_Transom}{2} - (D - Transom\_bh) * \tan(\alpha\_Transom\_up)$	$D - Transom\_bh$
T_4	$\frac{B\_Transom}{2}$	D
T_5	0	D

Table 4.17: Transom location points - Normal Shape

Point	Y [m]	Y [m]
T_1	0	$D - H\_Transom$
T_2	$\frac{B\_Transom}{2}$	D
T_3	0	D

4.2.6 Flat of Bottom

The FoB is created with six parameters. The aft and forward part are NURBS curve and the middle part is a line with the length of parallel mid body. In the figure 4.15 are the parameters used to define the FOB.

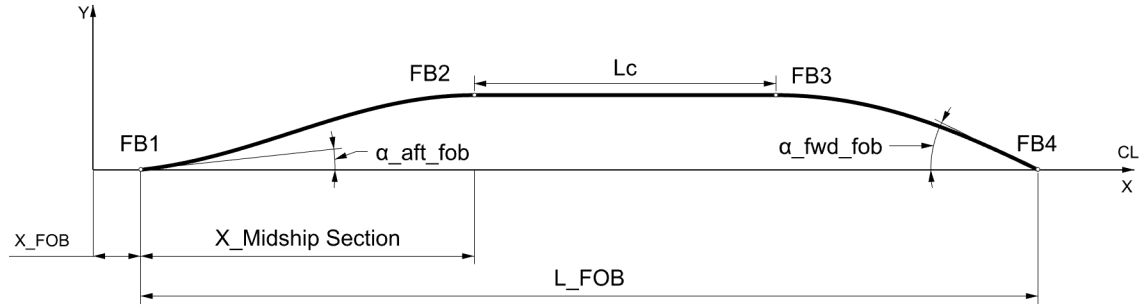

Figure 4.15: FOB Parameters

To define the FOB curve it is needed four points, as can be seen in figure 4.15. These points are created in XY plane at z = 0. The location of each point is presented in table 4.18.

Table 4.18: FoB points positions

Point	X [m]	Y [m]
FB_1	X_{FoB}	0
FB_2	$X_{MidshipSection}$	$\frac{B}{2} - FlatofKeel - Bilge_W - (tan(\alpha_{Side}) * (D - Bilge_H - H_{StraightSide}))$
FB_3	$X_{MidshipSection} + L_C$	$\frac{B}{2} - FlatofKeel - Bilge_W - (tan(\alpha_{Side}) * (D - Bilge_H - H_{StraightSide}))$
FB_4	$X_{FOB} + L_{FOB}$	0

4.2.7 Design Waterline

This geometric curve can be defined by five or six points depending on whether the waterline intersects the transom (six points) or not (five points). In figure 4.16 is presented the two situations. The DWL is developed on the XY plane.

When the DWL crosses the transom, an XY plane is created at Z = T and is later intersected with the transom curve to find the first two points of the DWL (W1, W2). The longitudinal coordinate of these two points is designated by X_DWL and the transverse coordinate is B_DWL. If there is no intersection with the transom, an XY plane is still created but the intersection is done with the stern contour curve with the result of this intersection being the point W1.

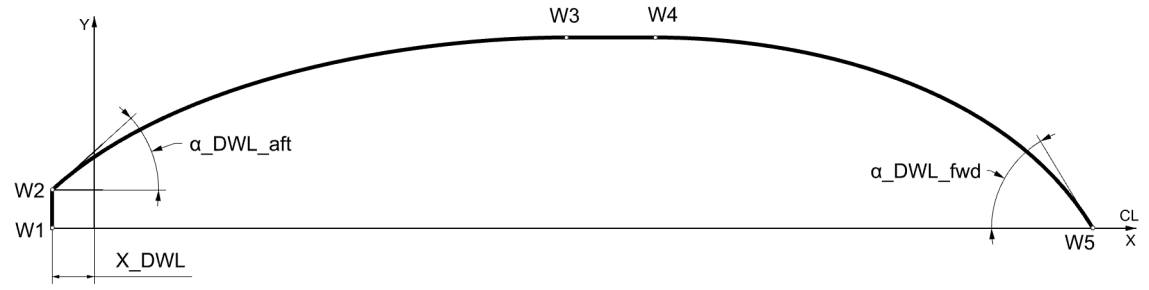

(a) DWL intersect Transom

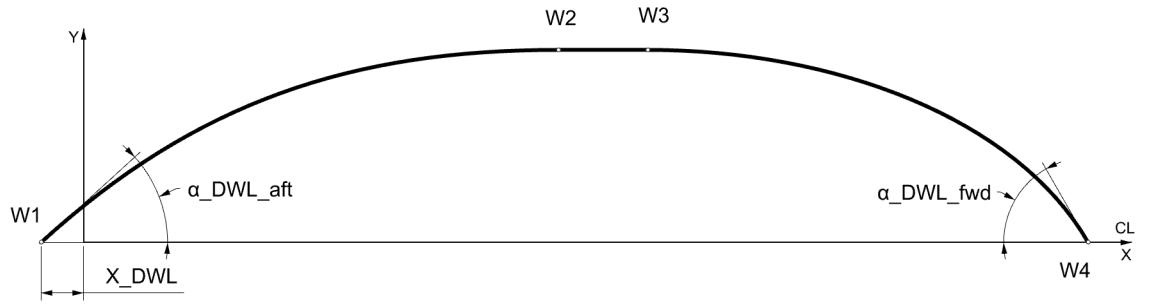

(b) DWL doesn't intersect Transom

Figure 4.16: DWL Parameters

The DWL curve is composed of two NURBS curves and one or two lines depending on whether or not it intersects the transom. The location of the points can be seen in the tables 4.19 and 4.20.

Table 4.19: Points Position - DWL intersect Transom

Point	**X [m]**	**Y [m]**
W_1	X_DWL	0
W_2	X_DWL	B_DWL
W_3	$X\_MidshipSection$	$\frac{B}{2}$
W_4	$X\_MidshipSection + L\_c$	$\frac{B}{2}$
W_5	L_{pp}	0

Table 4.20: Points Position - DWL doesn't intersect Transom

Point	**X [m]**	**Y [m]**
W_1	X_DWL	0
W_2	$X\_MidshipSection$	B
W_3	$X\_MidshipSection + L\_c$	B
W_4	L_{pp}	0

The area under the DWL curve is an important aspect as it is related to the water plane coefficient. To obtain the desired area, the script described in the introduction of chapter 4 was not enough, because despite the area being similar to the target area, the longitudinal distribution of the area was not accurate when compared to the real ships used in the validation. Because of this, two more parameters were created that individually control the area under the DWL forward and aft curve, which were called t_fullness_aft and t_fullness_fwd, respectively.

4.2.8 Deck Waterline

The deck waterline curve it is developed at xy plane at $z = D$, where D is depth. It is composed by two straight lines and two NURBS curves. If the breadth of the transom is equal to the breadth of the ship, the aft curve can become a straight line. As seen in chapter 3 this is more common in container and Ro-Ro ships. In figure 4.17 are represented the parameters and points necessary to define the deck waterline curve, with their description in table 4.2 and 4.21, respectively. It was assumed that the run angle of the forward curve is equal to 90 ° .

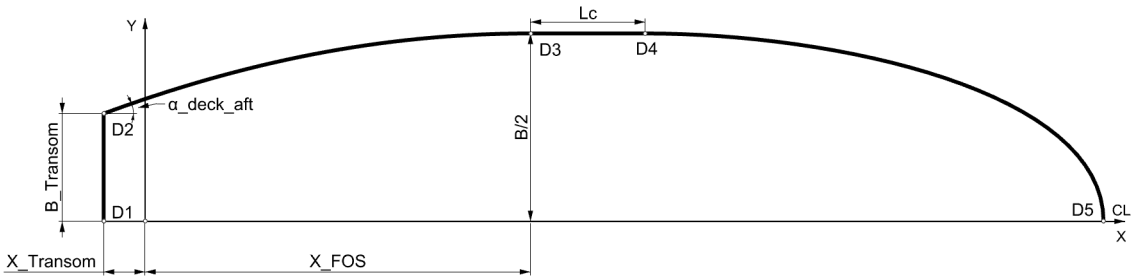

Figure 4.17: Deck Waterline Parameters

All of the points used to create the deck waterline contour are coincident with points of another curves. The first two points are coincident with points of the transom, the next two are the initial and end point of the FOS and the final point is the top point of the bow contour.

Table 4.21: Points Position - Deck Waterline

Point	X [m]	Y [m]
D_1	$X_{Transom}$	0
D_2	$X_{Transom}$	$B_{Transom}$
D_3	X_{FoS}	B
D_4	$X_{FoS} + L_C$	B
D_5	$L_{pp} + X_{Deck}$	0

4.3 Property Variation Curves

The property variation curves are curves that give some geometric properties of the hull shape along one direction. For example area or an entrance angle of a cross-section.

In the next subchapters, the way to parametrize each property variation curves will be presented. In the table 4.22 all the parameters used for the parametrization of the curves are described.

Table 4.22: Property Variation Curves Parameters

Parameter	Units	Description	Interval
Lpp	m	Length between perpendiculars	$0.0 \leq x \leq 400.0$
X_BulbTip	m	Horizontal distance from forward perpendicular to the bulb most forward point	$1.0 \leq x \leq 15.0$
X_DWL	m	Longitudinal position of design waterline from the aft perpendicular	[-]
X_Clearance	m	Longitudinal position at the most inward point for clearance	$0.0 \leq x \leq 20.0$
X_MidshipSection	m	Longitudinal position of the main frame	$10.0 \leq x \leq 150.0$
X_Transom	m	Longitudinal position of transom from the aft perpendicular	$-20.0 \leq x \leq 0.0$
X_Deck	m	Horizontal distance from forward perpendicular to most forward point of deck	$0.0 \leq x \leq 10.0$
X_FoS	m	Abscissa of first point from the aft prependicular	$-15.0 \leq x \leq 100.0$
X_FOB	m	Abscissa of the aft point of FoB	$0.0 \leq x \leq 50.0$
X_Boss	m	Longitudinal position for the propeller boss from the aft perpendicular	$1.0 \leq x \leq 15.0$
Lc	m	Length of parallel mid body	$0.0 \leq x \leq 125.0$
LCB	m	Longitudinal centre of buoyancy	$0.0 \leq x \leq 200.0$
D	m	Ship depth	$5.0 \leq x \leq 50.0$
H_Transom	m	Height of the transom panel	$2.0 \leq x \leq 30.0$
Z_Boss	m	Height of propeller boss from the aft perpendicular	$1.0 \leq x \leq 15.0$
R_Boss	m	Radius of propeller boss	$0.0 \leq x \leq 2.0$
A_TransomUW	m^2	Area of the transom panel that is underwater	[-]
A_MS	m^2	Area of the midship section	[-]
A_Bulb_T	m^2	Area of the bulb transverse section	[-]
α_aft	°	Angle of entrance in the aft curve of SAC	$0.0 \leq x \leq 90.0$
α_clearance	°	Angle of at the clearance point of SAC	$0.0 \leq x \leq 90.0$
α_fp	°	Angle at forward perpendicular	$0.0 \leq x \leq 90.0$
f_clearance	°	Area coefficient at long. position of propeller clearance	[-]

4.3.1 Sectional Area Curve

The SAC curve gives an area relative to a specific longitudinal position, and allows to change the distribution of underwater volume of the ship. A parameter with great influence on underwater volume distribution is the longitudinal centre of buoyancy (LCB). This curve is defined with 10 parameters. To create the SAC curve, three or seven points are needed depending on the complexity of the SAC. An example of a SAC with seven points is in figure 4.18.

This curve is created with three NURBS curves and with one line that represents the length of parallel mid body. The parameter A_TransUW is different than zero when the design waterline intersects with the transom panel but if the transom is above the water then the parameter is zero. When A_TransUW $\neq$ 0 its value is calculated by dividing the transom in two (a part underwater and part above water) and the area of the submerged part is calculated. The parameters A_MS and A_Bulb_T are related to the

parameters of the midship section curve and bulb cross-section curve, respectively. When the midship section curve is created, it must obey the midship section coefficient, with an error of less than 3% as indicated in subchapter 4.2.4. With this information it is possible to found the area corresponding to the midship section coefficient. The numerical value for A_Bulb_T is related to the cross section parameter (C_ABT), see table 3.3. When A_Bulb_T is equal to zero it means that there is no bulbous bow and the end point of the SAC is located at the forward perpendicular.

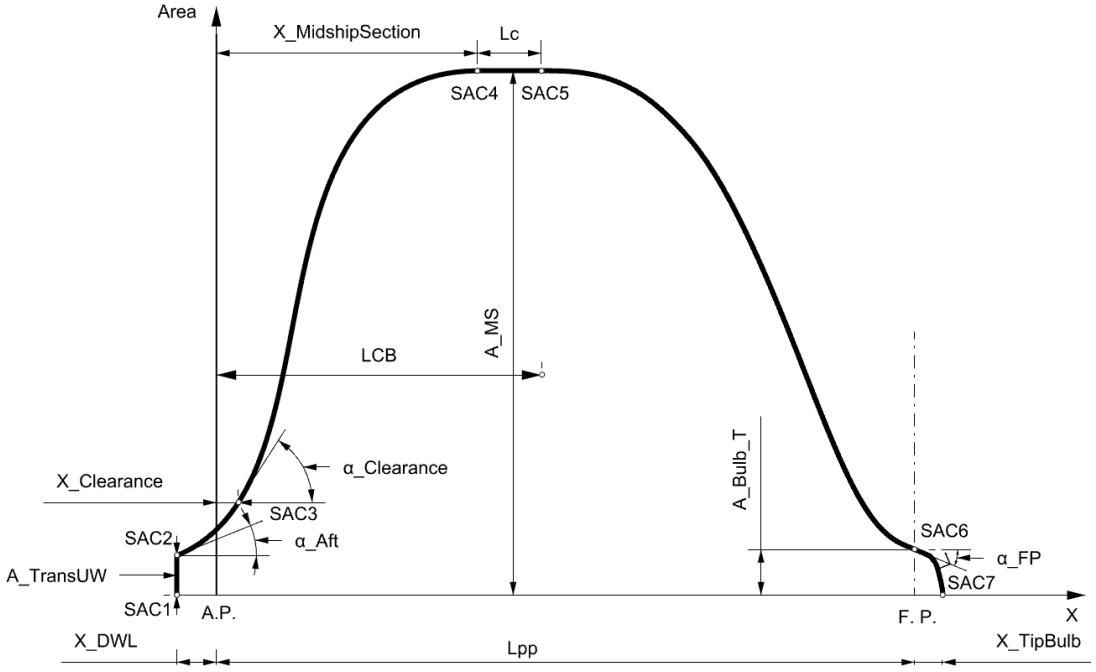

Figure 4.18: SAC Parameters

In table 4.23 are described the points location, that are created in the XY plane with the y axis representing the area at a longitudinal position. In the longitudinal position equal to the parameter X_Clearance there is a factor (f_Clearance) that allows to change the area in this location depending on the characteristics of the ship.

Table 4.23: Points Position - SAC

Point	**X [m]**	**Y [m]**
$SAC1$	X_DWL	0
$SAC2$	X_DWL	$A\_TransUW$
$SAC3$	$X\_Clearance$	$f\_Clearance * A\_MS$
$SAC4$	$X\_MidshipSection$	A_MS
$SAC5$	$X\_MidshipSection + Lc$	A_MS
$SAC6$	L_pp	A_Bulb_T
$SAC7$	$L\_pp + X\_TipBulb$	0

4.3.2 Longitudinal Variation of Section Angles

The section angle variation curve provides information on how angles vary along the length of the ship. Three curves are needed to define all the angles necessary to build a cross section at a given longitudinal position. These curves define the angles shown in the figure 3.9.

The definition of these curves was done using a Grasshopper plug-in called RichGraphMapper. An example of this component is present in figure 4.19. It is similar to a Grasshopper component called GraphMapper, but with the advantage of being able to choose more distributions and set the domain automatically. The distribution used was the Bézier distribution, as it can create very different types of distributions, as it is possible to define the start, mid and end points and the respective tangents.

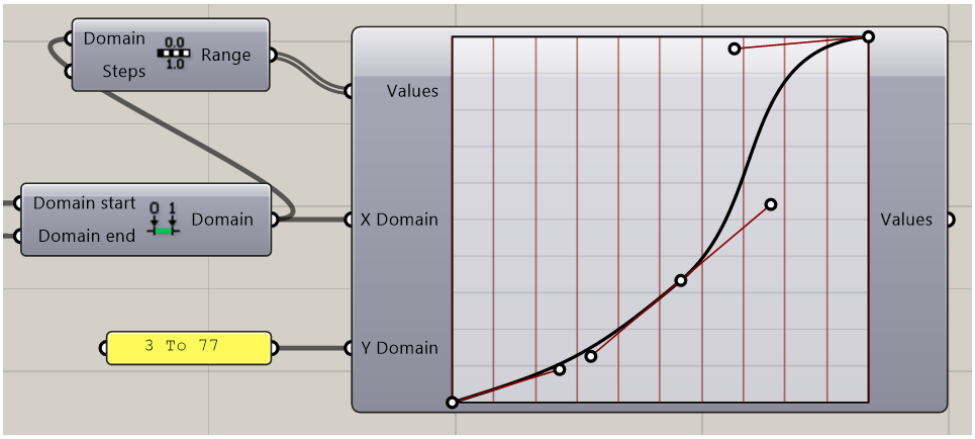

Figure 4.19: RichGraphMapper plug-in

In order to be able to create the curves, it is first necessary to define the domain for each of the three curves. For the curve that defines the entry angle of the sections (α_Bottom) the domain was as follows: [X_Transom $\leq$ X $\leq$ X_Clearance] $\bigcup$ [X_Clearance $<$ X $\leq$ X_FOB_Aft] $\bigcup$ [X_FOB_Aft $<$ X $<$ X_FOB_Fwd] $\bigcup$ [X_FOB_Fwd $\leq$ X $\leq$ X_Lpp]. For the curve that defines the run angle of the part of the underwater section (α_DWL) the domain was as follows: [X_Transom $\leq$ X $\leq$ X_Clearance] $\bigcup$ [X_Clearance $<$ X $\leq$ X_DWL_Aft] $\bigcup$ [X_DWL_Aft $<$ X $<$ X_DWL_Fwd] $\bigcup$ [X_DWL_Fwd $\leq$ X $\leq$ X_Lpp]. Finally, the domain of the angle variation curve of the section on the deck waterline is: [X_Transom $\leq$ X $\leq$ X_Clearance] $\bigcup$ [X_Clearance $<$ X $\leq$ X_FOS_Aft] $\bigcup$ [X_FOS_Aft $<$ X $<$ X_FOS_Fwd] $\bigcup$ [X_FOS_Fwd $\leq$ X $\leq$ X_Deck]. There are two assumptions made, one is that between the FOB length the angle is always 0° and the other is that the angle in the FOS region is always 90° . If there is a stern bulb or a bulbous bow, two separate curves are created to define the entry and exit angles of the sections. The domain for the stern bulb is as follows: [X_Boss $<$ X $<$ X_Clearance]. For the bulbous bow the domain is as follows: [X_Lpp $<$ X $<$ X_BulbTip]. With the domain and distribution defined for the three curves, it is possible in each domain to extract information from one hundred points to create a curve in Rhino associated with that domain.

4.3.3 Vertical Variation of Waterline Angles

For the waterlines, two curves were created to represent the vertical variation of angles. The process of creating these curves is the same as explained in the sub-chapter above, the only difference being the domains used to define the curves.

The water lines were divided into two regions: aft and forward regions. The forward region has two domains as follow: [0 $<$ Z $<$ T] $\bigcup$ [T $<$ Z $<$ D]. The aft region when there is a stern bulb has 4 domains as follow: [0 $<$ Z $<$ $Z\_Boss - R\_Boss$] $\bigcup$ [$Z\_Boss - R\_Boss \leq$ Z $\leq Z\_Boss + R\_Boss$] $\bigcup$ [$Z\_Boss + R\_Boss <$ Z $\leq D - H\_Transom$] $\bigcup$ [$D - H\_Transom <$ Z $<$ D]. It is assumed that for the domain [$Z\_Boss - R\_Boss \leq$ Z $\leq Z\_Boss + R\_Boss$] the angle is always 0° . When there isn't a presence of a stern bulb only two domains are necessary, namely: [0 $<$ Z $< D - H\_Transom$] $\bigcup$ [$D - H\_Transom \leq$ Z $<$ D].

4.4 Wireframe Model

Sections are an important aspect of a wireframe model, with the quality of both being related. With this in mind, ways were created to be able to create one or more sections so that it is possible to carry out hydrostatic calculations, etc.

To create a section it is necessary to discover its crossing points in a longitudinal position. This longitudinal position must be between the limits of the ship's hull, if this limit is not respected, it is not possible to create the section. When this happens, a window is created that warns that the limits have been violated and informs the possible limits. To find these crossing points, an intersection is made between a YZ plane, the geometric curves and two auxiliary water lines. These auxiliary curves are created at the height of the propeller clearance (z = Z_Clearance) and the height of the propeller boss (z = Z_Boss). The shape of these curves depends on whether the section is U or V shaped. Because of this it is possible to define the entrance and run angle for each curve. The point information is stored in a list. This list is then divided into two, one with the points under water and the other with the points above the water. The division is done by comparing the Z value of each crossing point with the draft value. When this division is done it is possible to create the section also dividing it in the part below and above the DWL. In addition to the crossing points, the angles represented in the figure 3.9 are also necessary, being defined in subchapter 4.3.2. When the section is created the underwater area is compared to the area designated in the SAC for the same longitudinal position. If there is an error greater than 3%, the curve is adjusted until the condition no longer exists. The process described above is for creating a section but the model is also prepared to give a specific number of sections. The method is the same only that waypoint information is stored in a data tree, with the tree having n branches where n is the number of desired sections.

The process for obtaining one or a certain number of waterlines is the same as the process for sections, with the difference that instead of intersecting the geometric curves with a YZ plane, it intersects with an XY plane, and the angles used come from the property curve described in sub chapter 4.3.3.

As stated in the analysis of the wireframe the buttocks were identified as the least important curves,

with the longitudinal contour and FOS being the only relevant buttocks, because of this only this two curves are presented in the wireframe.

Chapter 5

Validation

With the implementation of the parametric model completed, a validation was performed to verify if it could reproduce the different forms of merchant ships. To validate the parametric model, a graphical and numerical validation was chosen. The graphical validation was performed by creating a body plan with five sections in the aft and forward body, where the parametric sections were superimposed on the real sections. If the ship has a stern bulb, one section is added to the body plan and if there is a bulbous bow, two sections are added. Numerical validation was performed by obtaining some hydrostatic properties of the parametric model and comparing them with the real values. The validation was carried out for five ships with a bulk carrier, oil tanker and Ro-Ro, two container ships and each one of them presenting differences in characteristics between them. These ships were taken from the database created to study the different forms of ships.

The hydrostatic characteristics compared were: displacement (∇), Cb, Cm, Cwp, prismatic coefficient (Cp), LCB, buoyancy centre ordinate (KB), transverse metacentric radius (BMt), transverse metacentric height (KMt) and transverse moment of inertia (Ixx). The ship's displacement results from the measurement of the area under the SAC curve with the area information of forty sections. The LCB result is also related to the area under the SAC curve, as it is equal to the longitudinal position of the centroid area. The Cm and Cwp are calculated with the equation 3.1 and 3.2, respectively. To find KB, a section is created at the position of the LCB, then the centroid of the area is discovered, where the KB is equal to its height. The remainder of the hydrostatics is calculated with the following equations.

$$C_b = \frac{\nabla}{L_{pp} * B * T} \tag{5.1}$$

$$C_p = C_m * C_b \tag{5.2}$$

$$I_{xx} = \frac{2}{3} * \int_0^L y^3(x)dx \tag{5.3}$$

$$BM_t = \frac{I_{xx}}{\nabla} \tag{5.4}$$

$$KM_t = BM_t + KB \tag{5.5}$$

In order to solve the integral presented in equation 5.3, the 2nd rule of Simpson and the trapezoidal rule were used. The y values were removed by the code responsible for creating the sections in which the y value is equal to the y position of the section point that is in the vertical coordinate, z = T. The y values were removed by the code responsible for creating the sections in which the y value is equal to the y position of the section point that is in the vertical coordinate, z = T. The error used to compare the results between model and real ship was the relative error. The equations for the 2nd rule of Simpson, trapezoidal rule and relative error are presented in equations 5.6, 5.7 and 5.8, respectively. Where, h is the distance between x_i values (constant interval), $f(x_i)$ is the function value in x_i, Model is the value measured in the model ship and Real is the value measured at the the real ship.

$$I(f) = \frac{3 * h}{8} * [f(x_1) + 3 * f(x_2) + 3 * f(x_2) + f(x_4)] \tag{5.6}$$

$$I(f) = \frac{x_1 - x_0}{2} * [f(x_1) - f(x_0)] \tag{5.7}$$

$$RelativeError = \left| \frac{Model - Real}{Real} \right| * 100 \tag{5.8}$$

The position of the analysed aft midship sections is defined by dividing the distance between the longitudinal position of the midship section and the first point of the DWL by six (h_{aft}). The result of this division is added to the longitudinal position of the first point of the DWL and the result of this sum is added again to the value of the division and so on until reaching the position of the midship section. For the sections in the forward body the process is the same only that the division is made between the longitudinal position of the end of the cylindrical body and the longitudinal position of the tip of the bulb (h_{fwd}). The equations used to calculate these divisions are presented in the following equations. Where, X_MidshipSection is the longitudinal position of the midship section, X_DWL is the longitudinal position of the first point of DWL, X_BulbTip is the longitudinal position of the bulb tip and Lc is the length of the cylindrical mid body.

$$h_{aft} = \frac{X\_MidshipSection - X\_DWL}{6} \tag{5.9}$$

$$h_{fwd} = \frac{X\_BulbTip - (X\_MidshipSection + Lc)}{6} \tag{5.10}$$

5.1 Tanker - VLCC

This ship was chosen because it does not have a bulb on either the stern or the bow and since it is an oil tanker it has sections similar to a U shape. In table 5.1 presents the main dimensions of the ship.

Table 5.1: Main Dimensions of VLCC Ship

	Lpp	B	D	T
VLCC	333.37	54.24	26.21	20.42

In the figure 5.1 it is possible to see that the shape of the parametric sections is similar to the real sections. Section one and two presented the least similar shape, while section three is a near-perfect representation. Sections four, five and six, despite having a similar format, have a larger area, which is also verified in the forward sections, but with parametric sections number eight and nine presenting a smaller area. This happens due to the SAC curve despite having a closer displacement and a LCB, as seen in table 5.2, there are longitudinal positions that present differences between the parametrized and real SAC curve. The points located at DWL in sections with a bigger distance to midship present some difference with the exception of section eleven, but this can be visualised in section one, two and ten.

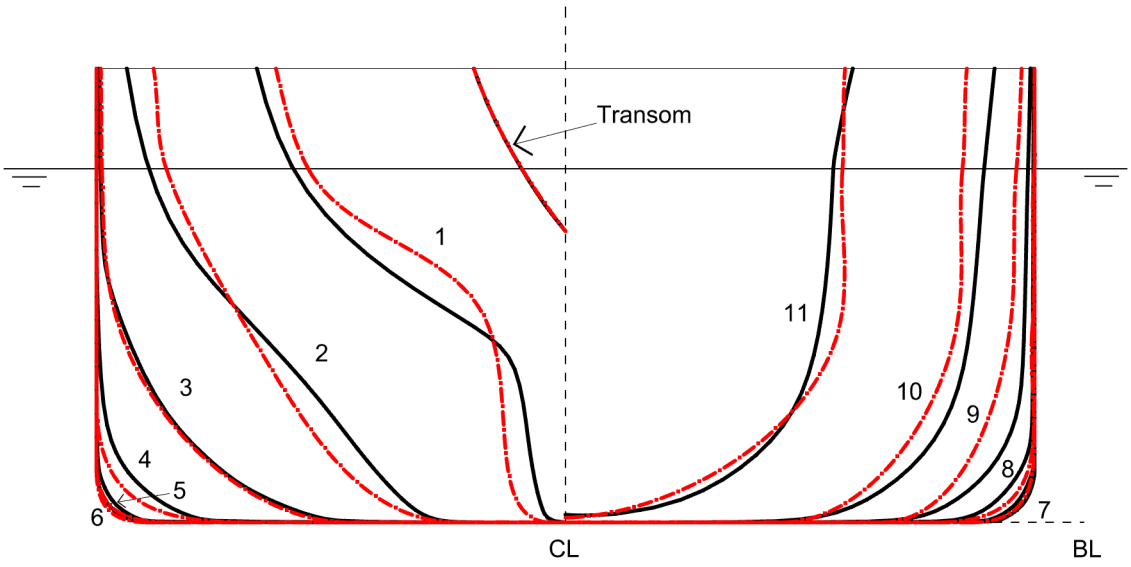

Figure 5.1: Comparative body plan of the real hull (black continuos line) and the parametric hull (red dash dot line) for the VLCC ship

The results for hydrostatics are shown in table 5.2, with displacement, form coefficients and LCB showing errors between zero and one percent, with the largest error being 0.89% in relation to the coefficient C_{wp}. The hydrostatic results referring to the equilibrium of the ship showed slightly higher errors, between one and four percent with largest error being related to the transverse moment of inertia. This is expected due to the differences of the y-coordinates of the points presented in the DWL, as can

be seen in figure 5.1.

Table 5.2: Hydrostatics results for VLCC ship

Hydrostatics	VLCC		
	Real	Model	Error
Displacement, t	308,870	309,225	0.11%
Cb, [-]	0.823	0.824	0.16%
Cm, [-]	0.996	0.997	0.10%
Cwp, [-]	0.896	0.888	0.89%
Cp, [-]	0.826	0.822	0.50%
LCB, [m]	177.51	176.59	0.52%
KB, [m]	10.59	10.24	3.31%
Ixx, [m^4]	3,678,642	3,543,483	3.67%
BMt, [m]	11.91	11.75	1.38%
KMt, [m]	22.50	21.99	2.29%

5.2 Container Ship - KCS

This container carrier was chosen because, in contrast to the above-mentioned ship, it has a bulb at the stern and bow, as well as its sections are more V shaped. In table 5.3 presents the main dimensions of the ship.

Table 5.3: Main Dimensions of KCS Ship

	Lpp	B	D	T
KCS	230.00	32.20	19.00	10.80

In the figure 5.2 is the comparison between the sections of the real hull and the parametric hull of the KCS. The aft sections have a good similarity to each other, with section 4 showing a more different shape, which may indicate a difference between the areas of the sections. This area difference means that in this region the parametrized SAC curve does not represent the real SAC curve well. The stern bulb section (section A) has a higher entry point which indicates that the stern contour does not reproduce well that zone where this point is located. In the frontal region, the sections have a similar shape, but with a lower section area. This happens because closer to the midship, the parametrized SAC does not present values of areas similar to the real ship, with this difference slowly decreasing as the sections approach the forward perpendicular. The bulb sections (section B and C) present very good results, as in both sections the form and area are similar.

In table 5.2 the hydrostatic results are presented. The results for the shape, LCB and displacement coefficients present good results, which indicates that the curves meet the area restrictions imposed by the model. The results related to the ship equilibrium present the biggest errors, being the biggest 7.72% corresponding to KB. The value of KMt is related to KB which makes its error bigger than the rest of the errors. In this ship, the transverse moment of inertia has a lower value than in the tanker, which is expected since the differences between the values of the y coordinate are smaller, as can be seen in

figure 5.2.

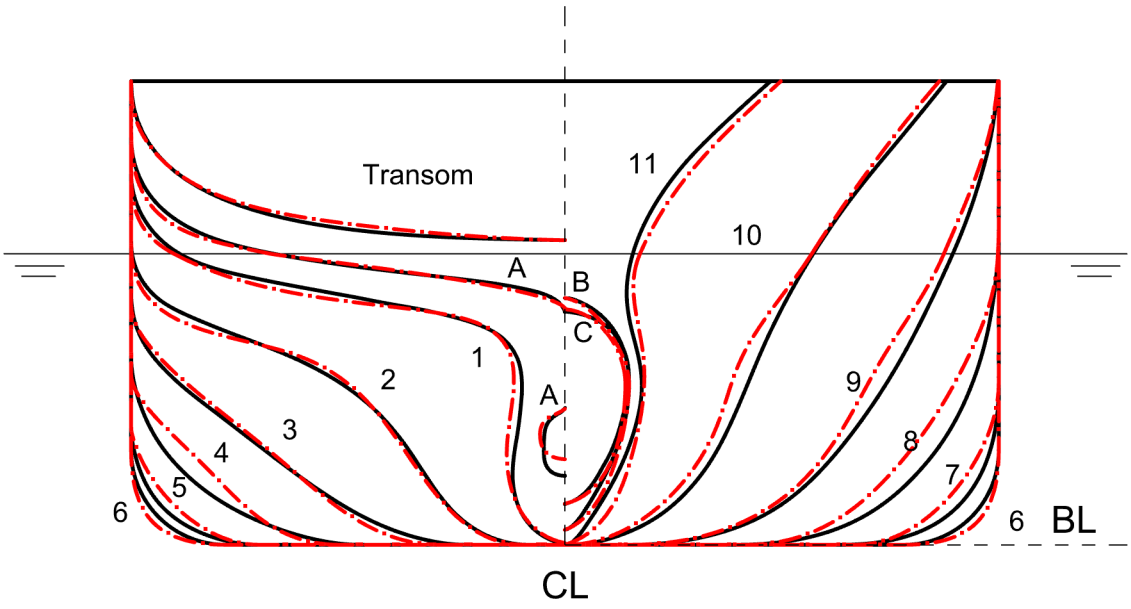

Figure 5.2: Comparative body plan of the real hull (black continuos line) and the parametric hull (red dash dot line) for the KCS ship

Table 5.4: Hydrostatics results for KCS ship

Hydrostatics	KCS		
	Real	Model	Error
Displacement, t	53,349	52,793	1.04%
Cb, [-]	0.643	0.644	0.15%
Cm, [-]	0.985	0.989	0.41%
Cwp, [-]	0.821	0.812	1.10%
Cp, [-]	0.654	0.637	2.62%
LCB, [m]	111.60	111.15	0.40%
KB, [m]	5.91	5.45	7.72%
Ixx, [m^4]	482,275	469,021	2.75%
BMt, [m]	9.04	8.88	1.72%
KMt, [m]	14.95	14.33	4.09%

5.3 Ro-Ro

The Ro-Ro ship was chosen because it has a larger transom panel than the ships previously presented, because on this type of ship is the bridge through which the vehicles enter. It also differs from the others in the area curve because it presents sections with larger area at the stern. In the table 5.5 it is described its main dimensions.

Table 5.5: Main Dimensions and Hydrostatics of Ro-Ro Ship

	L_{pp}	B	D	T
Ro-Ro	157.65	23.40	16.00	6.00

As seen in figure 5.3 the sections have similar shapes between parametric and real sections. The stern sections presented almost perfect shapes with some very small differences in relation to the section area. From section six to ten, the areas of the parametric sections present smaller values in relation to the real sections. This shows that the SAC curve parametrized, in this region has a notable area difference in relation to the real SAC curve. The bulb sections (section B and C) present very good results, as in both sections the form and area are similar.

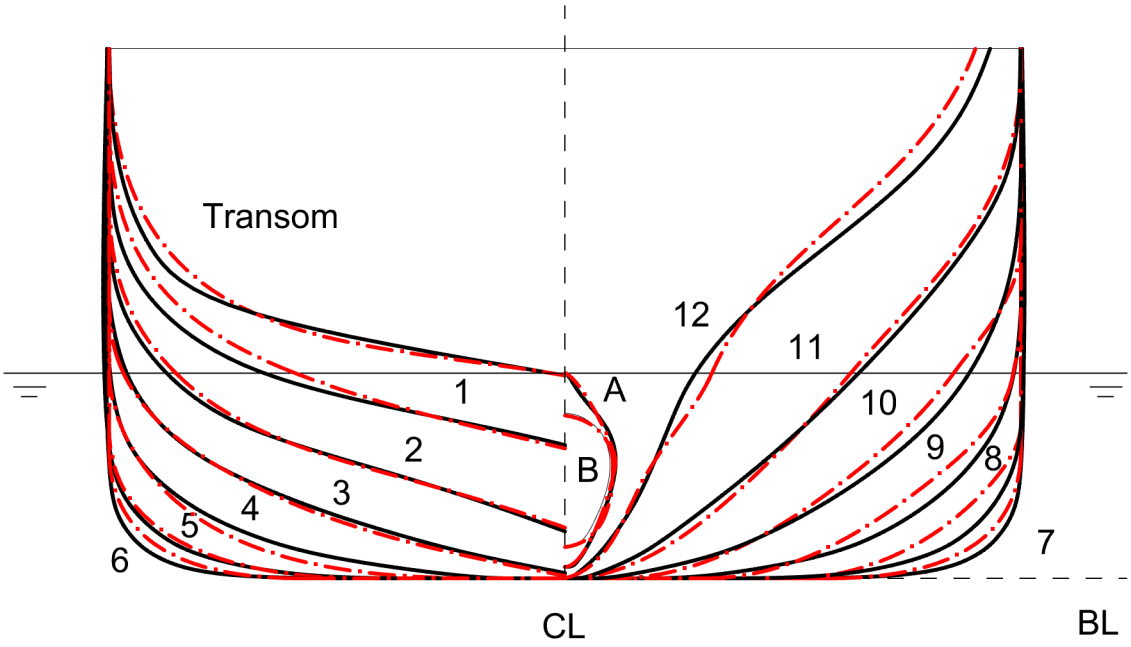

Figure 5.3: Comparative body plan of the real hull (black continuos line) and the parametric hull (red dash dot line) for the Ro-Ro ship

The hydrostatic comparison is shown in the table 5.6. The errors in this ship are slightly higher than the errors observed in the other ships used in the validation, which was not expected, since the quality of the sections is similar or better when compared to the other ships. Despite this, there is still a tendency to obtain worse results with equilibrium hydrostatics. The largest error is related with the KB and is equal to 8.53%.

Table 5.6: Hydrostatics results for Ro-Ro ship

Hydrostatics	Ro-Ro		
	Real	Model	Error
Displacement, t	15,650	15,412	1.54%
Cb, [-]	0.611	0.602	1.52%
Cm, [-]	0.946	0.955	0.93%
Cwp, [-]	0.798	0.818	2.51%
Cp, [-]	0.578	0.575	0.58%
LCB, [m]	70.52	70.12	0.56%
KB, [m]	3.54	3.24	8.53%
Ixx, [m^4]	177,392	171,554	3.29%
BMt, [m]	11.33	11.13	1.80%
KMt, [m]	15.16	14.37	5.21%

5.4 Bulk carrier

The bulk carrier chosen was the Japanese Bulk Carrier (JBC). The reasons to chose this ship were: a FOB with a big area, having a height of the bulb bigger than the others ship but at the same time the shorter distance between the forward perpendicular and the bulb tip, and presenting a FOS with straight segments. The main dimensions of the ship is presented in table 5.7.

Table 5.7: Main Dimensions and Hydrostatics of JBC Ship

	L_{pp}	B	D	T
JBC	280.00	45.00	25.00	16.50

The table 5.8 shows the hydrostatic results. This vessel showed the best hydrostatic results of the five ships used in the validation, with all errors between about zero and two percent, with KB and transverse moment of inertia being the only two hydrostatic characteristics that go slightly over two percent. The displacement and Cm presented an error equal to zero, with the errors of the other form coefficients around 1.50%, which are superior to the errors of KMt and BMt, which did not happen in previous ships.

Table 5.8: Hydrostatics results for JBC ship

Hydrostatics	JBC		
	Real	Model	Error
Displacement, t	182,950	182,946	0.00%
Cb, [-]	0.843	0.859	1.81%
Cm, [-]	0.998	0.998	0.00%
Cwp, [-]	0.910	0.921	1.21%
Cp, [-]	0.845	0.857	1.40%
LCB, [m]	147.03	146.79	0.16%
KB, [m]	8.44	8.26	2.13%
Ixx, [m^4]	1,853,284	1,812,623	2.19%
BMt, [m]	10.13	10.16	0.25%
KMt, [m]	18.58	18.42	0.88%

In the figure 5.4 it is possible to analyse the comparison between real and parametric sections. The stern sections had a similar shape and area, and section 1, despite having a similar shape, has a larger area. The aft bulb section (Section A) is similar in shape, but the section above the bulb has a larger area, which makes the shape slightly different. The forward sections have the same issue as the other parametric sections presented in the other ships, that is, the difference between the parametrized SAC curve and the real one, which leads to differences in shape. The bulb sections on the bulb in the bow contour (Section B and C) have similar shape and area, but the area distribution is not similar as it has a larger area under the bottom of the section and a lower area under the top of the section.

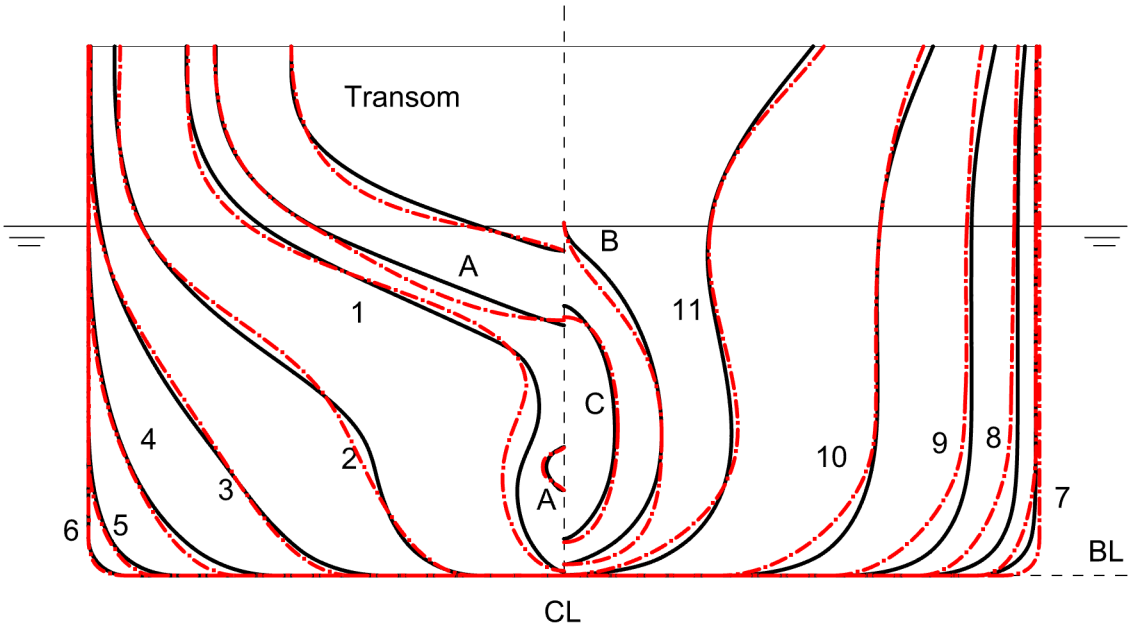

Figure 5.4: Comparative body plan of the real hull (black continuos line) and the parametric hull (red dash dot line) for the JBC ship

5.5 Container Ship - Colombo

This ship was chosen because it has characteristics that none of the other ships presented above have, which are: a transom with a U shape, an addition bulb in bow and a FOS curve that doesn't start at the height of the deck waterline. The main dimensions of the ship is presented in table 5.9.

Table 5.9: Main Dimensions and Hydrostatics of Colombo Ship

	L_{pp}	B	D	T
Colombo	319.00	42.80	27.50	13.00

In figure 5.5 it is possible to see that the aft bulb section (Section A) is reproduced with quality because it has similar shape and area. Section one presents a dissimilar form and area. Section two is the best one as it produces a very similar parametric section to the real. From section three to five the area of the sections are very different, with the biggest difference being presented in section four. The real section four is behind the parametric section five. The difference in area indicates that the parametrized SAC don't reproduce well the real SAC. This is also verified in the forward sections, with the exception of section nine, and in the bulb sections (Section B and C).

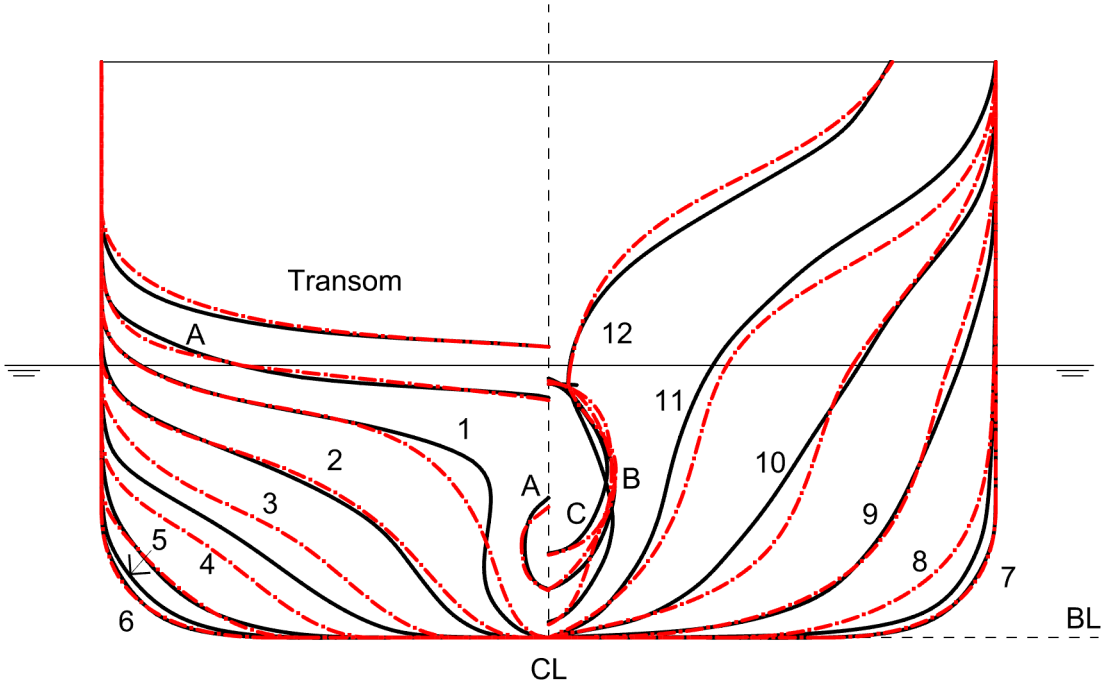

Figure 5.5: Comparative body plan of the real hull (black continuos line) and the parametric hull (red dash dot line) for the VLCC Colombo ship

As expected, the results for hydrostatics presented in table 5.10 show greater errors in the hydrostatic characteristics that depend on the quality of the sections, such as: displacement, Cb, Cp, LCB and KB. The biggest error is 7.20% which is related to KB. The lack of quality of the longitudinal distribution of the area given by the parametrized SAC is evidenced by the LCB error, as it presents a difference of 2.12 meters. The hydrostatics related to the geometric curves (Cm and Cwp) present low values, which indicates that these curves fulfil the restrictions imposed on them.

Table 5.10: Hydrostatics results for VLCC Colombo ship

Hydrostatics	Colombo		
	Real	Model	Error
Displacement, t	107,434	105,450	1.85%
Cb, [-]	0.591	0.580	1.84%
Cm, [-]	0.967	0.969	0.24%
Cwp, [-]	0.771	0.768	0.39%
Cp, [-]	0.571	0.562	1.61%
LCB, [m]	146.66	148.78	1.45%
KB, [m]	7.20	6.70	7.00%
Ixx, [m^4]	1,361,468	1,344,110	1.27%
BMt, [m]	12.99	13.07	0.58%
KMt, [m]	20.19	19.77	2.12%

5.6 Hydrostatics Results

In table 5.11 presents a compilation of the errors presented by all 5 ships previously presented.

Table 5.11: Hydrostatic Results

Hydrostatics	Relative Error Results				
	VLCC	JBC	Ro-Ro	KCS	Colombo
Displacement, t	0.11%	0.00%	1.54%	1.04%	1.85%
Cb, [-]	0.16%	1.81%	1.52%	0.15%	1.84%
Cm, [-]	0.10%	0.00%	0.93%	0.41%	0.24%
Cwp, [-]	0.89%	1.21%	2.51%	1.10%	0.39%
Cp, [-]	0.50%	1.40%	0.58%	2.62%	1.61%
LCB, [m]	0.52%	0.16%	0.56%	0.40%	1.45%
KB, [m]	3.31%	2.13%	8.53%	7.72%	7.00%
Ixx	3.67%	2.19%	3.29%	2.75%	1.27%
BMt, [m]	1.38%	0.25%	1.80%	1.72%	0.58%
KMt, [m]	2.29%	0.88%	5.21%	4.09%	2.12%

After analysing the table, it is possible to conclude that the hydrostatic characteristics that present the greatest errors in practically all ships are the transverse moment of inertia (Ixx) and the buoyancy centre ordinate (KB). The error related to Ixx is justifiable with the difference in the y coordinate of the points located in the DWL. The equation 5.3 used to calculate the Ixx also contributes to the increase in error since it uses the y coordinate, raising it to the cube. The KB hydrostatic error is justified by the differences shown in the ship transverse sections. This can be seen in the graphical validation presented earlier.

Chapter 6

Conclusions and Future Work

6.1 Conclusions

The objective of this thesis was to develop a fully parametric procedure to produce wireframe models able to represent the shape of the most common hull forms of merchant ships to be used in the concept design phase. Currently, surface models are considered the most complete representation of the hull shape, but there are more ways to represent it, such as: lines plan, offset table and a wireframe model. In the concept design phase, there is no need to have a complex surface model, as there are computer programs capable of producing the basic naval architecture computations from the selected sets of curves. In this thesis a wireframe procedure was developed, as it can provide all the curve information that is needed in the initial phases of the ship design.

To study the most common hull shapes, it was made a compilation and analysis of some different type of merchant ships. The objectives of this analysis were: identifying the most important curves to define hull's shape, the necessary parameters to define them and the values range of each parameter. The curves were classified in two types: geometric curves and property variation curves. Eight geometric curves were identified: bow and stern contours, midship section, FOB, FOS, transom, DWL and deck waterline. Three property distribution curves were identified: SAC, longitudinal variation of section angles and vertical variation of waterline angles. This study has some limitations because it was not possible to obtain sufficiently line plans or 3D models and some models presented modelling mistakes.

The procedure was implemented in a visual programming tool called Grasshopper, a plug-in of Rhinoceros 3D. The procedure starts with the input of eighty parameters, or less, depending on the complexity of the hull shape. With this data a number of points are created, then the geometric and property variation curves, and finally the wireframe model. Regarding the property variation curves the input parameters only define the domains. To complete the definition, it is necessary to manually set the minimum and maximum value of the angles and adjust the Bézier distribution in each domain. This is a positive aspect of a parametric approach as it allows modifying the hull representation. If the modifications do not produce good results, there is the possibility of undoing them and obtaining the initial shape of the hull. The final wireframe model produced can be detailed up to fifty sections and up to twenty

waterlines.

To validate the parametric model, five ships were selected for presenting different types of characteristics, such as presence or absence of bulbous bow, presence of cylindrical mid body, etc. Both numerical and graphical validations were made between the parametric hull and the real model. The numerical validation was the comparison of some hydrostatics properties values. This validation show good results for hydrostatics, with most results being between zero and four percent. Usually the biggest error presented was related to the KB, being around seven and eight percent. The ship with the best hydrostatic results was the bulk carrier, which exhibits errors between zero and two percent with only two hydrodynamic characteristics passing very slightly over two percent. The errors related to the ship equilibrium are usually larger by one or two percent, this is more visible on ships where there are some differences between the area of the parametric and real sections. The graphical validation was made by creating a body plan where the parametric sections were superimposed over the real sections. The parametric sections showed good shape despite some differences in areas, being more noticeable in the sections closer to midship. This indicates that the SAC parametrization has some limitations, as it is not capable of reproducing precise areas in the regions closest to the beginning and end of the cylindrical mid body. The ships with the best results were the KCS and the Ro-Ro, with the worst result being the tanker. The tanker presents the worst result because in addition of the problem with the SAC parametrization, also presents a noticeable variation in the y coordinates of the points located at the DWL. This happens because the parametrized DWL in this case is not able to reproduce with quality the real DWL curve, despite presenting good results for coefficient C_{WP}. Although, the cross sections produced may present some local discrepancies with the area from SAC, they present feasible shapes and lead to good hydrostatics results. Therefore, it was considered that the parametric procedure developed is capable of being used in the concept design phase, with the objective of this thesis being fulfilled.

The major achievements of this work, was the development of a fully parametric procedure, that is able to create a hull shape with the input of parameters. In addition, it has flexibility to do local shape adjustments allowing the designer the freedom to easily explore different shape features.

6.2 Future Work

The present parametric model have some limitations in aspects that are important for merchant ships shapes and the usability of the model.

At the moment the parametric procedure is able to create a knuckle only when there is an addition bulb, but the merchant ships can have more knuckles in other regions, for example when the transom panel presents a V shape section. In the future it would be interesting to investigate the possibility to create a knuckle at any desired location. Another limitation of the model is the capability to only reproduce stern contour with a single propeller. Another future work can be to develop parameters to reproduce ships with a twin-propeller. As identified in the section 3.2.1, there are two more types of bulb that are being used in certain types of ships instead of the traditional bulbs that the parametric model is able to create. These types are the X-bow and the axe-bow and it would be interesting if the model was

able to create them.

As identified in the validation of the parametric procedure, the parametrization of the SAC curve has some limitations, so in a later version of this parametric method it would be interesting to create more parameters that would create a more accurate SAC.

At this point the model is only focused in monohull, but because there are some merchant ships, mainly ferrys, that present a catamaran type hull it would be interesting if the parametric model was able to reproduce this type of hull.

For the parametric model to be used in more advanced stages of the ship design procedure, it is necessary to developed a quality surface model. To fulfil this objective, it is advisable to create parameters related to the surface to ensure that has good fairness.

To improve the usability of the model, it would be advantageous to develop a user interface that allows configuring and changing the input parameters in the Rhinoceros 3D software instead of having to look for the parameter slider in Grasshopper which can be a complex task if the person using the parametric model is not familiar with the location of it.

Bibliography

1. Bole, M. and Lee, B. Integrating parametric hull generation into early stage design. *Ship Technology Research*, 53:115–137, 7 2006. ISSN 0937-7255. doi: 10.1179/str.2006.53.3.003.

2. Taylor, D.W. Calculations of ships' forms and light thrown by model experiments upon resistance, propulsion and rolling of ships. In *Trans. International Engineering Congress, San Francisco*, 1915.

3. Benson, F.W. Mathematical ships's lines. *Transactions RINA 82*, 1940.

4. Kuiper, G. Preliminary design of ship lines by mathematical methods. *Journal of Ship Research*, 14 (01):52–65, 03 1970. ISSN 0022-4502. doi: https://doi.org/10.5957/jsr.1970.14.1.52.

5. Von Kerczek, C. and Tuckk, E. O. The Representation of Ship Hulls by Conformal Mapping Functions. *Journal of Ship Research*, 13(04):284–298, 12 1969. ISSN 0022-4502. doi: https://doi.org/10.5957/jsr.1969.13.4.284.

6. Reed, A. and Nowacki, H. Interactive creation of fair ship lines. *Journal of Ship Research*, 18: 96–112, 1974.

7. Bezier, P. *Numerical Control: Mathematics and Applications*. Wiley Series in Computing. J. Wiley, 1972. ISBN 9780835799447.

8. de Boor, C. On calculating with B-Splines. *Journal of Approximation Theory*, 6(1):50–62, 1972. doi: https://doi.org/10.1016/0021-9045(72)90080-9.

9. Piegl, L. and Tiller, W. *The NURBS Book*. Springer-Verlag, Berlin, Heidelberg, 1995. ISBN 3540615458.

10. Harries, S.; Abt, C.; and Hochkirch, K. Modeling meets simulation-process integration to improve design. *Honorary colloquium for Prof. Hagen, Prof. Schlüter and Prof. Thiel, Germany*, 2004.

11. Abt, C. and Harries, S. A new approach to integration of cad and cfd for naval architects. In *6th International Conference on Computer Applications and Information Technology in the Maritime Industries (COMPIT), Cortona, Italy,23-25 April 2007*, 467–479, 2007.

12. Lackenby, H. On the systematic geometrical variation of ship forms. *Transactions of The Royal Institute of Naval Architects (RINA)*, 92:289–315, 1950.

13. Hochkirch, K. and Bertram, V. Slow steaming bulbous bow optimization for a large containership. In *8th International Conperance on Computer and IT Applications in the Marine Industries (COMPIT), Budapest, Hugary,10 -12 May*, 390–398, 2009.

14. Zhang, Y.; Kim, D.; and Bahatmaka, A. Parametric method using grasshopper for bulbous bow generation. In *2018 International Conference on Computing, Electronics Communications Engineering (iCCECE), Southend, United Kingdom, 16-17 August*, 307–310, 2018. doi: 10.1109/iCCECOME.2018.8658464.

15. Pérez, F.; Suárez, J. A.; Clemente, J. A.; and Souto, A. Geometric modelling of bulbous bows with the use of non-uniform rational B-Spline surfaces. *Journal of Marine Science and Technology*, 12: 83–94, 6 2007. ISSN 09484280. doi: 10.1007/s00773-006-0225-6.

16. Nam, J. H. and Bang, N. S. A curve based hull form variation with geometric constraints of area and centroid. *Ocean Engineering*, 133:1–8, 2017. ISSN 00298018. doi: 10.1016/j.oceaneng.2017.01.031.

17. Buhmann, M. D. Radial basis functions. *Acta numerica*, 9:1–38, 2000.

18. Harries, S. and Uharek, S. Application of radial basis functions for partially-parametric modeling and principal component analysis for faster hydrodynamic optimization of a catamaran. *Journal of Marine Science and Engineering*, 9(10), 2021.

19. Choi, H. J. Hull-form optimization of a container ship based on bell-shaped modification function. *International Journal of Naval Architecture and Ocean Engineering*, 7:478–489, 2015. ISSN 20926790. doi: 10.1515/ijnaoe-2015-0034.

20. Lu, Y.; Chang, X.; Yin, X.; and Li, Z. Hydrodynamic design study on ship bow and stern hull form synchronous optimization covering whole speeds range. *Mathematical Problems in Engineering*, 2019:1–19, 08 2019. doi: 10.1155/2019/2356369.

21. Lu, Y.; Gu, Z.; Liu, S.; Chuang, Z.; Li, Z.; and Li, C. Scenario-based optimization design of ice-breaking bow for polar navigation. *Ocean Engineering*, 244:110365, 2022. ISSN 0029-8018. doi: https://doi.org/10.1016/j.oceaneng.2021.110365.

22. Sederberg, T. W. and Parry, S. R. Free-form deformation of solid geometric models. In *Proceedings of the 13th Annual Conference on Computer Graphics and Interactive Techniques, Dallas, United States of America, 18-22 August*, SIGGRAPH '86, 151–160. Association for Computing Machinery, 1986.

23. Brizzolara, S.; Vernengo, G.; Pasquinucci, C. A.; and Harries, S. Significance of parametric hull form definition on hydrodynamic performance optimization. In *VI International Conference on Computational Methods in Marine Engineering, Rome, Italy, 15-17 June*, 2015.

24. Ang, J.; Goh, C.; Jirafe, V.; and Li, Y. Efficient hull form design optimisation using hybrid evolutionary algorithm and morphing approach. In *International Conference on Computer Applications in Shipbuilding (iCCAS), Singapore, 26-29 September*, 09 2017.

25. Choo, C. T.; Ang, J. H.; Kuik, S.; Hui, L. C. M.; Li, Y.; and Goh, C. Ship design with a morphing evolutionary algorithm. In *2020 IEEE Congress on Evolutionary Computation (CEC), Glasgow, United Kingdom 19-24 July*, 1–8, 2020. doi: 10.1109/CEC48606.2020.9185645.

26. Harries, S. and Abt, C. Parametric design and optimization of sailing yachts. In *SNAME Chesapeake Sailing Yacht Symposium*, 1 1998.

27. Harries, S. and Abt, C. Parametric curve design applying fairness criteria. In *In International Workshop on creating fair and shape-preserving curves and surfaces. Berlin (Potsdam, Teubner): Network Fairshape*, 1998.

28. Nowacki, H. and Harries, S. Form parameter approach to the design of fair hull shapes. In *In 10th International conference on Computer Applications (ICCAS), Cambridge, United States of America, 7-11 June*, 1999.

29. Zhang, P.; Zhu, D. X.; and Leng, W. H. Parametric approach to design of hull forms. *Journal of Hydrodynamics*, 20:804–810, December 2008. ISSN 10016058. doi: 10.1016/S1001-6058(09)60019-6.

30. Abt, C.; Bade, S. D.; Birk, L.; and Harries, S. Parametric hull form design - a step towards one week ship design. In *8th International Symposium on Pratical Design of Ships and Other Floating Structure (PRADS), Shanghai, September*, 67–74, 2001.

31. Hochkirch, K.; Röder, K.; Abt, C.; and Harries, S. Advanced parametric yacht design. In *High Performance Yacht Design Conference (HPYD), Auckland, New Zealand, December*, 2002.

32. Maisonneuve, J.J.; Harries, S.; Marzi, J.; Raven, H.C.; Viviani, U.; and Piippo, H. Towards optimal design of ship hull shapes. In *Proceedings of the 8th International Marine Design Conference (IMDC), Athens, Greece, 5-8 May*, 31–42, 2003.

33. Abt, C.; Harries, S.; and Heimann, J. From redesign to optimal hull lines by means of parametric modeling. In *2nd Intl. Conf. Computer Applications and Information Technology in the Maritime Industries (COMPIT), Hamburg, Germany, May*, 444–458, 2003.

34. Papanikolaou, A.; Harries, S.; Wilken, M.; and Zaraphonitis, G. Integrated design and multiobjective optimization approach to ship design. In *RINA, Royal Institution of Naval Architects - International Conference on Computer Applications in Shipbuilding (ICCAS), Gyeonnggi-do, South Korea, 26-29 October*, volume 3, 31–42, 2011. ISBN 9781905040872. doi: 10.3940/rina.iccas.2011.50.

35. Han, S.; Lee, Y. S.; and Choi, Y. B. Hydrodynamic hull form optimization using parametric models. *Journal of Marine Science and Technology*, 17:1–17, 3 2012. ISSN 09484280. doi: 10.1007/s00773-011-0148-8.

36. Sanches, F. M. Parametric modelling of hull form for ship optimization. Master's Thesis, Instituto Superior Técnico, 2016.

37. Sener, B. Parametric design of a surface combatant for simulation-driven design and hydrodynamic optimization. *International Journal of Mechanical And Production Engineering*, 4:2320–2092, 2016.

38. Feng, Y.; Moctar, O.; and Schellin, T. Hydrodynamic optimisation of a multi-purpose wind offshore supply vessel. *Ship Technology Research*, 67:1–15, 04 2019. doi: 10.1080/09377255.2019.1602976.

39. Feng, Y.; el Moctar, O.; and Schellin, T. E. Hydrodynamic Optimization of a Containership. In *International Conference on Offshore Mechanics and Arctic Engineering (OMAE), 3-7 August*, volume Volume 2B: Structures, Safety, and Reliability, 2020. doi: https://doi.org/10.1115/OMAE2020-18616.

40. Feng, Y.; Moctar, O.; and Schellin, T. Parametric hull form optimization of containerships for minimum resistance in calm water and in waves. *Journal of Marine Science and Application*, 01 2022. doi: 10.1007/s11804-021-00243-w.

41. Bole, M. *A Hull Surface Generation Technique Based on a Form Topology and Geometric Constraint Approach*. PhD Thesis, University of Strathclyde, 2003.

42. Bole, M. and Lee, B. An hierarchical approach to hull form design. 2003.

43. Bole, M. A strategy for closely integrating parametric generation and interactive manipulation in hull surface design. In *18th International Conference on Computer and IT Applications in the Maritime Industries (COMPIT), Tullamore, Ireland, 25-27 March*, 2019.

44. Bole, M. Interactive hull form transformations using curve network deformation. *Ship Technology Research*, 58:46–64, 2011.

45. Kim, H. C. and Nowacki, H. Parametric design of complex hull forms. *Ship and Ocean Technology*, 9:47–63, March 2005.

46. Pérez, F. L.; Clemente, J. A.; Suárez, J. A.; and González, J. M. Parametric generation, modeling, and fairing of simple hull lines with the use of nonuniform rational b-spline surfaces. *Journal of Ship Research*, 52:1–15, 2008.

47. Calkins, D.E; Schachter, R.D; and Oliveira, L.T. An automated computational method for planing hull form definition in concept design. *Ocean Engineering*, 28(3):297–327, 2001. ISSN 0029-8018.

48. Pérez-Arribas, F. Parametric generation of planing hulls. *Ocean Engineering*, 81:89–104, 5 2014. ISSN 00298018. doi: 10.1016/j.oceaneng.2014.02.016.

49. Khan, S.; Gunpinar, E.; and Dogan, K. M. A novel design framework for generation and parametric modification of yacht hull surfaces. *Ocean Engineering*, 136:243–259, 2017. ISSN 00298018. doi: 10.1016/j.oceaneng.2017.03.013.

50. Khan, S.; Gunpinar, E.; and Sener, B. Genyacht: An interactive generative design system for computer-aided yacht hull design. *Ocean Engineering*, 191:106462, 2019. ISSN 0029-8018.

51. Kostas, K. V.; Ginnis, A. I.; Politis, C. G.; and Kaklis, P. D. Ship-hull shape optimization with a T-Spline based BEM-isogeometric solver. *Computer Methods in Applied Mechanics and Engineering*, 284:611–622, 2 2015. ISSN 00457825. doi: 10.1016/j.cma.2014.10.030.

52. Ginnis, A. I.; Feurer, C.; Belibassakis, K. A.; Kaklis, P. D.; Kostas, K. V.; Gerostathis, Th P.; and Politis, C. G. A catia® ship-parametric model for isogeometric hull optimization with respect to wave resistance. In *RINA, Royal Institution of Naval Architects - International Conference on Computer Applications in Shipbuilding (ICCAS), Gyeonnggi-do, South Korea, 26-29 October*, 9–20, 2011. ISBN 9781905040872.

53. Katsoulis, T.; Wang, X.; and Kaklis, P. D. A T-Splines-based parametric modeller for computer-aided ship design. *Ocean Engineering*, 191, 11 2019. ISSN 00298018. doi: 10.1016/j.oceaneng.2019.106433.

54. Ingrassia, T.; Mancuso, A.; Nigrelli, V.; Saporito, A.; and Tumino, D. Parametric hull design with rational bézier curves and estimation of performances. *Journal of Marine Science and Engineering*, 9, 4 2021. ISSN 20771312. doi: 10.3390/jmse9040360.

55. Guan, G.; Wang, L.; Geng, J.; Zhuang, Z.; and Yang, Q. Parametric automatic optimal design of usv hull form with respect to wave resistance and seakeeping. *Ocean Engineering*, 235:109462, 2021. ISSN 0029-8018. doi: https://doi.org/10.1016/j.oceaneng.2021.109462.

56. Pérez-Arribas, F. and Calderon-Sanchez, J. A parametric methodology for the preliminary design of SWATH hulls. *Ocean Engineering*, 197:106823, 2020. ISSN 0029-8018. doi: https://doi.org/10.1016/j.oceaneng.2019.106823.

57. Romanelli, F. Parametric modelling of hulls for small craft. Master's Thesis, Instituto Superior Técnico, 2021.

58. Zhou, H.; Feng, B.; Liu, Z.; Chang, H.; and Cheng, X. Nurbs-based parametric design for ship hull form. *Journal of Marine Science and Engineering*, 10, 2022. ISSN 2077-1312. doi: 10.3390/jmse10050686.

59. Kracht, A. M. Design of bulbous bows. *SNAME Transactions*, 86:197–217, 1978.

Appendix A

Parametric Model Grasshopper Code - Examples

In this appendix is presented some visual Grasshopper codes. The boxes are called components, with the ability to create points, curves, vectors. In addition there are components called ”sliders” that allow to set and modify the input parameters. The components have inputs (left side) and outputs (right side), with the connection between them being made by wires (black lines in the drawing). There are components with the ability to compile code in Python (figure A.1), C++ and Visual Basic. In figure A.3 the rightmost component is an example of a python compiler. This compiler was used multiple times in the parametric procedure. In figure A.2 it is presented the fully parametric procedure, with some examples of the code to create the geometric (section A.2), properties variation curves (section A.3) and the wireframe model (section A.4).

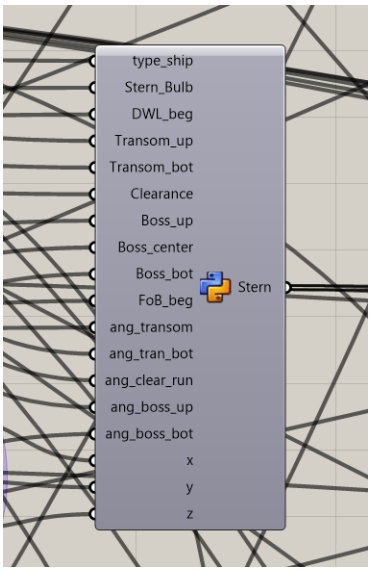

Figure A.1: Python Compiler Component

A.1 Fully Parametric Procedure

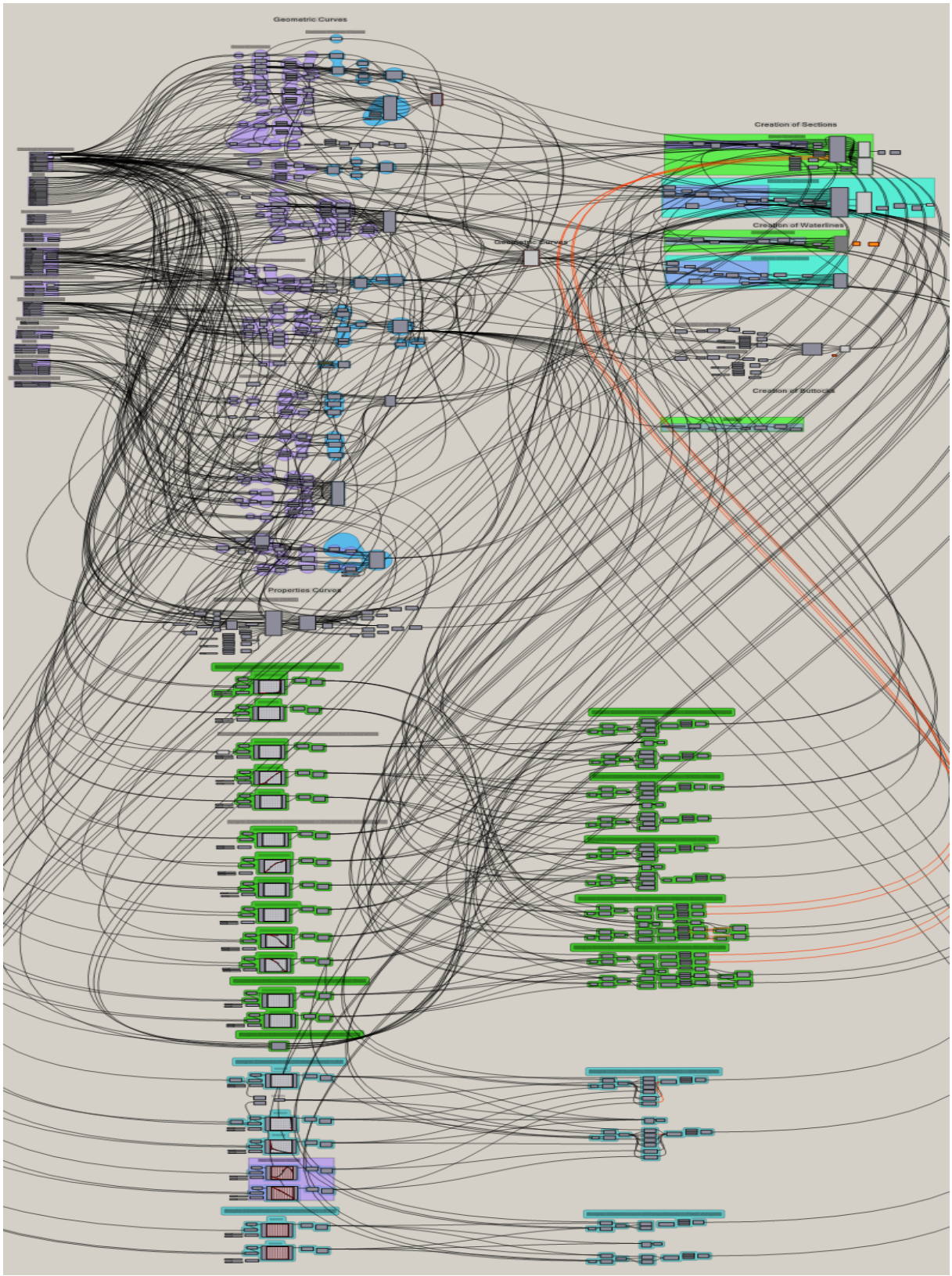

Figure A.2: Fully Parametric Procedure

A.2 Geometric Curves

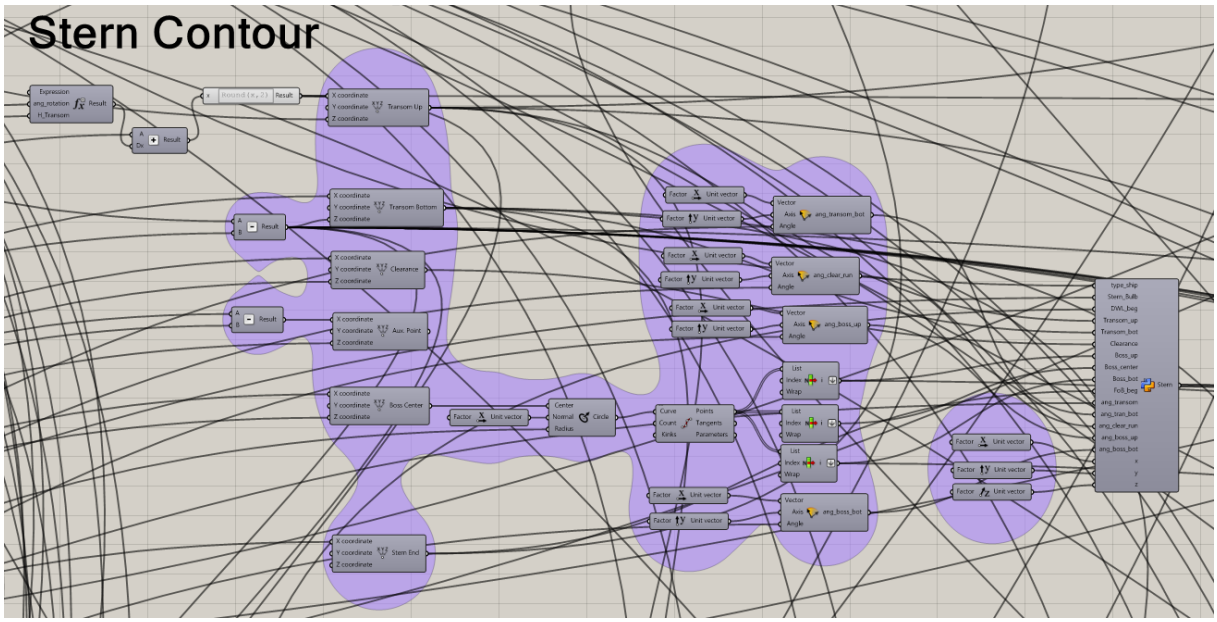

Figure A.3: Geometric Curve Example - Stern Contour

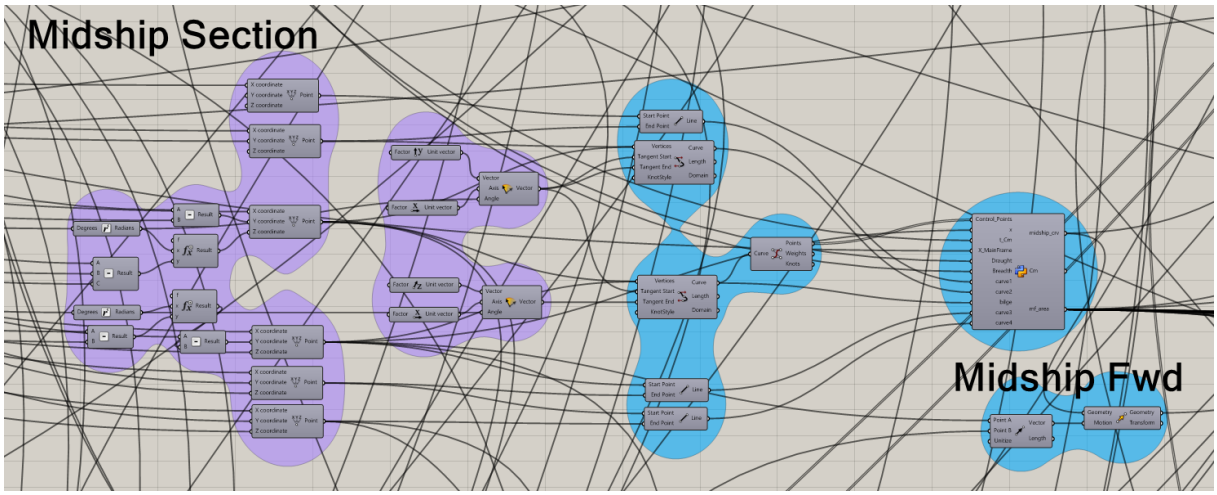

Figure A.4: Geometric Curve Example - Midship Section Curve

A.3 Property Variation Curves

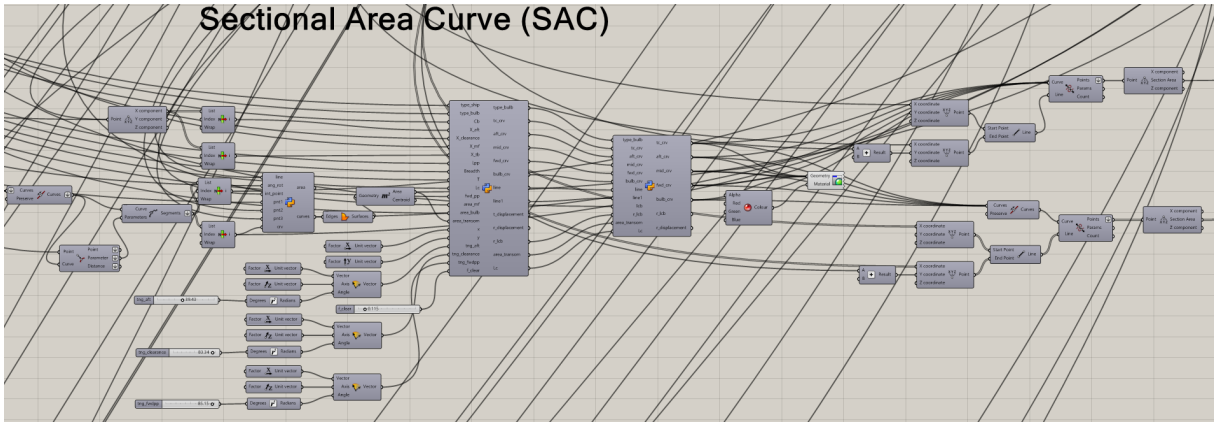

Figure A.5: Property Variation Curves Example - SAC Curve

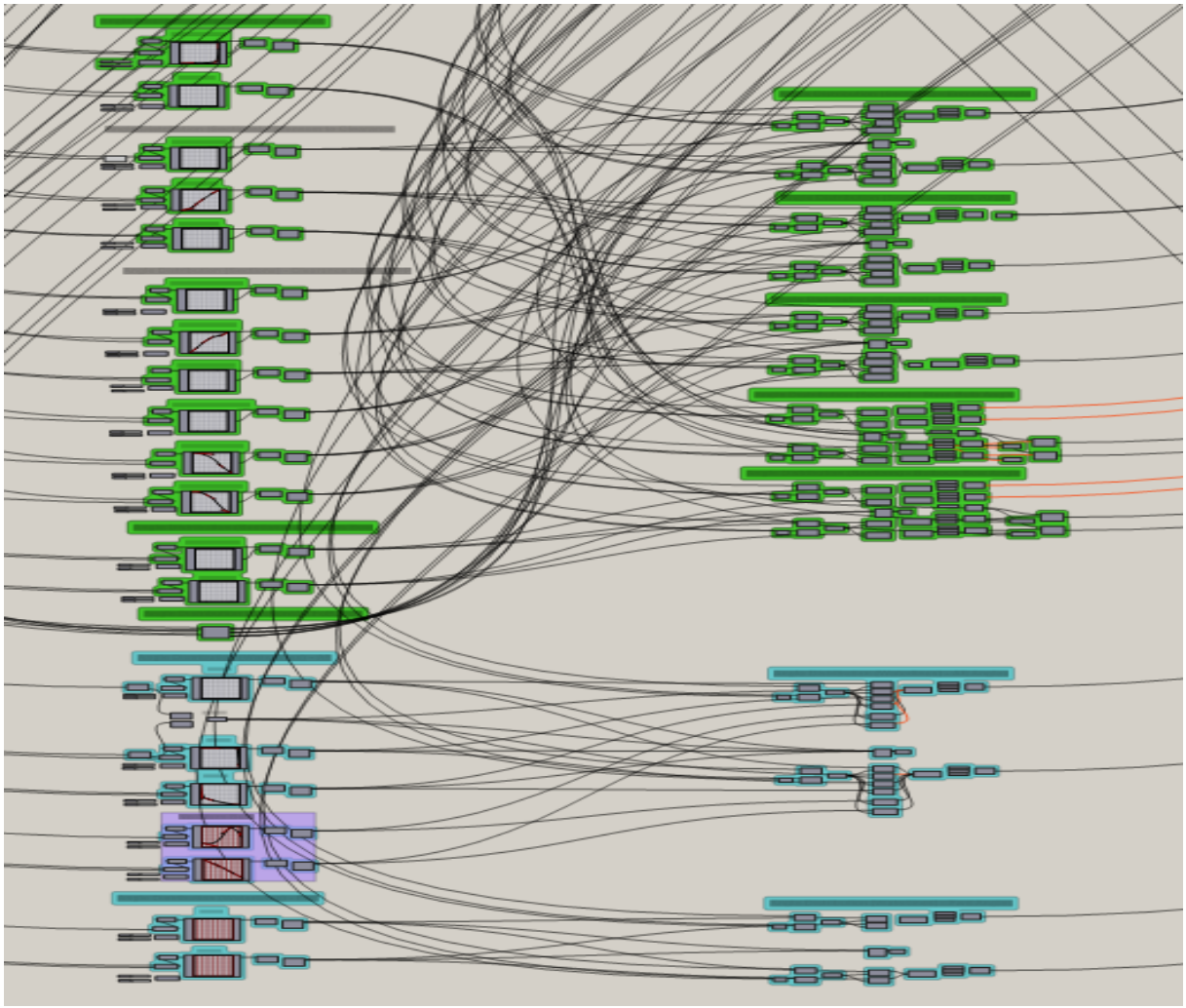

Figure A.6: Property Variation Curves Example - Longitudinal and Vertical Angles Variation

A.4 Sections and Waterlines Creation

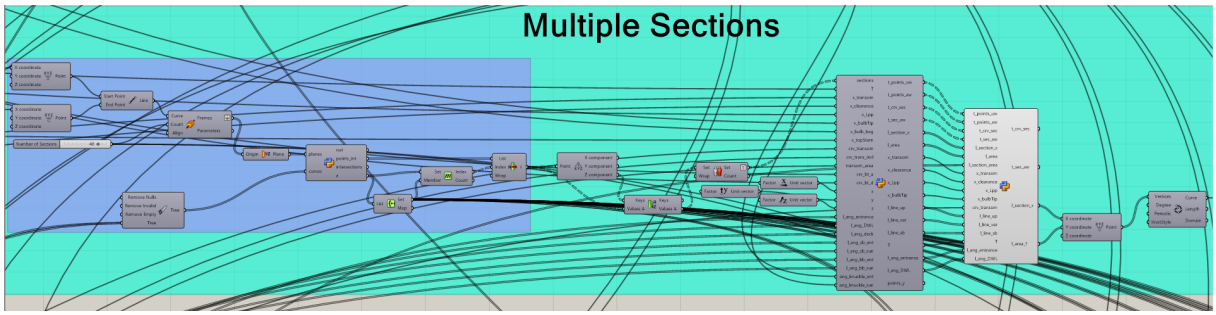

Figure A.7: Sections Creation

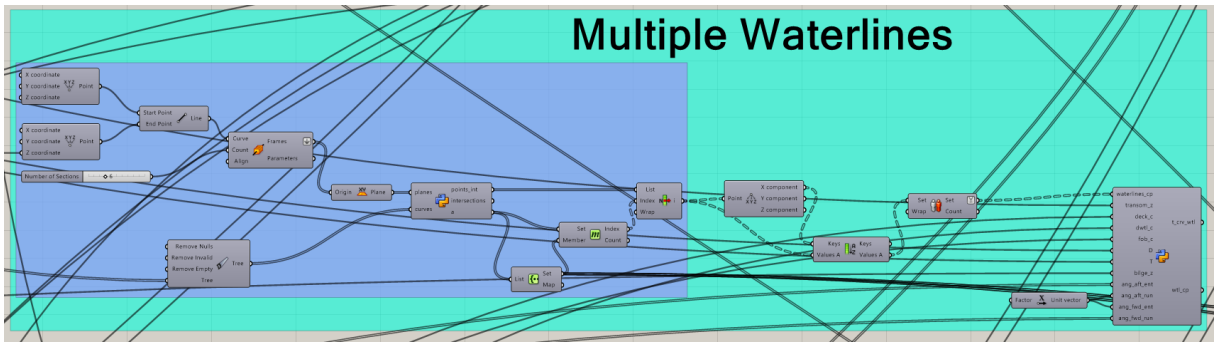

Figure A.8: Waterlines Creation